Technische Universität Graz
Institut für Festigkeitslehre
Kopernikusgasse 24/I
8010 Graz

Stephan Teichtmeister

Gradient-extended viscoplasticity at small strains and its numerical implementation with enhanced-strain finite elements.

Masterarbeit
zur Erlangung des akademischen Grades eines Diplom–Ingenieurs

Technische Universität Graz
Fakultät für Maschinenbau und Wirtschaftswissenschaften

Studienrichtung:
Maschinenbau

Betreuer: O.Univ.–Prof. Dipl.–Ing. Dr.techn. Christian C. Celigoj

Deutsche Fassung:
Beschluss der Curricula-Kommission für Bachelor-, Master- und Diplomstudien vom 10.11.2008
Genehmigung des Senates am 1.12.2008

EIDESSTATTLICHE ERKLÄRUNG

Ich erkläre an Eides statt, dass ich die vorliegende Arbeit selbstständig verfasst, andere als die angegebenen Quellen/Hilfsmittel nicht benutzt, und die den benutzten Quellen wörtlich und inhaltlich entnommenen Stellen als solche kenntlich gemacht habe.

Graz, am …… ……..
(Unterschrift)

Englische Fassung:

STATUTORY DECLARATION

I declare that I have authored this thesis independently, that I have not used other than the declared sources / resources, and that I have explicitly marked all material which has been quoted either literally or by content from the used sources.

…… ……..
date (signature)

Vorwort

Die vorliegende Arbeit entstand von Juli 2013 bis Dezember 2013 am Institut für Festigkeitslehre der TU Graz unter Betreuung von Prof. Christian C. Celigoj, dem ich hier für dessen intensive Betreuung meinen Dank aussprechen will. Besonders bedanken möchte ich mich auch bei Dr. Stefan Hollerer für sein Interesse und seine tatkräftige Unterstützung. Weiters waren die fachlichen Diskussionen mit Dr. Manfred Ulz stets sehr hilfreich.

Für die Förderung und die Möglichkeit an diversen Konferenzen teilzunehmen, möchte ich mich vor allem bei Prof. Günter Brenn vom Institut für Strömungslehre und Wärmeübertragung der TU Graz und bei Prof. Olaf Steinbach vom Institut für Numerische Mathematik der TU Graz bedanken.

Schließlich gebührt ein ganz großes Dankeschön meinen Eltern Günter und Gabriele, sowie meiner Schwester Vanessa, die mich während meiner Studienzeit immer wieder ermutigt und aufgebaut haben.

Stephan Teichtmeister, Graz, am 21.12.2013

Abstract
This thesis deals with a thermodynamically consistent, nonlocal multifield-continuum theory to describe viscous softening materials. For this purpose we introduce beside the classical local internal variables, which are only treated on integration point level, so called generalized internal variables, which build together with its dual quantities additional degrees of freedom. The nonlocality comes in with the consideration of the gradient of the generalized internal variables. The presented continuum theory is applied to von-Mises viscoplasticity. To prevent locking, a mixed FE-formulation with additional macroscopic strains, based on the Hu-Washizu principle, has been realized. Numerical examples compare the results of the local and the nonlocal theory and show clearly the regularization effect of the gradient-extended theory.

Kurzfassung
Diese Arbeit beschäftigt sich mit einer thermodynamisch konsistenten, nichtlokalen Mehrfeld-Kontinuumstheorie zur Beschreibung viskoser entfestigender Materialien. Hierfür werden neben den klassischen lokalen internen Variablen, welche nur auf Integrationspunktlevel behandelt werden, so genannte generalisierte interne Variablen eingeführt, welche zusammen mit ihren dualen Größen zusätzliche Freiheitsgrade bilden. Die Nichtlokalität kommt schließlich durch Berücksichtigung des Gradienten der generalisierten internen Variablen ins Spiel. Die vorgestellte Kontinuumstheorie wird schließlich auf die von-Mises Viskoplastizität angewandt. Zur Verhinderung von locking Effekten wurde basierend auf dem Hu-Washizu Prinzip eine gemischte FE-Formulierung mit erweiterten makroskopischen Verzerrungen realisiert. Numerische Beispiele stellen die Ergebnisse der lokalen und nichtlokalen Theorie gegenüber und machen die regularisierende Wirkung der gradientenerweiterten Theorie klar ersichtlich.

Contents

List of Figures

List of Tables

1. Basics of geometrically linear local continuum mechanics

In this chapter we give an introduction to classical geometrically linear local continuum thermodynamics. Starting from fundamental balance laws and the second law of thermodynamics, we will discuss some aspects of constitutive theory. We will also look at standard dissipative materials and will apply the concept to rate-independent and rate-dependent plasticity. The main references for the first three sections of this chapter are [1], [8], [16] and [27]. Most of the information in Section 1.4 is taken from [17] and [24].

1.1. Geometry and basic physical quantities

Let the material body under focus $\mathscr{B} \subset \mathbb{R}^3$ be a bounded and simply connected domain with sufficiently smooth boundary $\partial\mathscr{B}$. The body is assumed to be a continuous set of particles $\mathsf{x} \in \mathscr{B}$. The position of a particle x is given by the vector $\boldsymbol{x} = x_i \boldsymbol{e}_i$ with respect to a fixed cartesian coordinate system $\{x_i\}$ with basis vectors $\boldsymbol{e}_i$. The attention on the motion of the body under external loading will be restricted to a time intervall $\mathscr{T} = [0, T]$. The following kinematic quantities will be used throughout the text: the displacement field $\boldsymbol{u}(\boldsymbol{x}, t)\colon \mathscr{B} \times \mathscr{T} \to \mathbb{R}^3$, the velocity field

$$\boldsymbol{v}(\boldsymbol{x}, t)\colon \begin{cases} \mathscr{B} \times \mathscr{T} \to \mathbb{R}^3 \\ (\boldsymbol{x}, t) \mapsto \frac{\partial}{\partial t} \boldsymbol{u}(\boldsymbol{x}, t) \end{cases}$$

and the strain field

$$\boldsymbol{\varepsilon}(\boldsymbol{x}, t)\colon \begin{cases} \mathscr{B} \times \mathscr{T} \to Sym \\ (\boldsymbol{x}, t) \mapsto \frac{1}{2}\left[\nabla \boldsymbol{u} + (\nabla \boldsymbol{u})^T\right] \end{cases},$$

where Sym denotes the space of symmetric second order tensors. In the following the abbreviation $\dot{(\cdot)} := \frac{\partial}{\partial t}(\cdot)$ will be used.
Furthermore the existence of a traction field $\boldsymbol{t}(\boldsymbol{x}, t, \boldsymbol{n})\colon \mathscr{B} \times \mathscr{T} \times \mathbb{R}^3 \to \mathbb{R}^3$ is postulated, which represents the force acting on a surface element, the orientation of which is given by its normal vector $\boldsymbol{n}$. Cauchy's theorem states, that there exists a unique tensor field $\boldsymbol{\sigma}(\boldsymbol{x}, t)$, called stress tensor field, such that

$$\boldsymbol{t}(\boldsymbol{x}, t, \boldsymbol{n}) = \boldsymbol{\sigma}(\boldsymbol{x}, t)\boldsymbol{n}\,. \tag{1.1}$$

By using the balance of angular momentum it can be shown that $\boldsymbol{\sigma}(\boldsymbol{x}, t) \in Sym$.
At last the heat flux $q(\boldsymbol{x}, t, \boldsymbol{n})\colon \mathscr{B} \times \mathscr{T} \times \mathbb{R}^3 \to \mathbb{R}$ is introduced. In full analogy to Cauchy's theorem, the heat flux can be expressed by the linear relationship

$$q(\boldsymbol{x}, t, \boldsymbol{n}) = \boldsymbol{q}(\boldsymbol{x}, t) \cdot \boldsymbol{n}\,, \tag{1.2}$$

where $\boldsymbol{q}(\boldsymbol{x}, t)\colon \mathscr{B} \times \mathscr{T} \to \mathbb{R}^3$ denotes the heat flux vector.
For all further considerations all fields shall be assumed to be smooth enough.

1.2. Balance principles

Balance principles, which are the conservation of mass, the balance of linear and angular momentum and the first law of thermodynamics, must be fulfilled by every material. Furthermore the second law of thermodynamics, which is formulated by an inequality, is a fundamental requirement for every constitutive law.

1.2.1. Balance of mass

We assume that $\mathscr{V} \subset \mathscr{B}$ is a sufficiently smooth open set. The balance of mass postulates, that the temporal change of the total mass of the body $\mathscr{V}$ is zero:

$$\frac{\mathrm{d}}{\mathrm{d}t} \int_{\mathscr{V}} \rho \, \mathrm{d}v = 0 \,,$$

where $\rho(\boldsymbol{x}, t)$ denotes the mass density field. Because $\mathscr{V}$ is not time dependent in the linear theory, we can switch integration and differentiation, and obtain the local statement of balance of mass as

$$\frac{\mathrm{d}}{\mathrm{d}t} \rho(\boldsymbol{x}, t) = 0 \,.$$

Hence, we simply get $\rho = \rho_0$, where $\rho_0(\boldsymbol{x})$ is the initial mass density field.

1.2.2. Balance of linear momentum

Let $\mathscr{V} \subset \mathscr{B}$ be a sufficiently smooth open set. The linear momentum is defined by

$$\boldsymbol{J}(t) := \int_{\mathscr{V}} \rho \boldsymbol{v} \, \mathrm{d}v \,.$$

It is postulated, that the temporal change of the linear momentum equals the external forces acting on $\mathscr{V}$ and its boundary $\partial\mathscr{V}$:

$$\frac{\mathrm{d}}{\mathrm{d}t} \boldsymbol{J}(t) = \boldsymbol{F}_{ext} \,,$$

where the external forces consist of mass specific body forces, e.g. gravity acceleration, and boundary tractions:

$$\boldsymbol{F}_{ext} := \int_{\mathscr{V}} \rho \boldsymbol{f}^B \, \mathrm{d}v + \int_{\partial\mathscr{V}} \boldsymbol{t} \, \mathrm{d}s_{\boldsymbol{x}} \,.$$

Using the representation (1.1) and transforming the boundary integral into a volume integral by using Gauss' theorem, yields after localization Cauchy's equation of motion:

$$\mathrm{div}[\boldsymbol{\sigma}] + \rho \boldsymbol{f}^B = \rho \dot{\boldsymbol{v}} \tag{1.3}$$

for $(\boldsymbol{x}, t) \in \mathscr{V} \times \mathscr{T}$.

1.2.3. First law of thermodynamics

As before the open subset $\mathscr{V} \subset \mathscr{B}$ is assumed to be smooth enough. The first law of thermodynamics postulates the conservation of energy during a thermodynamic process. The temporal change of total energy $\mathcal{E}$ stored in the body $\mathscr{V}$ equals the sum of mechanical power P_{ext} of all external forces and the power Q due to heat flow:

$$\frac{\mathrm{d}}{\mathrm{d}t} \mathcal{E}(t) = P_{ext} + Q \,. \tag{1.4}$$

The total energy is the sum of the kinetic energy $\mathcal{K}$ and the internal energy $\mathcal{U}$, given by

$$\mathcal{K}(t) = \int_{\mathscr{V}} \frac{1}{2}\rho \boldsymbol{v}\cdot\boldsymbol{v}\,\mathrm{d}v \quad \text{and} \quad \mathcal{U}(t) = \int_{\mathscr{V}} \rho e\,\mathrm{d}v\,,$$

where $e(\boldsymbol{x},t)$ denotes the mass specific internal energy. The applied powers read

$$P_{ext} = \int_{\mathscr{V}} \rho \boldsymbol{f}^B\cdot\boldsymbol{v}\,\mathrm{d}v + \int_{\partial\mathscr{V}} \boldsymbol{t}\cdot\boldsymbol{v}\,\mathrm{d}s_{\boldsymbol{x}} \quad \text{and} \quad Q = \int_{\mathscr{V}} \rho r\,\mathrm{d}v - \int_{\partial\mathscr{V}} q\,\mathrm{d}s_{\boldsymbol{x}}\,,$$

where thermal power arises from internal heat sources, described by the mass specific quantity $r(\boldsymbol{x},t)$, and from heat flowing across the boundary. Here one should be aware of the minus sign which takes care of the fact, that an incoming heat flux, which after (1.2) forms an obtuse angle with the normal vector $\boldsymbol{n}$, must raise the total energy.
Transforming the surface integral arising in P_{ext} into a volume integral and using Cauchy's equation of motion (1.3), allows to rewrite the global balance of energy in terms of the internal stress power $P_{int} := -\int_{\mathscr{V}} \boldsymbol{\sigma} : \dot{\boldsymbol{\varepsilon}}\,\mathrm{d}v$ as

$$\frac{\mathrm{d}}{\mathrm{d}t}\mathcal{U}(t) = -P_{int} + Q\,, \tag{1.5}$$

or in local form

$$\rho\dot{e} = \boldsymbol{\sigma} : \dot{\boldsymbol{\varepsilon}} + \rho r - \mathrm{div}[\boldsymbol{q}] \tag{1.6}$$

for $(\boldsymbol{x},t) \in \mathscr{V}\times\mathscr{T}$. Insertion of (1.5) in (1.4) yields the global balance of mechanical energy

$$\frac{\mathrm{d}}{\mathrm{d}t}\mathcal{K}(t) = P_{ext} + P_{int}\,. \tag{1.7}$$

1.2.4. Second law of thermodynamics

Thermodynamic processes are not only restricted by the first law of thermodynamics, which does not give an information about the direction of a process, e.g. heat always flows from higher to lower temperature. To describe the latter and the irreversibility of a thermodynamic process, a new state variable, the entropy $\mathcal{S}$, is introduced. The second law of thermodynamics states, that the temporal change of the entropy is given by the sum of some entropy input S_{inp} across the boundary and some entropy production S_{pro} inside the body:

$$\frac{\mathrm{d}}{\mathrm{d}t}\mathcal{S}(t) = S_{inp} + S_{pro} \quad \text{with} \quad S_{pro} \geq 0\,,$$

where $S_{pro} = 0$ for reversible processes. The entropy can be written in terms of the mass specific entropy $\eta(\boldsymbol{x},t)$ as

$$\mathcal{S}(t) = \int_{\mathscr{V}} \rho\eta\,\mathrm{d}v$$

and the entropy inputs are given by

$$S_{inp} = \int_{\mathscr{V}} \frac{\rho r}{\theta}\,\mathrm{d}v - \int_{\partial\mathscr{V}} \frac{\boldsymbol{q}\cdot\boldsymbol{n}}{\theta}\,\mathrm{d}s_{\boldsymbol{x}} \quad \text{and} \quad S_{pro} = \int_{\mathscr{V}} \frac{d}{\theta}\,\mathrm{d}v\,,$$

where $d(\boldsymbol{x},t)$ denotes the dissipation power density and $\theta(\boldsymbol{x},t)$ the absolute temperature which must be strictly positive for all $(\boldsymbol{x},t) \in \mathscr{V}\times\mathscr{T}$. Incorporation of (1.6) gives after localization the so called Clausius-Duhem inequality:

$$d = \boldsymbol{\sigma} : \dot{\boldsymbol{\varepsilon}} - \rho\dot{e} + \theta\rho\dot{\eta} - \boldsymbol{q}\cdot\nabla\ln[\theta] \geq 0 \tag{1.8}$$

for $(\boldsymbol{x},t) \in \mathscr{V} \times \mathscr{T}$. Introducing the local dissipation power density $d_{loc} := \boldsymbol{\sigma} : \dot{\boldsymbol{\varepsilon}} - \rho\dot{e} + \theta\rho\dot{\eta}$, which describes the local internal dissipation, and the conductive dissipation power density $d_{cond} := -\boldsymbol{q} \cdot \nabla \ln[\theta]$, which describes the dissipation due to heat conduction, the stronger restrictions

$$d_{loc} \geq 0 \quad \text{and} \quad d_{cond} \geq 0 \tag{1.9}$$

are assumed. The first inequality is known as Clausius-Planck inequality and the second one as Fourier inequality. Looking at $(1.9)_1$ a good parametrisation for the specific internal energy would be $e = e(\boldsymbol{\varepsilon}, \eta)$, and we obtain from $(1.9)_1$ the relations $\theta = \partial_\eta e$ and $\boldsymbol{\sigma} = \rho\partial_{\boldsymbol{\varepsilon}} e$. However, since the entropy is a state variable which is difficult to handle practically, the so called Helmholtz free energy $\bar{\psi}$ is introduced via a Legendre transformation

$$\bar{\psi}(\boldsymbol{\varepsilon}, \theta) := \min_{\eta} \{e(\boldsymbol{\varepsilon}, \eta) - \theta\eta\} = e(\boldsymbol{\varepsilon}, \eta(\theta)) - \theta\eta(\theta)\,,$$

see Definition 5 in Appendix A. In an analogue way, one can also derive other thermodynamic potentials like the Gibbs free enthalpy $\bar{\varphi} = \bar{\varphi}(\boldsymbol{\sigma}, \theta)$ and the enthalpy $\bar{h} = \bar{h}(\boldsymbol{\sigma}, \eta)$. Rewriting (1.8) in terms of $\bar{\psi}$ gives

$$d = \boldsymbol{\sigma} : \dot{\boldsymbol{\varepsilon}} - \rho\dot{\bar{\psi}} - \rho\dot{\theta}\eta - \boldsymbol{q} \cdot \nabla \ln[\theta] \geq 0 \tag{1.10}$$

for $(\boldsymbol{x},t) \in \mathscr{V} \times \mathscr{T}$.

1.3. Coleman-Noll procedure

To ensure physical and mathematical consistence, constitutive equations have to fulfil several assumptions. The most important of them are

1. the principle of equipresence,
2. the principle of material objectivity and
3. the principle of thermodynamic consistence.

Principle of equipresence
This principle states, that all constitutive laws of the material model must contain the same set of independent variables, unless constraints are given by some physical rule or some invariance rule. Let the constitutive state be chosen as

$$\mathfrak{c}_t := \{\boldsymbol{u}, \nabla\boldsymbol{u}, \theta, \nabla\theta\}\ ,$$

and let a set of internal variables $\boldsymbol{\mathcal{I}}(\boldsymbol{x},t)$ be taken into account, which describe dissipative processes in the body, e.g. plastification, damage, ... Since the internal variables are additional unknown fields, additional equations in form of evolution equations are needed together with some initial conditions[1]. The principle of equipresence demands

$$\bar{\psi} = \bar{\psi}(\mathfrak{c}_t, \boldsymbol{\mathcal{I}})\,, \quad \boldsymbol{\sigma} = \boldsymbol{\sigma}(\mathfrak{c}_t, \boldsymbol{\mathcal{I}})\,, \quad \eta = \eta(\mathfrak{c}_t, \boldsymbol{\mathcal{I}}) \quad \text{and} \quad \boldsymbol{q} = \boldsymbol{q}(\mathfrak{c}_t, \boldsymbol{\mathcal{I}})\,.$$

Principle of material objectivity
This principle states, that constitutive laws are not allowed to depend on the choice or on the motion of the reference frame. As an example we look at the Helmholtz free energy $\bar{\psi}$.

[1] It will be seen later that, depending on the constitutive model, we may also have to take into account boundary conditions for the internal variables.

The principle of material objectivity demands the invariance of $\bar{\psi}(\mathfrak{c}_t, \boldsymbol{\mathcal{I}})$ under rigid body motions, this means

$$\bar{\psi}(\mathfrak{c}_t^+, \boldsymbol{\mathcal{I}}^+) = \bar{\psi}(\mathfrak{c}_t, \boldsymbol{\mathcal{I}})$$

with $\mathfrak{c}_t^+ := \{\boldsymbol{u}^+, \nabla\boldsymbol{u}^+, \theta^+, \nabla\theta^+\}$ being a collection of the transformed states

$$\begin{aligned} \boldsymbol{u}^+(\boldsymbol{x}, t) &:= \boldsymbol{u}(\boldsymbol{x}, t) + \boldsymbol{c}(t) + \boldsymbol{Q}(t)\boldsymbol{x}\,, \\ \theta^+(\boldsymbol{x}, t) &:= \theta(\boldsymbol{x}, t)\,, \end{aligned}$$

where $\boldsymbol{c}(t)\colon \mathscr{T} \to \mathbb{R}^3$ describes a translation and $\boldsymbol{Q}(t)\colon \mathscr{T} \to \mathbb{R}^{3\times 3}$ a rotation with $\boldsymbol{Q}(t) = -[\boldsymbol{Q}(t)]^T$ and $\det[\boldsymbol{Q}(t)] = 1$ for all $t \in \mathscr{T}$. It is immediately seen that $\bar{\psi}$ cannot depend on $\boldsymbol{u}$ explicitly. Every second order tensor can be decomposed into a symmetric and a skew symmetric tensor, i.e.

$$\begin{aligned} \nabla\boldsymbol{u}^+ &= \mathrm{Sym}[\nabla\boldsymbol{u}^+] + \mathrm{Skew}[\nabla\boldsymbol{u}^+] \\ &= \mathrm{Sym}[\nabla\boldsymbol{u}] + \mathrm{Sym}[\boldsymbol{Q}] + \mathrm{Skew}[\nabla\boldsymbol{u}] + \mathrm{Skew}[\boldsymbol{Q}]\,, \end{aligned}$$

and we see that $\mathrm{Sym}[\nabla\boldsymbol{u}^+] = \mathrm{Sym}[\nabla\boldsymbol{u}]$ due to $\mathrm{Sym}[\boldsymbol{Q}] = 0$. This means that $\bar{\psi}$ cannot depend on $\mathrm{Skew}[\nabla\boldsymbol{u}]$ but on $\mathrm{Sym}[\nabla\boldsymbol{u}] = \boldsymbol{\varepsilon}$. Therefore, together with $\boldsymbol{\mathcal{I}}$ the new constitutive state is

$$\mathfrak{c} := \{\boldsymbol{\varepsilon}, \theta, \nabla\theta\}\ .$$

Of course it is assumed that the chosen internal variables $\boldsymbol{\mathcal{I}}$ are in agreement with the principle of material objectivity.
Because needed soon, the time derivative of $\bar{\psi}$ reads

$$\dot{\bar{\psi}} = \partial_{\boldsymbol{\varepsilon}}\bar{\psi} : \dot{\boldsymbol{\varepsilon}} + \partial_\theta\bar{\psi}\cdot\dot{\theta} + \partial_{\nabla\theta}\bar{\psi}\cdot\nabla\dot{\theta} + \partial_{\boldsymbol{\mathcal{I}}}\bar{\psi}\cdot\dot{\boldsymbol{\mathcal{I}}}\,, \tag{1.11}$$

where of course in the last term, depending on the mathematical nature of the internal variables (scalar, vector or tensor of higher order), the appropriate multiplication must be chosen.

Principle of thermodynamic consistence

As pointed out before, it is a crucial point for a constitutive law to be consistent with the second law of thermodynamics. Therefore the Clausius-Duhem inequality (1.10) must be fulfilled for all processes $\boldsymbol{u}(\boldsymbol{x}, t)$ and $\theta(\boldsymbol{x}, t)$ for all $(\boldsymbol{x}, t) \in \mathscr{V} \times \mathscr{T}$. Inserting (1.11) into (1.10) gives with the definition $\psi := \rho\bar{\psi}$

$$d = (\boldsymbol{\sigma} - \partial_{\boldsymbol{\varepsilon}}\psi) : \dot{\boldsymbol{\varepsilon}} - (\rho\eta + \partial_\theta\psi)\,\dot{\theta} - \partial_{\nabla\theta}\psi\cdot\nabla\dot{\theta} - \boldsymbol{q}\cdot\nabla\ln[\theta] - \partial_{\boldsymbol{\mathcal{I}}}\psi\cdot\dot{\boldsymbol{\mathcal{I}}} \geq 0\,. \tag{1.12}$$

From a physical point of view it is clear, that $\boldsymbol{\varepsilon}$ and $\dot{\boldsymbol{\varepsilon}}$, θ and $\dot{\theta}$, and $\nabla\theta$ and $\nabla\dot{\theta}$ can be controlled independently. As a result every single term of the first three terms in (1.12) can be positive or negative. In order to fulfil (1.12) it is maybe obvious to claim

$$\boldsymbol{\sigma} = \partial_{\boldsymbol{\varepsilon}}\psi\,, \quad \eta = -\frac{1}{\rho}\partial_\theta\psi \quad \text{and} \quad \partial_{\nabla\theta}\psi = 0\,.$$

The last condition states, that ψ is not allowed to be a function of $\nabla\theta$. Using the Fourier inequality $(1.9)_2$ one now obtains from (1.12) the so called reduced dissipation inequality

$$\boldsymbol{\mathcal{F}}\cdot\dot{\boldsymbol{\mathcal{I}}} \geq 0 \quad \text{with} \quad \boldsymbol{\mathcal{F}} := -\partial_{\boldsymbol{\mathcal{I}}}\psi(\boldsymbol{\varepsilon}, \theta, \boldsymbol{\mathcal{I}})\,, \tag{1.13}$$

which has to be fulfilled for all $(\boldsymbol{x}, t) \in \mathscr{V} \times \mathscr{T}$ by every evolution law for the internal variables. The defined quantity $\boldsymbol{\mathcal{F}}$ is in some sense responsible for the temporal change of the internal variables $\boldsymbol{\mathcal{I}}$ and is therefore called thermodynamic driving force conjugate to $\boldsymbol{\mathcal{I}}$.

For all further considerations the temperature field $\theta(\boldsymbol{x}, t)$ is assumed to be homogeneous and constant in time. From now on we will also look at the whole body $\mathscr{B}$ when formulating global equations.

1.4. Standard dissipative solids

In standard dissipative materials the evolution law for $\boldsymbol{\mathcal{I}}$ is governed by a scalar dissipation potential function ϕ, which is assumed to depend on $\dot{\boldsymbol{\mathcal{I}}}$. Let two linear functionals be introduced as

$$\Psi(\boldsymbol{\varepsilon}, \boldsymbol{\mathcal{I}}) := \int_{\mathscr{V}} \psi(\boldsymbol{\varepsilon}, \boldsymbol{\mathcal{I}}) \, \mathrm{d}v \quad \text{and} \quad \Phi(\dot{\boldsymbol{\mathcal{I}}}) := \int_{\mathscr{V}} \phi(\dot{\boldsymbol{\mathcal{I}}}) \, \mathrm{d}v \,,$$

where the first one describes the energy storage due to deformation and is therefore called stored energy functional, and where the second one describes the dissipation due to internal mechanisms and is therefore called dissipation potential functional.
We now define the internal rate potential per unit volume

$$\pi(\boldsymbol{\varepsilon}, \boldsymbol{\mathcal{I}}, \dot{\boldsymbol{\varepsilon}}, \dot{\boldsymbol{\mathcal{I}}}) := \frac{\mathrm{d}}{\mathrm{d}t} \psi(\boldsymbol{\varepsilon}, \boldsymbol{\mathcal{I}}) + \phi(\dot{\boldsymbol{\mathcal{I}}}) \,.$$

The functions ψ and ϕ are related through Biot's constitutive differential equation

$$\partial_{\boldsymbol{\mathcal{I}}} \psi(\boldsymbol{\varepsilon}, \boldsymbol{\mathcal{I}}) + \partial_{\dot{\boldsymbol{\mathcal{I}}}} \phi(\dot{\boldsymbol{\mathcal{I}}}) = 0$$

for $(\boldsymbol{x}, t) \in \mathscr{B} \times \mathscr{T}$, see [17] and the references therein. This allows the thermodynamic driving force to be written as $\boldsymbol{\mathcal{F}} = \partial_{\dot{\boldsymbol{\mathcal{I}}}} \phi(\dot{\boldsymbol{\mathcal{I}}})$. Then the reduced dissipation inequality (1.13) reads

$$d = \partial_{\dot{\boldsymbol{\mathcal{I}}}} \phi(\dot{\boldsymbol{\mathcal{I}}}) \cdot \dot{\boldsymbol{\mathcal{I}}} \geq 0 \tag{1.14}$$

for $(\boldsymbol{x}, t) \in \mathscr{B} \times \mathscr{T}$, which restricts the dissipation function ϕ. Assuming ϕ to be convex with respect to $\dot{\boldsymbol{\mathcal{I}}}$, see Definition 2 in Appendix A, we get, according to Lemma 2 in Appendix A, $d \geq \phi(\dot{\boldsymbol{\mathcal{I}}}) - \phi(\boldsymbol{0})$ for all $\dot{\boldsymbol{\mathcal{I}}}$. From this we can immediately see, that (1.14) is automatically fulfilled if $\phi(\dot{\boldsymbol{\mathcal{I}}}) \geq 0$ for all $\dot{\boldsymbol{\mathcal{I}}}$ and $\phi(\boldsymbol{0}) = 0$.
In summary the internal stress power can be written as

$$P_{int} = -\int_{\mathscr{B}} \dot{\psi} \, \mathrm{d}v - \int_{\mathscr{B}} d \, \mathrm{d}v = -\dot{\Psi} - \mathcal{D} \quad \text{with} \quad \mathcal{D} := \int_{\mathscr{B}} \partial_{\dot{\boldsymbol{\mathcal{I}}}} \phi(\dot{\boldsymbol{\mathcal{I}}}) \cdot \dot{\boldsymbol{\mathcal{I}}} \, \mathrm{d}v \tag{1.15}$$

being the dissipation power.
Let us further look at the case, when ϕ is a positively homogeneous function of order one, this means $\phi(\alpha \dot{\boldsymbol{\mathcal{I}}}) = \alpha \phi(\dot{\boldsymbol{\mathcal{I}}})$ for all $\alpha \in \mathbb{R}_+$, see Definition 7 in Appendix A. Such a type of ϕ, e.g., occurs for rate-independent plasticity, and we get after differentiation with respect to α an easy relation between d and ϕ, namely

$$d = \partial_{\dot{\boldsymbol{\mathcal{I}}}} \phi(\dot{\boldsymbol{\mathcal{I}}}) \cdot \dot{\boldsymbol{\mathcal{I}}} = \phi(\dot{\boldsymbol{\mathcal{I}}}) \,, \tag{1.16}$$

where $\partial_{\dot{\boldsymbol{\mathcal{I}}}}(\cdot)$ has to be understood as sub-differential since ϕ is not differentiable in $\dot{\boldsymbol{\mathcal{I}}} = 0$ in the classical sense, see [3] and [21]. We observe that for the fulfilment of (1.14) only the condition $\phi(\dot{\boldsymbol{\mathcal{I}}}) \geq 0$ has to be enforced; from (1.16) we immediately get $\phi(\boldsymbol{0}) = 0$, and for an arbitrary but fixed $\boldsymbol{\mathcal{F}}$ we have $\phi(\dot{\boldsymbol{\mathcal{I}}}_1 + \dot{\boldsymbol{\mathcal{I}}}_2) = \boldsymbol{\mathcal{F}} \dot{\boldsymbol{\mathcal{I}}}_1 + \boldsymbol{\mathcal{F}} \dot{\boldsymbol{\mathcal{I}}}_2 = \phi(\dot{\boldsymbol{\mathcal{I}}}_1) + \phi(\dot{\boldsymbol{\mathcal{I}}}_2)$ and hence convexity follows from Lemma 5 in Appendix A. Later it will be helpful to introduce the dual dissipation function, which is defined via a Legendre transformation

$$\phi^*(\boldsymbol{\mathcal{F}}) := \max_{\dot{\boldsymbol{\mathcal{I}}}} \{ \boldsymbol{\mathcal{F}} \cdot \dot{\boldsymbol{\mathcal{I}}} - \phi(\dot{\boldsymbol{\mathcal{I}}}) \} \,.$$

Since ϕ is convex with respect to $\dot{\boldsymbol{\mathcal{I}}}$, this transformation is involutoric. This means the dual of the dual dissipation function is the dissipation function itself, i.e.

$$\phi(\dot{\boldsymbol{\mathcal{I}}}) = \max_{\boldsymbol{\mathcal{F}}} \{ \boldsymbol{\mathcal{F}} \cdot \dot{\boldsymbol{\mathcal{I}}} - \phi^*(\boldsymbol{\mathcal{F}}) \} \,, \tag{1.17}$$

see Lemma 3 in Appendix A.

1.4.1. Application to plasticity

Plasticity always comes along with dissipation. First we look at the rate-independent case. Let all admissible states in the space of thermodynamic driving forces $\boldsymbol{\mathcal{F}}$ be defined by the set

$$\mathbb{E}_{\boldsymbol{\mathcal{F}}}(\boldsymbol{\mathcal{I}}) := \left\{ \bar{\boldsymbol{\mathcal{F}}} \colon \varphi(\bar{\boldsymbol{\mathcal{F}}}, \boldsymbol{\mathcal{I}}) \leq 0 \quad \text{for a given } \boldsymbol{\mathcal{I}} \right\} ,$$

where $\varphi(\bar{\boldsymbol{\mathcal{F}}}, \boldsymbol{\mathcal{I}})$ is called yield function. The elastic domain is given by the interior of $\mathbb{E}_{\boldsymbol{\mathcal{F}}}(\boldsymbol{\mathcal{I}})$ defined as

$$\mathrm{int}[\mathbb{E}_{\boldsymbol{\mathcal{F}}}(\boldsymbol{\mathcal{I}})] := \left\{ \bar{\boldsymbol{\mathcal{F}}} \colon \varphi(\bar{\boldsymbol{\mathcal{F}}}, \boldsymbol{\mathcal{I}}) < 0 \quad \text{for a given } \boldsymbol{\mathcal{I}} \right\} .$$

Therefore a plastic state is only reached on the yield surface $\partial\mathbb{E}_{\boldsymbol{\mathcal{F}}}(\boldsymbol{\mathcal{I}}) = \mathbb{E}_{\boldsymbol{\mathcal{F}}}(\boldsymbol{\mathcal{I}}) \backslash \mathrm{int}[\mathbb{E}_{\boldsymbol{\mathcal{F}}}(\boldsymbol{\mathcal{I}})]$.

Remark 1. If the yield function $\varphi(\bar{\boldsymbol{\mathcal{F}}}, \boldsymbol{\mathcal{I}})$ is convex with respect to $\bar{\boldsymbol{\mathcal{F}}}$, then $\mathbb{E}_{\boldsymbol{\mathcal{F}}}(\boldsymbol{\mathcal{I}})$ is a convex set. This shall be shown here. Due to Definition 2 in Appendix A, we have

$$\varphi(\lambda\bar{\boldsymbol{\mathcal{F}}}_1 + (1-\lambda)\bar{\boldsymbol{\mathcal{F}}}_2, \boldsymbol{\mathcal{I}}) \leq \lambda\varphi(\bar{\boldsymbol{\mathcal{F}}}_1, \boldsymbol{\mathcal{I}}) + (1-\lambda)\varphi(\bar{\boldsymbol{\mathcal{F}}}_2, \boldsymbol{\mathcal{I}})$$

for all $\lambda \in [0,1]$ and for all $\bar{\boldsymbol{\mathcal{F}}}_1, \bar{\boldsymbol{\mathcal{F}}}_2 \in \mathbb{E}_{\boldsymbol{\mathcal{F}}}(\boldsymbol{\mathcal{I}})$. We get $\varphi(\lambda\bar{\boldsymbol{\mathcal{F}}}_1 + (1-\lambda)\bar{\boldsymbol{\mathcal{F}}}_2, \boldsymbol{\mathcal{I}}) \leq 0$, and accordingly $\mathbb{E}_{\boldsymbol{\mathcal{F}}}(\boldsymbol{\mathcal{I}})$ is a convex set, see Definition 1 in Appendix A.

In order to derive the dissipation function ϕ we make use of a very important principle - the principle of maximum plastic dissipation. It demands that the actual thermodynamic driving force $\boldsymbol{\mathcal{F}} \in \mathbb{E}_{\boldsymbol{\mathcal{F}}}(\boldsymbol{\mathcal{I}})$ maximizes the plastic dissipation power density $d_p := d = \bar{\boldsymbol{\mathcal{F}}} \cdot \dot{\boldsymbol{\mathcal{I}}}$ with a given rate $\dot{\boldsymbol{\mathcal{I}}}$. So $\boldsymbol{\mathcal{F}}$ can be derived through the constrained optimization problem

$$\boldsymbol{\mathcal{F}} = \underset{\bar{\boldsymbol{\mathcal{F}}} \in \mathbb{E}_{\boldsymbol{\mathcal{F}}}(\boldsymbol{\mathcal{I}})}{\arg\max} [\bar{\boldsymbol{\mathcal{F}}} \cdot \dot{\boldsymbol{\mathcal{I}}}] \quad \text{and} \quad \boldsymbol{\mathcal{F}} = \underset{\bar{\boldsymbol{\mathcal{F}}} \in \mathbb{E}_{\boldsymbol{\mathcal{F}}}(\boldsymbol{\mathcal{I}})}{\arg\min} [-\bar{\boldsymbol{\mathcal{F}}} \cdot \dot{\boldsymbol{\mathcal{I}}}] , \tag{1.18}$$

respectively, for $\boldsymbol{\mathcal{I}}$ being given. Since for rate-independent plasticity $d = \phi$, the dissipation function at the actual admissible state can be obtained by the same task:

$$\phi(\dot{\boldsymbol{\mathcal{I}}}) = \max_{\bar{\boldsymbol{\mathcal{F}}} \in \mathbb{E}_{\boldsymbol{\mathcal{F}}}(\boldsymbol{\mathcal{I}})} \{\bar{\boldsymbol{\mathcal{F}}} \cdot \dot{\boldsymbol{\mathcal{I}}}\} ,$$

which gives by comparison with (1.17) $\phi^*(\boldsymbol{\mathcal{F}}) = 0$ for $\varphi(\boldsymbol{\mathcal{F}}, \boldsymbol{\mathcal{I}}) \leq 0$. Assuming $(1.18)_2$ to have one optimal solution, the principle of maximum plastic dissipation implies

1. the evolution law for $\boldsymbol{\mathcal{I}}$,
2. the Karush-Kuhn-Tucker conditions (in short KKT conditions) and
3. the convexity of $\mathbb{E}_{\boldsymbol{\mathcal{F}}}(\boldsymbol{\mathcal{I}})$,

see [24]. To show point 1, we introduce the Lagrangian functional $\mathcal{L}(\bar{\boldsymbol{\mathcal{F}}}, \boldsymbol{\mathcal{I}}, \lambda) := -\bar{\boldsymbol{\mathcal{F}}} \cdot \dot{\boldsymbol{\mathcal{I}}} + \lambda\varphi(\bar{\boldsymbol{\mathcal{F}}}, \boldsymbol{\mathcal{I}})$, where $\lambda \in \mathbb{R}$ is the Lagrange multiplier, and obtain the wanted evolution law for the internal variables as

$$\partial_{\boldsymbol{\mathcal{F}}}\mathcal{L}(\boldsymbol{\mathcal{F}}, \boldsymbol{\mathcal{I}}, \lambda) = 0 \quad \Leftrightarrow \quad \dot{\boldsymbol{\mathcal{I}}} = \lambda\partial_{\boldsymbol{\mathcal{F}}}\varphi(\boldsymbol{\mathcal{F}}, \boldsymbol{\mathcal{I}}) . \tag{1.19}$$

To get some information about the Lagrange multiplier λ we do a case-by-case analysis. If $\varphi(\boldsymbol{\mathcal{F}}, \boldsymbol{\mathcal{I}}) < 0$, the constraint $\boldsymbol{\mathcal{F}} \in \mathbb{E}_{\boldsymbol{\mathcal{F}}}(\boldsymbol{\mathcal{I}})$ has no influence on the solution $\boldsymbol{\mathcal{F}}$, see Figure 1.1(b). Therefore we can say $\lambda = 0$. On the other hand, if $\varphi(\boldsymbol{\mathcal{F}}, \boldsymbol{\mathcal{I}}) = 0$ we have $\lambda \neq 0$ in general, see Figure 1.1(c). This leads to the condition $\lambda\varphi(\boldsymbol{\mathcal{F}}, \boldsymbol{\mathcal{I}}) = 0$. Next, we look at the evolution law $(1.19)_2$ rewritten as $\partial_{\boldsymbol{\mathcal{F}}}[-d_p(\boldsymbol{\mathcal{F}}, \boldsymbol{\mathcal{I}})] = \lambda\partial_{\boldsymbol{\mathcal{F}}}\varphi(\boldsymbol{\mathcal{F}}, \boldsymbol{\mathcal{I}})$. The emerging partial derivatives are vectors lying normal to the surfaces $\varphi(\bar{\boldsymbol{\mathcal{F}}}, \boldsymbol{\mathcal{I}})$, and $-d_p(\bar{\boldsymbol{\mathcal{F}}}, \dot{\boldsymbol{\mathcal{I}}})$ in

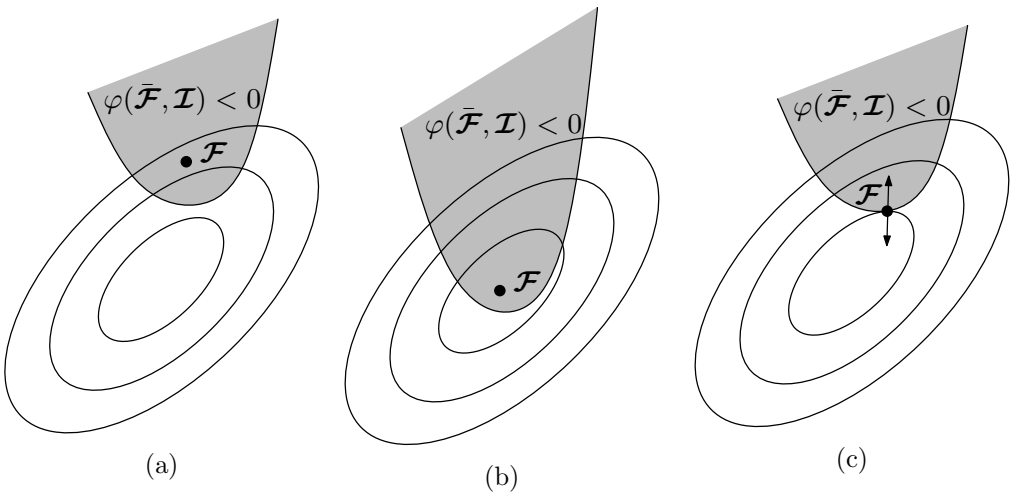

Figure 1.1. Derivation of the KKT conditions: (a) impossible situation, (b) solution for $\varphi(\boldsymbol{\mathcal{F}},\boldsymbol{\mathcal{I}}) < 0$, (c) solution for $\varphi(\boldsymbol{\mathcal{F}},\boldsymbol{\mathcal{I}}) = 0$.

point $\boldsymbol{\mathcal{F}}$, see Figure 1.1(c), which is the reason why the evolution law $(1.19)_2$ is often called normality rule. Since these normal vectors have the same direction but different orientation, the Lagrange multiplier must be positive. So we conclude

$$\lambda \geq 0\,, \quad \varphi(\boldsymbol{\mathcal{F}},\boldsymbol{\mathcal{I}}) \leq 0 \quad \text{and} \quad \lambda\varphi(\boldsymbol{\mathcal{F}},\boldsymbol{\mathcal{I}}) = 0\,, \tag{1.20}$$

which are the well known KKT conditions. Physically spoken, these conditions are nothing else then the loading/unloading conditions, see [6].

Remark 2. Note, that the function which has to minimized, namely $-d_p$, is linear (and therefore convex) in $\bar{\boldsymbol{\mathcal{F}}}$. Hence, $\boldsymbol{\mathcal{F}}$ can only lie on the boundary $\partial\mathbb{E}_{\boldsymbol{\mathcal{F}}}(\boldsymbol{\mathcal{I}})$, which is in agreement with our assumption that plastic states are only reached on the yield surface.

It remains to show point 3. According to Lemma 2 in Appendix A, an equivalent condition for the yield function φ to be convex is

$$\varphi(\bar{\boldsymbol{\mathcal{F}}}_1,\boldsymbol{\mathcal{I}}) - \varphi(\bar{\boldsymbol{\mathcal{F}}}_2,\boldsymbol{\mathcal{I}}) \geq \partial_{\bar{\boldsymbol{\mathcal{F}}}_2}\varphi(\bar{\boldsymbol{\mathcal{F}}}_2,\boldsymbol{\mathcal{I}}) \cdot (\bar{\boldsymbol{\mathcal{F}}}_1 - \bar{\boldsymbol{\mathcal{F}}}_2) \tag{1.21}$$

for all $\bar{\boldsymbol{\mathcal{F}}}_1, \bar{\boldsymbol{\mathcal{F}}}_2 \in \mathbb{E}_{\boldsymbol{\mathcal{F}}}(\boldsymbol{\mathcal{I}})$. It is sufficient to set $\bar{\boldsymbol{\mathcal{F}}}_2 = \boldsymbol{\mathcal{F}}$ with $\varphi(\boldsymbol{\mathcal{F}},\boldsymbol{\mathcal{I}}) = 0$ and the convexity condition (1.21) reduces to

$$0 \geq (\bar{\boldsymbol{\mathcal{F}}} - \boldsymbol{\mathcal{F}}) \cdot \partial_{\boldsymbol{\mathcal{F}}}\varphi(\boldsymbol{\mathcal{F}},\boldsymbol{\mathcal{I}}) \tag{1.22}$$

for all $\bar{\boldsymbol{\mathcal{F}}} \in \mathbb{E}_{\boldsymbol{\mathcal{F}}}(\boldsymbol{\mathcal{I}})$. From the principle of maximum plastic dissipation we have $\boldsymbol{\mathcal{F}}\cdot\dot{\boldsymbol{\mathcal{I}}} \geq \bar{\boldsymbol{\mathcal{F}}}\cdot\dot{\boldsymbol{\mathcal{I}}}$ for all $\bar{\boldsymbol{\mathcal{F}}} \in \mathbb{E}_{\boldsymbol{\mathcal{F}}}(\boldsymbol{\mathcal{I}})$ and incorporating the evolution law $(1.19)_2$ yields

$$0 \geq \lambda(\bar{\boldsymbol{\mathcal{F}}} - \boldsymbol{\mathcal{F}}) \cdot \partial_{\boldsymbol{\mathcal{F}}}\varphi(\boldsymbol{\mathcal{F}},\boldsymbol{\mathcal{I}})$$

for all $\bar{\boldsymbol{\mathcal{F}}} \in \mathbb{E}_{\boldsymbol{\mathcal{F}}}(\boldsymbol{\mathcal{I}})$. From the KKT conditions we have $\lambda \geq 0$ and accordingly we obtain (1.22). Finally, the convexity of $\mathbb{E}_{\boldsymbol{\mathcal{F}}}(\boldsymbol{\mathcal{I}})$ follows from Remark 1.

In summary, the principle of maximum plastic dissipation is a convex optimization problem, see [3] for the mathematical background.

Remark 3. If the convex function which has to be minimized or the convex function occurring in the inequality constraint has cones, e.g. one thinks about Tresca's yield surface [6], sub-differentials must be used.

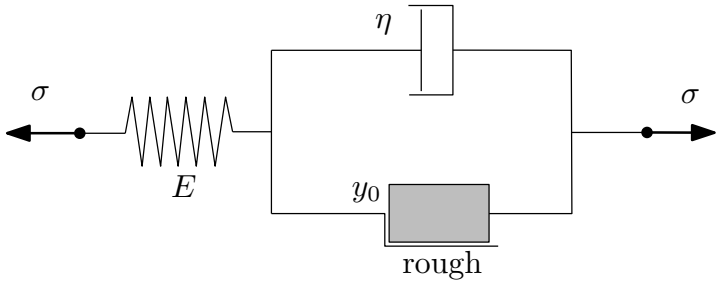

Figure 1.2. One-dimensional model of viscoplasticity, with E being Young's modulus, η being the viscosity and y_0 being the yield stress.

In rate-dependent plasticity states $\boldsymbol{\mathcal{F}}$ outside the closure of the elastic domain are allowed. In the one dimensional rheological model the rate-dependency can be taken into account by a dashpot with viscosity $\eta \in (0, \infty)$, see Figure 1.2.
As pointed out in [24] viscoplasticity can be interpreted as a regularization. The viscosity plays the rule of a penalty factor and the principle of maximum plastic dissipation can be written as an unconstrained optimization problem:

$$\phi(\dot{\boldsymbol{\mathcal{I}}}) = \max_{\bar{\boldsymbol{\mathcal{F}}}} \{ \bar{\boldsymbol{\mathcal{F}}} \cdot \dot{\boldsymbol{\mathcal{I}}} - \frac{1}{2\eta} \langle \varphi(\bar{\boldsymbol{\mathcal{F}}}, \boldsymbol{\mathcal{I}}) \rangle^2 \} \,, \tag{1.23}$$

where $\langle \cdot \rangle$ depicts the so called Macaulay brackets $\langle x \rangle := \frac{1}{2}(x + |x|)$ for $x \in \mathbb{R}$. Details can be found in [20]. In an analogous way as before, we obtain the evolution law for the internal variables as

$$\dot{\boldsymbol{\mathcal{I}}} = \frac{1}{\eta} \langle \varphi(\boldsymbol{\mathcal{F}}, \boldsymbol{\mathcal{I}}) \rangle \partial_{\boldsymbol{\mathcal{F}}} \varphi(\boldsymbol{\mathcal{F}}, \boldsymbol{\mathcal{I}}) \,. \tag{1.24}$$

A comparison with (1.19) identifies the Lagrange multiplier as $\lambda = \frac{1}{\eta} \langle \varphi(\boldsymbol{\mathcal{F}}, \boldsymbol{\mathcal{I}}) \rangle$, which of course cannot be negative.

2. Geometrically linear continuum mechanics of gradient-type dissipative solids

In this chapter the theory of gradient-extended standard dissipative solids is presented. For this purpose the major sources are [28] and [18]. We will see, that so called generalized internal variables lead to an additional elliptic partial differential equation, which makes it necessary to prescribe boundary conditions for the generalized internal variables. After the derivation of the rate-dependent strong form of the full coupled system of equations by using the balance of mechanical energy (1.7), we will switch to an equivalent potential formulation. The time incremental formulation of this potential will be consistent with the strong form. Finally, we do a discretization by finite elements, see [30] and [29].

2.1. Geometry

The macroscopic setting has already been stated in Section 1.1. However, here we also look at some additional microscopic fields, which describe the microscopic state of the solid. To distinguish between the two scales we introduce the notation $\bar{(\cdot)}(\boldsymbol{x},t)$ for the macroscopic fields and the notation $\check{(\cdot)}(\boldsymbol{x},t)$ for the microscopic fields. We define the microscopic deformation map

$$\check{\boldsymbol{\varphi}}(\boldsymbol{x},t)\colon \begin{cases} \mathscr{B}\times\mathscr{T}\to\mathbb{R}^m \\ (\boldsymbol{x},t)\mapsto \check{\boldsymbol{u}}(\boldsymbol{x},t)\,, \end{cases}$$

with $m\in\mathbb{N}$, see Figure 2.1. The array $\check{\boldsymbol{u}}$ is called microscopic displacement and consists of m scalars, which describe dissipative processes in the material and can therefore be seen as internal variables. However, in contrast to standard internal variables, $\check{\boldsymbol{u}}$ is also affected by additional balance equations, which makes it also necessary to prescribe boundary conditions for $\check{\boldsymbol{u}}$. This circumstance is the reason to call $\check{\boldsymbol{u}}$ an array of generalized internal variables. The fact that we are following a multi-field approach here, demands different decompositions of the boundary $\partial\mathscr{B}$. They are $\partial\mathscr{B}=\overline{\partial\mathscr{B}}_{\bar{\boldsymbol{u}}}\cup\overline{\partial\mathscr{B}}_{\bar{\boldsymbol{t}}}$, $\partial\mathscr{B}_{\bar{\boldsymbol{u}}}\cap\partial\mathscr{B}_{\bar{\boldsymbol{t}}}=\emptyset$ and $\partial\mathscr{B}=\overline{\partial\mathscr{B}}_{\check{\boldsymbol{u}}}\cup\overline{\partial\mathscr{B}}_{\check{\boldsymbol{t}}}$, $\partial\mathscr{B}_{\check{\boldsymbol{u}}}\cap\partial\mathscr{B}_{\check{\boldsymbol{t}}}=\emptyset$, where on $\partial\mathscr{B}_{\bar{\boldsymbol{u}}}$ and $\partial\mathscr{B}_{\check{\boldsymbol{u}}}$ the macroscopic and microscopic displacement fields $\bar{\boldsymbol{u}}_D(\boldsymbol{x},t)$ and $\check{\boldsymbol{u}}_D(\boldsymbol{x},t)$, respectively, are prescribed (Dirichlet boundary), and where on $\partial\mathscr{B}_{\bar{\boldsymbol{t}}}$ and $\partial\mathscr{B}_{\check{\boldsymbol{t}}}$ the macroscopic and microscopic traction fields $\bar{\boldsymbol{t}}_N(\boldsymbol{x},t)$ and $\check{\boldsymbol{t}}_N(\boldsymbol{x},t)$, respectively, are prescribed (Neumann boundary).

The crucial point of the presented gradient-extended theory is the incorporation of microscopic information of the neighbourhood, which is handled by introducing the length scale parameter $l\in\mathbb{R}^+$. Consequently we are dealing with a nonlocal continuum theory.

2.2. Strong form of the coupled system of equations

Because we also take micro-mechanical fields into account, we adopt the constitutive state $\mathfrak{c}$ introduced in Section 1.3:

$$\mathfrak{c}(\mathfrak{u}):=\{\bar{\boldsymbol{\varepsilon}},\check{\boldsymbol{u}},\nabla\check{\boldsymbol{u}}\}\quad\text{with}\quad\mathfrak{u}:=\{\bar{\boldsymbol{u}},\check{\boldsymbol{u}}\}\,. \tag{2.1}$$

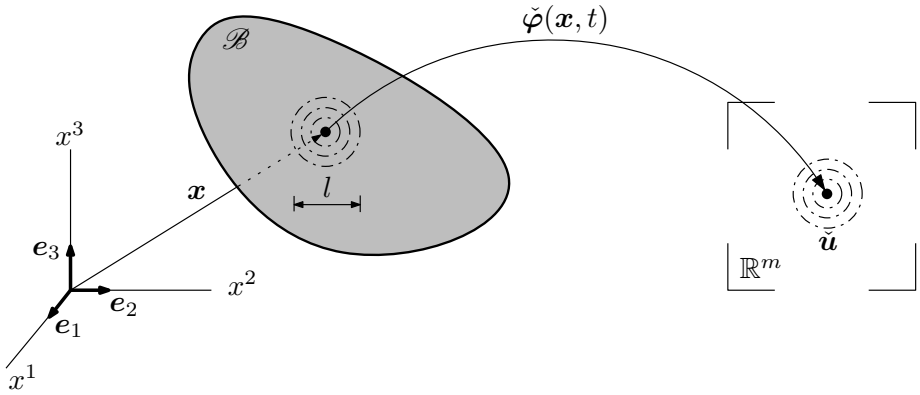

Figure 2.1. Geometrical setting when dealing with microscopic information, which is summarized in the array $\check{\boldsymbol{u}}$. The length scale parameter l provides for the nonlocality of the gradient-extended theory.

The consideration of the gradient of the microscopic displacement field in the constitutive state is not standard and gives the theory its name. Since $\check{\boldsymbol{u}}$ also describes dissipative processes we write the stored energy functional and the dissipation potential functional, introduced in Section 1.4, as

$$\Psi(\mathfrak{c},\boldsymbol{\mathcal{I}}) = \int_{\mathscr{B}} \psi(\mathfrak{c},\boldsymbol{\mathcal{I}})\,\mathrm{d}v \quad \text{and} \quad \Phi(\dot{\mathfrak{c}},\dot{\boldsymbol{\mathcal{I}}}) = \int_{\mathscr{B}} \phi(\dot{\mathfrak{c}},\dot{\boldsymbol{\mathcal{I}}})\,\mathrm{d}v\,, \tag{2.2}$$

where we have also taken into account some local internal variables $\boldsymbol{\mathcal{I}}$, which were treated in the last chapter. Of course the constitutive state (2.1) must be in agreement with the principle of material objectivity, this means

$$\psi(\mathfrak{c}^+,\boldsymbol{\mathcal{I}}^+) = \psi(\mathfrak{c},\boldsymbol{\mathcal{I}}) \quad \text{and} \quad \phi(\mathfrak{c}^+,\boldsymbol{\mathcal{I}}^+) = \phi(\mathfrak{c},\boldsymbol{\mathcal{I}})\,,$$

where again the plus sign denotes the translated and rotated state. Since the entries of $\check{\boldsymbol{u}}$ are scalar fields we can say

$$\check{\boldsymbol{u}}^+(\boldsymbol{x},t) = \check{\boldsymbol{u}}(\boldsymbol{x},t)\,,$$

which immediately identifies $\mathfrak{c}$ as an objective constitutive state.
To obtain the coupled system of equations we use the global balance of mechanical energy (1.7). Here we restrict ourselves to the quasi-static case, which means

$$P_{int} + P_{ext} = 0\,. \tag{2.3}$$

Looking at the representation (1.15) for the internal power, we calculate

$$\dot{\psi} = \partial_{\bar{\boldsymbol{\varepsilon}}}\psi : \dot{\bar{\boldsymbol{\varepsilon}}} + \partial_{\check{\boldsymbol{u}}}\psi \cdot \dot{\check{\boldsymbol{u}}} + \partial_{\nabla\check{\boldsymbol{u}}}\psi : \nabla\dot{\check{\boldsymbol{u}}} + \partial_{\boldsymbol{\mathcal{I}}}\psi \cdot \dot{\boldsymbol{\mathcal{I}}} \tag{2.4}$$

and extend the dissipation power density d according to the dependencies of the dissipation potential function in (2.2) as

$$d = \bar{\boldsymbol{\mathcal{F}}} : \dot{\bar{\boldsymbol{\varepsilon}}} + \check{\boldsymbol{f}} \cdot \dot{\check{\boldsymbol{u}}} + \check{\boldsymbol{\mathcal{F}}} : \nabla\dot{\check{\boldsymbol{u}}} + \boldsymbol{\mathcal{F}} \cdot \dot{\boldsymbol{\mathcal{I}}}\,,$$

where $\bar{\boldsymbol{\mathcal{F}}} := \partial_{\bar{\boldsymbol{\varepsilon}}}\phi$ is conjugate to $\bar{\boldsymbol{\varepsilon}}$ and stands for dissipative macroscopic stresses, $\check{\boldsymbol{f}} := \partial_{\check{\boldsymbol{u}}}\phi$ conjugate to $\check{\boldsymbol{u}}$ and $\check{\boldsymbol{\mathcal{F}}} := \partial_{\nabla\check{\boldsymbol{u}}}\phi$ conjugate to $\nabla\check{\boldsymbol{u}}$. These new thermodynamic driving forces are concluded in the array

$$\mathfrak{f} := \left\{\bar{\boldsymbol{\mathcal{F}}}, \check{\boldsymbol{f}}, \check{\boldsymbol{\mathcal{F}}}\right\}\,.$$

By introducing a microscopic body force per unit mass $\check{\boldsymbol{f}}^B$, the external power can be written as

$$P_{ext} = \int_{\mathscr{B}} \rho \bar{\boldsymbol{f}}^B \cdot \dot{\bar{\boldsymbol{u}}} \, \mathrm{d}v + \int_{\partial\mathscr{B}_{\bar{\boldsymbol{t}}}} \bar{\boldsymbol{t}}_N \cdot \dot{\bar{\boldsymbol{u}}} \, \mathrm{d}s_{\boldsymbol{x}} + \int_{\mathscr{B}} \rho \check{\boldsymbol{f}}^B \cdot \dot{\check{\boldsymbol{u}}} \, \mathrm{d}v + \int_{\partial\mathscr{B}_{\check{\boldsymbol{t}}}} \check{\boldsymbol{t}}_N \cdot \dot{\check{\boldsymbol{u}}} \, \mathrm{d}s_{\boldsymbol{x}} \, .$$

Finally, the global balance of mechanical energy (2.3) yields after integration by parts

$$\begin{aligned} 0 = &- \int_{\mathscr{B}} \operatorname{div}[\partial_{\bar{\boldsymbol{\varepsilon}}}\psi + \bar{\boldsymbol{\mathcal{F}}}] \cdot \dot{\bar{\boldsymbol{u}}} \, \mathrm{d}v - \int_{\mathscr{B}} \rho \bar{\boldsymbol{f}}^B \cdot \dot{\bar{\boldsymbol{u}}} \, \mathrm{d}v + \int_{\partial\mathscr{B}_{\bar{\boldsymbol{t}}}} [(\partial_{\bar{\boldsymbol{\varepsilon}}}\psi + \bar{\boldsymbol{\mathcal{F}}}) \cdot \boldsymbol{n} - \bar{\boldsymbol{t}}_N] \cdot \dot{\bar{\boldsymbol{u}}} \, \mathrm{d}s_{\boldsymbol{x}} \\ &- \int_{\mathscr{B}} \operatorname{div}[\partial_{\nabla\check{\boldsymbol{u}}}\psi + \check{\boldsymbol{\mathcal{F}}}] \cdot \dot{\check{\boldsymbol{u}}} \, \mathrm{d}v + \int_{\mathscr{B}} (\partial_{\check{\boldsymbol{u}}}\psi + \check{\boldsymbol{f}} - \rho \check{\boldsymbol{f}}^B) \cdot \dot{\check{\boldsymbol{u}}} \, \mathrm{d}v \\ &+ \int_{\partial\mathscr{B}_{\check{\boldsymbol{t}}}} [(\partial_{\nabla\check{\boldsymbol{u}}}\psi + \check{\boldsymbol{\mathcal{F}}}) \cdot \boldsymbol{n} - \check{\boldsymbol{t}}_N] \cdot \dot{\check{\boldsymbol{u}}} \, \mathrm{d}s_{\boldsymbol{x}} + \int_{\mathscr{B}} (\partial_{\boldsymbol{\mathcal{I}}}\psi + \boldsymbol{\mathcal{F}}) \cdot \dot{\boldsymbol{\mathcal{I}}} \, \mathrm{d}v \, , \end{aligned} \tag{2.5}$$

which has to be fulfilled for all $\dot{\bar{\boldsymbol{u}}} \in \mathcal{V}^0_{\bar{\boldsymbol{u}}}$, $\dot{\check{\boldsymbol{u}}} \in \mathcal{V}^0_{\check{\boldsymbol{u}}}$ and $\dot{\boldsymbol{\mathcal{I}}} \in \mathcal{L}_2(\mathscr{B})$, where we have introduced the function spaces

$$\begin{aligned} \mathcal{V}^0_{\bar{\boldsymbol{u}}} &:= \left\{ \boldsymbol{w}(\cdot,t) \in [\mathcal{H}^1(\mathscr{B})]^3 \colon \boldsymbol{w} = \boldsymbol{0} \quad \text{on } \partial\mathscr{B}_{\bar{\boldsymbol{u}}} \right\} , \\ \mathcal{V}^0_{\check{\boldsymbol{u}}} &:= \left\{ \boldsymbol{w}(\cdot,t) \in [\mathcal{H}^1(\mathscr{B})]^m \colon \boldsymbol{w} = \boldsymbol{0} \quad \text{on } \partial\mathscr{B}_{\check{\boldsymbol{u}}} \right\} \end{aligned}$$

with $\mathcal{H}^1(\mathscr{B})$ being the space of functions in $\mathcal{L}_2(\mathscr{B})$, the first derivative(s) of which is (are) square integrable, see Appendix A. Note, that the size of the array $\dot{\boldsymbol{\mathcal{I}}}$ is unspecified and we mean by $\dot{\boldsymbol{\mathcal{I}}} \in \mathcal{L}_2(\mathscr{B})$, that every single element from the array $\dot{\boldsymbol{\mathcal{I}}}$ is from $\mathcal{L}_2(\mathscr{B})$. Consequently, if an array size is not given, we will suppress the information of the array size in the notion of the corresponding function space. Furthermore, from now on we will just write $\mathcal{L}_2$ instead of $\mathcal{L}_2(\mathscr{B})$.
As pointed out in Subsection 1.4.1, it is important to distinguish between rate-independency and rate-dependency. The mathematical main difference is, that for the rate-dependent case the Lagrange multiplier λ is explicitly known, namely $\lambda = \frac{1}{\eta}\langle\varphi(\mathfrak{f}, \boldsymbol{\mathcal{F}}, \mathfrak{c}, \boldsymbol{\mathcal{I}})\rangle$. The resulting coupled system of equations, which is obtained from (2.5), is summarized for rate-dependency in Table 2.1.

2.3. Potential formulation and time incrementation

Especially for the purpose with finite elements, we switch to an equivalent potential formulation. For this we write the internal rate potential per unit volume, introduced in Section 1.4, as

$$\pi(\mathfrak{c}, \boldsymbol{\mathcal{I}}, \dot{\mathfrak{c}}, \dot{\boldsymbol{\mathcal{I}}}) = \frac{\mathrm{d}}{\mathrm{d}t}\psi(\mathfrak{c}, \boldsymbol{\mathcal{I}}) + \phi(\dot{\mathfrak{c}}, \dot{\boldsymbol{\mathcal{I}}})$$

and construct the potential

$$\begin{aligned} \Pi(\dot{\bar{\boldsymbol{u}}}, \dot{\check{\boldsymbol{u}}}, \dot{\boldsymbol{\mathcal{I}}}) &:= \int_{\mathscr{B}} \pi(\mathfrak{c}, \boldsymbol{\mathcal{I}}, \dot{\mathfrak{c}}, \dot{\boldsymbol{\mathcal{I}}}) \, \mathrm{d}v - P_{ext}(\dot{\mathfrak{u}}, t) \\ &= \frac{\mathrm{d}}{\mathrm{d}t}\Psi(\mathfrak{c}, \boldsymbol{\mathcal{I}}) + \Phi(\dot{\mathfrak{c}}, \dot{\boldsymbol{\mathcal{I}}}) - P_{ext}(\dot{\mathfrak{u}}, t) \end{aligned}$$

for a given state $\{\bar{\boldsymbol{u}}, \check{\boldsymbol{u}}, \boldsymbol{\mathcal{I}}\}$ at a given time t. Since the expression $\frac{\mathrm{d}}{\mathrm{d}t}\Psi(\mathfrak{c}, \boldsymbol{\mathcal{I}})$ is linear in $\{\dot{\mathfrak{c}}, \dot{\boldsymbol{\mathcal{I}}}\}$, the convexity of ϕ with respect to $\{\dot{\mathfrak{c}}, \dot{\boldsymbol{\mathcal{I}}}\}$ confers to the potential Π. As a result the temporal change of the macro- and microscopic displacement fields and of the internal variables is given by the minimization principle

$$\{\dot{\bar{\boldsymbol{u}}}, \dot{\check{\boldsymbol{u}}}, \dot{\boldsymbol{\mathcal{I}}}\} = \arg\{ \min_{\dot{\bar{\boldsymbol{u}}} \in \mathcal{V}^0_{\bar{\boldsymbol{u}}}} \min_{\dot{\check{\boldsymbol{u}}} \in \mathcal{V}^0_{\check{\boldsymbol{u}}}} \min_{\dot{\boldsymbol{\mathcal{I}}} \in \mathcal{L}_2} [\Pi(\dot{\bar{\boldsymbol{u}}}, \dot{\check{\boldsymbol{u}}}, \dot{\boldsymbol{\mathcal{I}}})] \} \, . \tag{2.6}$$

Macroscopic equilibrium:

$$\begin{aligned} -\mathrm{div}[\partial_{\bar{\boldsymbol{\varepsilon}}}\psi + \bar{\boldsymbol{\mathcal{F}}}] - \rho\bar{\boldsymbol{f}}^B &= \boldsymbol{0} && \text{in } \mathscr{B} \\ \bar{\boldsymbol{u}} &= \bar{\boldsymbol{u}}_D && \text{on } \partial\mathscr{B}_{\bar{\boldsymbol{u}}} \\ (\partial_{\bar{\boldsymbol{\varepsilon}}}\psi + \bar{\boldsymbol{\mathcal{F}}}) \cdot \boldsymbol{n} &= \bar{\boldsymbol{t}}_N && \text{on } \partial\mathscr{B}_{\bar{\boldsymbol{t}}} \end{aligned}$$

Microscopic balance equation:

$$\begin{aligned} -\mathrm{div}[\partial_{\nabla\check{\boldsymbol{u}}}\psi + \check{\boldsymbol{\mathcal{F}}}] + \partial_{\check{\boldsymbol{u}}}\psi + \check{\boldsymbol{f}} - \rho\check{\boldsymbol{f}}^B &= \boldsymbol{0} && \text{in } \mathscr{B} \\ \check{\boldsymbol{u}} &= \check{\boldsymbol{u}}_D && \text{on } \partial\mathscr{B}_{\check{\boldsymbol{u}}} \\ (\partial_{\nabla\check{\boldsymbol{u}}}\psi + \check{\boldsymbol{\mathcal{F}}}) \cdot \boldsymbol{n} &= \check{\boldsymbol{t}}_N && \text{on } \partial\mathscr{B}_{\check{\boldsymbol{t}}} \end{aligned}$$

Conjugate problem for local internal variables:

$$\partial_{\boldsymbol{\mathcal{I}}}\psi + \boldsymbol{\mathcal{F}} = \boldsymbol{0} \quad \text{in } \mathscr{B}$$

Evolution equations with $\lambda = \frac{1}{\eta}\langle\varphi(\mathfrak{f}, \boldsymbol{\mathcal{F}}, \mathfrak{c}, \boldsymbol{\mathcal{I}})\rangle$:

$$\begin{aligned} \dot{\mathfrak{c}} &= \lambda\partial_{\mathfrak{f}}\varphi && \text{in } \mathscr{B} \\ \mathfrak{c}(t=0) &= \mathfrak{c}_0 && \text{in } \mathscr{B} \\ \dot{\boldsymbol{\mathcal{I}}} &= \lambda\partial_{\boldsymbol{\mathcal{F}}}\varphi && \text{in } \mathscr{B} \\ \boldsymbol{\mathcal{I}}(t=0) &= \boldsymbol{\mathcal{I}}_0 && \text{in } \mathscr{B} \end{aligned}$$

Table 2.1. Strong form of rate-dependent coupled system of equations for gradient-type solids.

By considering the new dependencies, the dissipation function ϕ reads in terms of its Legendre transform ϕ^*

$$\phi(\dot{\mathfrak{c}}, \dot{\boldsymbol{\mathcal{I}}}) = \max_{\mathfrak{f}\in\mathcal{L}_2} \max_{\boldsymbol{\mathcal{F}}\in\mathcal{L}_2} \{\mathfrak{f}\cdot\dot{\mathfrak{c}} + \boldsymbol{\mathcal{F}}\cdot\dot{\boldsymbol{\mathcal{I}}} - \phi^*(\mathfrak{f}, \boldsymbol{\mathcal{F}})\}\,, \tag{2.7}$$

see (1.17). If we incorporate this representation, we can introduce an extended internal rate potential per unit volume as

$$\pi^*(\mathfrak{c}, \boldsymbol{\mathcal{I}}, \dot{\mathfrak{c}}, \dot{\boldsymbol{\mathcal{I}}}, \mathfrak{f}, \boldsymbol{\mathcal{F}}) := \frac{\mathrm{d}}{\mathrm{d}t}\psi(\mathfrak{c}, \boldsymbol{\mathcal{I}}) + \mathfrak{f}\cdot\dot{\mathfrak{c}} + \boldsymbol{\mathcal{F}}\cdot\dot{\boldsymbol{\mathcal{I}}} - \phi^*(\mathfrak{f}, \boldsymbol{\mathcal{F}})\,, \tag{2.8}$$

and accordingly we can define an extended potential as

$$\Pi^*(\dot{\bar{\boldsymbol{u}}}, \dot{\check{\boldsymbol{u}}}, \dot{\boldsymbol{\mathcal{I}}}, \mathfrak{f}, \boldsymbol{\mathcal{F}}) := \int_{\mathscr{B}} \pi^*(\mathfrak{c}, \boldsymbol{\mathcal{I}}, \dot{\mathfrak{c}}, \dot{\boldsymbol{\mathcal{I}}}, \mathfrak{f}, \boldsymbol{\mathcal{F}})\,\mathrm{d}v - P_{ext}(\dot{\boldsymbol{u}}, t) \tag{2.9}$$

for a given state $\{\bar{\boldsymbol{u}}, \check{\boldsymbol{u}}, \boldsymbol{\mathcal{I}}\}$ at a given time t. Then the extended variational principle reads

$$\{\dot{\bar{\boldsymbol{u}}}, \dot{\check{\boldsymbol{u}}}, \dot{\boldsymbol{\mathcal{I}}}, \mathfrak{f}, \boldsymbol{\mathcal{F}}\} = \arg\{\min_{\dot{\bar{\boldsymbol{u}}}\in\mathcal{V}^0_{\bar{\boldsymbol{u}}}} \min_{\dot{\check{\boldsymbol{u}}}\in\mathcal{V}^0_{\check{\boldsymbol{u}}}} \min_{\dot{\boldsymbol{\mathcal{I}}}\in\mathcal{L}_2} \max_{\mathfrak{f}\in\mathcal{L}_2} \max_{\boldsymbol{\mathcal{F}}\in\mathcal{L}_2} [\Pi^*(\dot{\bar{\boldsymbol{u}}}, \dot{\check{\boldsymbol{u}}}, \dot{\boldsymbol{\mathcal{I}}}, \mathfrak{f}, \boldsymbol{\mathcal{F}})]\}\,, \tag{2.10}$$

where the two max-operations come from the Legendre transformation (2.7). Note, that due to the formulation of the dissipation function ϕ in terms of its dual ϕ^*, the minimization principle (2.6) has been transformed into a saddle point problem.
So far no distinction has been made between rate-independent and rate-dependent processes. As in the last section, we will specialize to the latter case, for which we can replace the dual dissipation function by $\frac{1}{2\eta}\langle\varphi(\mathfrak{f}, \boldsymbol{\mathcal{F}}, \mathfrak{c}, \boldsymbol{\mathcal{I}})\rangle^2$, see (1.23). Accordingly (2.8) reads

$$\pi^*_\eta(\mathfrak{c}, \boldsymbol{\mathcal{I}}, \dot{\mathfrak{c}}, \dot{\boldsymbol{\mathcal{I}}}, \mathfrak{f}, \boldsymbol{\mathcal{F}}) := \frac{\mathrm{d}}{\mathrm{d}t}\psi(\mathfrak{c}, \boldsymbol{\mathcal{I}}) + \mathfrak{f}\cdot\dot{\mathfrak{c}} + \boldsymbol{\mathcal{F}}\cdot\dot{\boldsymbol{\mathcal{I}}} - \frac{1}{2\eta}\langle\varphi(\mathfrak{f}, \boldsymbol{\mathcal{F}}, \mathfrak{c}, \boldsymbol{\mathcal{I}})\rangle^2\,. \tag{2.11}$$

Of course Π^*_η is defined by just replacing π^* by π^*_η in (2.9). Naturally, also the variational principle (2.10) is adopted just by plugging in Π^*_η. At this point we should check if the variational problem gives the strong form summarized in Table 2.1. To make Π^*_η stationary, it is necessary that

$$\delta\Pi^*_\eta(\dot{\bar{\boldsymbol{u}}}, \dot{\check{\boldsymbol{u}}}, \dot{\boldsymbol{\mathcal{I}}}, \mathfrak{f}, \boldsymbol{\mathcal{F}}) = \delta_{\dot{\bar{\boldsymbol{u}}}}\Pi^*_\eta + \delta_{\dot{\check{\boldsymbol{u}}}}\Pi^*_\eta + \delta_{\dot{\boldsymbol{\mathcal{I}}}}\Pi^*_\eta + \delta_{\mathfrak{f}}\Pi^*_\eta + \delta_{\boldsymbol{\mathcal{F}}}\Pi^*_\eta = 0$$

for all $\delta\dot{\bar{\boldsymbol{u}}} \in \mathcal{V}^0_{\bar{\boldsymbol{u}}}$, $\delta\dot{\check{\boldsymbol{u}}} \in \mathcal{V}^0_{\check{\boldsymbol{u}}}$, $\delta\dot{\boldsymbol{\mathcal{I}}} \in \mathcal{L}_2$, $\delta\mathfrak{f} \in \mathcal{L}_2$ and $\delta\boldsymbol{\mathcal{F}} \in \mathcal{L}_2$. Calculating the single variations, as it will be done at the end of the section for the time discrete case, and doing integration by parts in fact really gives the strong form of coupled equations.

For the numerical implementation it is necessary to do a numerical time integration of the corresponding evolution equations, see Table 2.1. Hence we divide $\mathscr{T} = [0, T]$ into a number of uniform time increments with time step τ. Then the discrete times are given by $t_n = \tau n$ for $n = 0, 1, 2, \dots$. We assume all fields to be known at t_n and want to obtain the fields at time t_{n+1}. For a shorter notation we will skip the index $n+1$, e.g.

$$\bar{\boldsymbol{u}}_n := \bar{\boldsymbol{u}}(\boldsymbol{x}, t_n) \quad \text{and} \quad \bar{\boldsymbol{u}} := \bar{\boldsymbol{u}}(\boldsymbol{x}, t_{n+1})\,.$$

One-step procedures are the easiest methods to solve an initial value problem numerically. Because of being unconditionally stable, it would be convenient to use the implicit Euler scheme here, which reads applied to the evolution problems in Table 2.1

$$\begin{aligned} \mathfrak{c} &= \mathfrak{c}_n + \tau\frac{1}{\eta}\langle\varphi(\mathfrak{f}, \boldsymbol{\mathcal{F}}, \mathfrak{c}, \boldsymbol{\mathcal{I}})\rangle\partial_{\mathfrak{f}}\varphi(\mathfrak{f}, \boldsymbol{\mathcal{F}}, \mathfrak{c}, \boldsymbol{\mathcal{I}})\,, \\ \boldsymbol{\mathcal{I}} &= \boldsymbol{\mathcal{I}}_n + \tau\frac{1}{\eta}\langle\varphi(\mathfrak{f}, \boldsymbol{\mathcal{F}}, \mathfrak{c}, \boldsymbol{\mathcal{I}})\rangle\partial_{\boldsymbol{\mathcal{F}}}\varphi(\mathfrak{f}, \boldsymbol{\mathcal{F}}, \mathfrak{c}, \boldsymbol{\mathcal{I}}) \end{aligned} \tag{2.12}$$

for $n = 0, 1, 2, \dots$. However, as in the continuous case, we will follow a potential approach here. To obtain the time incremental version of the potential Π^*_η, we do an integration with respect to time t from t_n to t_{n+1}

$$\Pi^{*\tau}_\eta := \int_{t_n}^{t_{n+1}} \Pi^*_\eta \,\mathrm{d}t = \int_{\mathscr{B}} \underbrace{\int_{t_n}^{t_{n+1}} \pi^*_\eta \,\mathrm{d}t}_{=:\pi^{*\tau}_\eta} \,\mathrm{d}v - \underbrace{\int_{t_n}^{t_{n+1}} P_{ext} \,\mathrm{d}t}_{=:P^\tau_{ext}}\,.$$

By assuming time independent macro- and microscopic external forces, we find the time incremental external power as

$$\begin{aligned} P^\tau_{ext} = &\int_{\mathscr{B}} \rho\bar{\boldsymbol{f}}^B \cdot (\bar{\boldsymbol{u}} - \bar{\boldsymbol{u}}_n)\,\mathrm{d}v + \int_{\partial\mathscr{B}_{\bar{\boldsymbol{t}}}} \bar{\boldsymbol{t}}_N \cdot (\bar{\boldsymbol{u}} - \bar{\boldsymbol{u}}_n)\,\mathrm{d}s_{\boldsymbol{x}} \\ &+ \int_{\mathscr{B}} \rho\check{\boldsymbol{f}}^B \cdot (\check{\boldsymbol{u}} - \check{\boldsymbol{u}}_n)\,\mathrm{d}v + \int_{\partial\mathscr{B}_{\check{\boldsymbol{t}}}} \check{\boldsymbol{t}}_N \cdot (\check{\boldsymbol{u}} - \check{\boldsymbol{u}}_n)\,\mathrm{d}s_{\boldsymbol{x}}\,. \end{aligned}$$

The time incremental internal rate potential per unit volume is

$$\pi^{*\tau}_\eta = \mathrm{IAlgo}\{\pi^*_\eta\}\,,$$

where $\mathrm{IAlgo}\{\cdot\}$ stands for a consistent integration algorithm. This means, that the integration must be done in such a way, that we obtain the macroscopic equilibrium, the microscopic balance equation and the conjugate problem for local internal variables, see Table 2.1, at time t_{n+1} from the time incremental potential formulation. The time

discrete versions of the evolution equations are the result of such a consistent approach. By introducing an extended constitutive state at time t_{n+1} as

$$\mathfrak{c}^*(\mathfrak{u}^*) := \{\bar{\boldsymbol{\varepsilon}}, \check{\boldsymbol{u}}, \nabla\check{\boldsymbol{u}}, \mathfrak{f}\} \quad \text{with} \quad \mathfrak{u}^* := \{\bar{\boldsymbol{u}}, \check{\boldsymbol{u}}, \mathfrak{f}\} \tag{2.13}$$

and the set of local internal variables together with its dual forces at t_{n+1}

$$\mathfrak{s} := \{\boldsymbol{\mathcal{I}}, \boldsymbol{\mathcal{F}}\}\,, \tag{2.14}$$

we write for the time incremental rate potential per unit volume

$$\begin{aligned}\pi_\eta^{*\tau}(\mathfrak{c}^*, \mathfrak{c}_n^*, \mathfrak{s}, \mathfrak{s}_n) = \psi(\mathfrak{c}, \boldsymbol{\mathcal{I}}) - \psi(\mathfrak{c}_n, \boldsymbol{\mathcal{I}}_n) + \mathfrak{f}\cdot(\mathfrak{c} - \mathfrak{c}_n) + \boldsymbol{\mathcal{F}}\cdot(\boldsymbol{\mathcal{I}} - \boldsymbol{\mathcal{I}}_n) \\ - \frac{\tau}{2\eta}\langle\varphi(\mathfrak{f}, \boldsymbol{\mathcal{F}}, \mathfrak{c}_n, \boldsymbol{\mathcal{I}}_n)\rangle^2\,.\end{aligned} \tag{2.15}$$

Once again we write down the time incremental potential, but now with its dependencies, as

$$\Pi_\eta^{*\tau}(\bar{\boldsymbol{u}}, \check{\boldsymbol{u}}, \boldsymbol{\mathcal{I}}, \mathfrak{f}, \boldsymbol{\mathcal{F}}) = \int_{\mathscr{B}} \pi_\eta^{*\tau}(\mathfrak{c}^*, \mathfrak{c}_n^*, \mathfrak{s}, \mathfrak{s}_n)\,\mathrm{d}v - P_{ext}^\tau(\mathfrak{u}, \mathfrak{u}_n)\,.$$

The macro- and microscopic displacement fields, the local internal variables and the thermodynamic driving forces at time t_{n+1} are obtained via the variational principle

$$\{\bar{\boldsymbol{u}}, \check{\boldsymbol{u}}, \boldsymbol{\mathcal{I}}, \mathfrak{f}, \boldsymbol{\mathcal{F}}\} = \arg\{\min_{\bar{\boldsymbol{u}}\in\mathcal{V}_{\bar{\boldsymbol{u}}}} \min_{\check{\boldsymbol{u}}\in\mathcal{V}_{\check{\boldsymbol{u}}}} \min_{\boldsymbol{\mathcal{I}}\in\mathcal{L}_2} \max_{\mathfrak{f}\in\mathcal{L}_2} \max_{\boldsymbol{\mathcal{F}}\in\mathcal{L}_2} [\Pi_\eta^{*\tau}(\bar{\boldsymbol{u}}, \check{\boldsymbol{u}}, \boldsymbol{\mathcal{I}}, \mathfrak{f}, \boldsymbol{\mathcal{F}})]\}\,,$$

with

$$\begin{aligned}\mathcal{V}_{\bar{\boldsymbol{u}}} &:= \{\boldsymbol{w}(\cdot) \in [\mathcal{H}^1(\mathscr{B})]^3 \colon \boldsymbol{w} = \bar{\boldsymbol{u}}_D \quad \text{on } \partial\mathscr{B}_{\bar{\boldsymbol{u}}}\}\,, \\ \mathcal{V}_{\check{\boldsymbol{u}}} &:= \{\boldsymbol{w}(\cdot) \in [\mathcal{H}^1(\mathscr{B})]^m \colon \boldsymbol{w} = \check{\boldsymbol{u}}_D \quad \text{on } \partial\mathscr{B}_{\bar{\boldsymbol{u}}}\}\,.\end{aligned}$$

For this it is necessary that the first variation of $\Pi_\eta^{*\tau}$ vanishes:

$$\delta\Pi_\eta^{*\tau}(\bar{\boldsymbol{u}}, \check{\boldsymbol{u}}, \boldsymbol{\mathcal{I}}, \mathfrak{f}, \boldsymbol{\mathcal{F}}) = \delta_{\bar{\boldsymbol{u}}}\Pi_\eta^{*\tau} + \delta_{\check{\boldsymbol{u}}}\Pi_\eta^{*\tau} + \delta_{\boldsymbol{\mathcal{I}}}\Pi_\eta^{*\tau} + \delta_{\mathfrak{f}}\Pi_\eta^{*\tau} + \delta_{\boldsymbol{\mathcal{F}}}\Pi_\eta^{*\tau} = 0 \tag{2.16}$$

for all $\delta\bar{\boldsymbol{u}} \in \mathcal{V}_{\bar{\boldsymbol{u}}}^0$, $\delta\check{\boldsymbol{u}} \in \mathcal{V}_{\check{\boldsymbol{u}}}^0$, $\delta\boldsymbol{\mathcal{I}} \in \mathcal{L}_2$, $\delta\mathfrak{f} \in \mathcal{L}_2$ and $\delta\boldsymbol{\mathcal{F}} \in \mathcal{L}_2$. Using $\delta_{\bar{\boldsymbol{u}}}\mathfrak{c} = \{\delta\bar{\boldsymbol{\varepsilon}}, \boldsymbol{0}, \boldsymbol{0}\}$ and $\delta_{\check{\boldsymbol{u}}}\mathfrak{c} = \{\boldsymbol{0}, \delta\check{\boldsymbol{u}}, \nabla\delta\check{\boldsymbol{u}}\}$, the single variations read

$$\begin{aligned}\delta_{\bar{\boldsymbol{u}}}\Pi_\eta^{*\tau} &= \int_{\mathscr{B}} (\partial_{\bar{\boldsymbol{\varepsilon}}}\psi + \bar{\boldsymbol{\mathcal{F}}}) : \delta\bar{\boldsymbol{\varepsilon}}\,\mathrm{d}v + \int_{\mathscr{B}} \rho\bar{\boldsymbol{f}}^B\cdot\delta\bar{\boldsymbol{u}}\,\mathrm{d}v - \int_{\partial\mathscr{B}_{\bar{\boldsymbol{t}}}} \bar{\boldsymbol{t}}_N\cdot\delta\bar{\boldsymbol{u}}\,\mathrm{d}s_{\boldsymbol{x}}\,, \\ \delta_{\check{\boldsymbol{u}}}\Pi_\eta^{*\tau} &= \int_{\mathscr{B}} [(\partial_{\check{\boldsymbol{u}}}\psi + \check{\boldsymbol{f}})\cdot\delta\check{\boldsymbol{u}} + (\partial_{\nabla\check{\boldsymbol{u}}}\psi + \check{\boldsymbol{\mathcal{F}}}) : \nabla\delta\check{\boldsymbol{u}}]\,\mathrm{d}v + \int_{\mathscr{B}} \rho\check{\boldsymbol{f}}^B\cdot\delta\check{\boldsymbol{u}}\,\mathrm{d}v \\ &\quad - \int_{\partial\mathscr{B}_{\check{\boldsymbol{t}}}} \check{\boldsymbol{t}}_N\cdot\delta\check{\boldsymbol{u}}\,\mathrm{d}s_{\boldsymbol{x}}\,, \\ \delta_{\boldsymbol{\mathcal{I}}}\Pi_\eta^{*\tau} &= \int_{\mathscr{B}} (\partial_{\boldsymbol{\mathcal{I}}}\psi + \boldsymbol{\mathcal{F}})\cdot\delta\boldsymbol{\mathcal{I}}\,\mathrm{d}v\,, \\ \delta_{\mathfrak{f}}\Pi_\eta^{*\tau} &= \int_{\mathscr{B}} (\mathfrak{c} - \mathfrak{c}_n - \frac{\tau}{\eta}\langle\varphi\rangle\partial_{\mathfrak{f}}\varphi)\cdot\delta\mathfrak{f}\,\mathrm{d}v\,, \\ \delta_{\boldsymbol{\mathcal{F}}}\Pi_\eta^{*\tau} &= \int_{\mathscr{B}} (\boldsymbol{\mathcal{I}} - \boldsymbol{\mathcal{I}}_n - \frac{\tau}{\eta}\langle\varphi\rangle\partial_{\boldsymbol{\mathcal{F}}}\varphi)\cdot\delta\boldsymbol{\mathcal{F}}\,\mathrm{d}v\,.\end{aligned} \tag{2.17}$$

Doing integration by parts and localizing, gives the time discrete strong form of the governing equations for gradient-type dissipative solids, see Table 2.2. Here we see, that the chosen integration algorithm for π_η^* is indeed consistent. Furthermore we should point out the difference between the implicit Euler scheme (2.12) and the time discrete evolution

Macroscopic equlibrium:

$$\begin{aligned} -\mathrm{div}[\partial_{\bar{\boldsymbol{\varepsilon}}}\psi + \bar{\boldsymbol{\mathcal{F}}}] - \rho\bar{\boldsymbol{f}}^B &= \boldsymbol{0} && \text{in } \mathscr{B} \\ \bar{\boldsymbol{u}} &= \bar{\boldsymbol{u}}_D && \text{on } \partial\mathscr{B}_{\bar{\boldsymbol{u}}} \\ (\partial_{\bar{\boldsymbol{\varepsilon}}}\psi + \bar{\boldsymbol{\mathcal{F}}}) \cdot \boldsymbol{n} &= \bar{\boldsymbol{t}}_N && \text{on } \partial\mathscr{B}_{\bar{\boldsymbol{t}}} \end{aligned}$$

Microscopic balance equation:

$$\begin{aligned} -\mathrm{div}[\partial_{\nabla\check{\boldsymbol{u}}}\psi + \check{\boldsymbol{\mathcal{F}}}] + \partial_{\check{\boldsymbol{u}}}\psi + \check{\boldsymbol{f}} - \rho\check{\boldsymbol{f}}^B &= \boldsymbol{0} && \text{in } \mathscr{B} \\ \check{\boldsymbol{u}} &= \check{\boldsymbol{u}}_D && \text{on } \partial\mathscr{B}_{\check{\boldsymbol{u}}} \\ (\partial_{\nabla\check{\boldsymbol{u}}}\psi + \check{\boldsymbol{\mathcal{F}}}) \cdot \boldsymbol{n} &= \check{\boldsymbol{t}}_N && \text{on } \partial\mathscr{B}_{\check{\boldsymbol{t}}} \end{aligned}$$

Conjugate problem for local internal variables:

$$\partial_{\boldsymbol{\mathcal{I}}}\psi + \boldsymbol{\mathcal{F}} = \boldsymbol{0} \quad \text{in } \mathscr{B}$$

Evolution equations with $\lambda = \frac{1}{\eta}\langle\varphi(\mathfrak{f}, \boldsymbol{\mathcal{F}}, \mathfrak{c}_n, \boldsymbol{\mathcal{I}}_n)\rangle$:

$$\begin{aligned} \mathfrak{c} &= \mathfrak{c}_n + \tau\lambda\partial_{\mathfrak{f}}\varphi(\mathfrak{f}, \boldsymbol{\mathcal{F}}, \mathfrak{c}_n, \boldsymbol{\mathcal{I}}_n) && \text{in } \mathscr{B} \\ \mathfrak{c}(t=0) &= \mathfrak{c}_0 && \text{in } \mathscr{B} \\ \boldsymbol{\mathcal{I}} &= \boldsymbol{\mathcal{I}}_n + \tau\lambda\partial_{\boldsymbol{\mathcal{F}}}\varphi(\mathfrak{f}, \boldsymbol{\mathcal{F}}, \mathfrak{c}_n, \boldsymbol{\mathcal{I}}_n) && \text{in } \mathscr{B} \\ \boldsymbol{\mathcal{I}}(t=0) &= \boldsymbol{\mathcal{I}}_0 && \text{in } \mathscr{B} \end{aligned}$$

Table 2.2. Time discrete strong form of rate-dependent coupled system of equations for gradient-type solids.

equations in Table 2.2. However, when we apply the gradient-extended theory to von-Mises plasticity, this disagreement will disappear since the von-Mises yield function does not depend on $\mathfrak{c}$, $\boldsymbol{\mathcal{I}}$ and $\mathfrak{c}_n$, $\boldsymbol{\mathcal{I}}_n$, respectively.
If one takes a closer look at the time discrete conjugate problem and the evolution equation for the local internal variables $\boldsymbol{\mathcal{I}}$, given in Table 2.2, one can see, that for a known actual state $\mathfrak{c}^*$, $\mathfrak{s}$ can be solved via a decoupled local solution algorithm, which will be specified in the next chapter for von-Mises plasticity. As a result $\boldsymbol{\mathcal{I}}$ and $\boldsymbol{\mathcal{F}}$ will not be discretized globally, which means, that these quantities only exist on integration point level. Therefore we can reduce the necessary condition (2.16) to

$$\delta_{\bar{\boldsymbol{u}}}\Pi_\eta^{*\tau} + \delta_{\check{\boldsymbol{u}}}\Pi_\eta^{*\tau} + \delta_{\mathfrak{f}}\Pi_\eta^{*\tau} = 0 \tag{2.18}$$

for all $\delta\bar{\boldsymbol{u}} \in \mathcal{V}^0_{\bar{\boldsymbol{u}}}$, $\delta\check{\boldsymbol{u}} \in \mathcal{V}^0_{\check{\boldsymbol{u}}}$ and $\delta\mathfrak{f} \in \mathcal{L}_2$. Introducing the arrays $\mathfrak{g} := \{\bar{\boldsymbol{f}}^B, \check{\boldsymbol{f}}^B, \boldsymbol{0}\}$, $\mathfrak{t}_N := \{\bar{\boldsymbol{t}}_N, \check{\boldsymbol{t}}_N, \boldsymbol{0}\}$, $\delta\mathfrak{u}^* := \{\delta\bar{\boldsymbol{u}}, \delta\check{\boldsymbol{u}}, \delta\mathfrak{f}\}$ and $\delta_{\mathfrak{u}^*}\mathfrak{c}^* := \{\delta\bar{\boldsymbol{\varepsilon}}, \delta\check{\boldsymbol{u}}, \nabla\delta\check{\boldsymbol{u}}, \delta\mathfrak{f}\}$, we can write the system of equations in a short way, since every single variation in (2.18) must be zero on its own:

$$\delta_{\mathfrak{u}^*}\Pi_\eta^{*\tau} := \begin{bmatrix} \delta_{\bar{\boldsymbol{u}}}\Pi_\eta^{*\tau} \\ \delta_{\check{\boldsymbol{u}}}\Pi_\eta^{*\tau} \\ \delta_{\mathfrak{f}}\Pi_\eta^{*\tau} \end{bmatrix} = \int_{\mathscr{B}} \partial_{\mathfrak{c}^*}\pi_\eta^{*\tau} \cdot \delta_{\mathfrak{u}^*}\mathfrak{c}^* \,\mathrm{d}v - \int_{\mathscr{B}} \rho\mathfrak{g} \cdot \delta\mathfrak{u}^* \,\mathrm{d}v - \int_{\partial\mathscr{B}_{\mathfrak{t}}} \mathfrak{t}_N \cdot \delta\mathfrak{u}^* \,\mathrm{d}s_{\boldsymbol{x}} = \boldsymbol{0}$$

for all $\delta\bar{\boldsymbol{u}} \in \mathcal{V}^0_{\bar{\boldsymbol{u}}}$, $\delta\check{\boldsymbol{u}} \in \mathcal{V}^0_{\check{\boldsymbol{u}}}$ and $\delta\mathfrak{f} \in \mathcal{L}_2$. The numerical solution of this variational principle is discussed in the following section.

2.4. Standard finite element formulation

Let the body $\mathscr{B}_h \approx \mathscr{B} \subset \mathbb{R}^3$ or $\mathscr{B}_h \approx \mathscr{B} \subset \mathbb{R}^2$ be regularly decomposed[1] into N finite elements $\mathscr{B}_h^e$ with $e = 1, \ldots, N$ and let M denote the number of nodes of the whole mesh.

[1] A non-regular decomposition is characterized by hanging nodes.

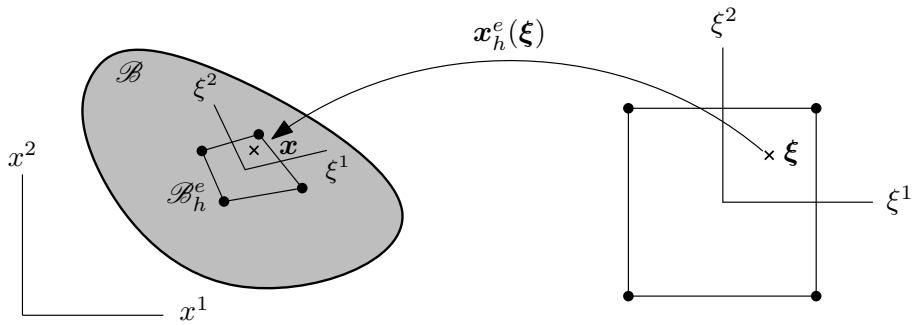

Figure 2.2. Interpolation of the geometry.

Following the isoparametric concept, the geometry is described on element level by the ansatz

$$\boldsymbol{x}_h^e(\boldsymbol{\xi}) := \sum_{i=1}^{M^e} h_i(\boldsymbol{\xi}) \boldsymbol{x}_i^e \,,$$

where M^e denotes the number of nodes of element $\mathscr{B}_h^e$, $\boldsymbol{\xi}$ the natural coordinates, $h_i(\boldsymbol{\xi})$ the shape functions and

$$\boldsymbol{x}_i^e := \begin{bmatrix} x_i^1 \\ x_i^2 \\ x_i^3 \end{bmatrix}^e \,,$$

the coordinates of the node with local number i belonging to the element $\mathscr{B}_h^e$, see Figure 2.2 for the two-dimensional case. Note, that the shape functions h_i are constructed in such a way, that they are one at node i, and zero at every other node of the element.
Principally the same ansatz is also chosen for the element-wise approximation of the global fields $\bar{\boldsymbol{u}}$, $\check{\boldsymbol{u}}$ and $\mathfrak{f}$:

$$\bar{\boldsymbol{u}}_h^e(\boldsymbol{x}) = \sum_{i=1}^{M^e} h_i(\boldsymbol{\xi}) \bar{\boldsymbol{d}}_i^e \,, \quad \check{\boldsymbol{u}}_h^e(\boldsymbol{x}) = \sum_{i=1}^{M^e} h_i(\boldsymbol{\xi}) \check{\boldsymbol{d}}_i^e \quad \text{and} \quad \mathfrak{f}_h^e(\boldsymbol{x}) = \sum_{i=1}^{M^e} h_i(\boldsymbol{\xi}) \mathfrak{f}_i^e \,. \tag{2.19}$$

These functions are uniquely determined by their nodal values

$$\bar{\boldsymbol{d}}_i^e = \begin{bmatrix} \bar{d}_i^1 \\ \bar{d}_i^2 \\ \bar{d}_i^3 \end{bmatrix}^e \,, \quad \check{\boldsymbol{d}}_i^e = \begin{bmatrix} \check{d}_i^1 \\ \vdots \\ \check{d}_i^m \end{bmatrix}^e \quad \text{and} \quad \mathfrak{f}_i^e \,.$$

Remark 4. One has to be careful in choosing the shape functions of the different global fields. To satisfy the discrete BBL-condition this cannot be done arbitrarily. But we follow a rather pragmatical approach here and will choose the same shape functions for the macro- and microscopical displacement fields and for the thermodynamic driving forces without caring about the stability condition. However this choice turns out to be disadvantageous in the sense that a locking effect occurs. To prevent this, the finite element formulation will be adopted in the next section by an enhanced strain field.

The element-wise representations in (2.19) can also be written in form of matrix-vector products:

$$\bar{\boldsymbol{u}}_h^e(\boldsymbol{x}) = \bar{\boldsymbol{H}}^e(\boldsymbol{\xi}) \bar{\boldsymbol{d}}^e \,, \quad \check{\boldsymbol{u}}_h^e(\boldsymbol{x}) = \check{\boldsymbol{H}}^e(\boldsymbol{\xi}) \check{\boldsymbol{d}}^e \quad \text{and} \quad \mathfrak{f}_h^e(\boldsymbol{x}) = \boldsymbol{H}_{\mathfrak{f}}^e(\boldsymbol{\xi}) \mathfrak{f}^e \,,$$

where e.g.

$$\bar{\boldsymbol{H}}^e = \begin{bmatrix} h_1 & 0 & 0 & \dots & h_{M^e} & 0 & 0 \\ 0 & h_1 & 0 & \dots & 0 & h_{M^e} & 0 \\ 0 & 0 & h_1 & \dots & 0 & 0 & h_{M^e} \end{bmatrix} \quad \text{and} \quad \bar{\boldsymbol{d}}^e = \begin{bmatrix} \bar{\boldsymbol{d}}_1^e \\ \vdots \\ \bar{\boldsymbol{d}}_{M^e}^e \end{bmatrix}.$$

Using the assembling operator A, we can summarize the global approximation of $\mathfrak{u}^*$ as

$$\mathfrak{u}_h^*(\boldsymbol{x}) = \mathop{\mathsf{A}}_{e=1}^{N} \begin{bmatrix} \bar{\boldsymbol{u}}_h^e \\ \check{\boldsymbol{u}}_h^e \\ \mathfrak{f}_h^e \end{bmatrix} = \mathop{\mathsf{A}}_{e=1}^{N} \underbrace{\begin{bmatrix} \bar{\boldsymbol{H}}^e & \boldsymbol{0} & \boldsymbol{0} \\ \boldsymbol{0} & \check{\boldsymbol{H}}^e & \boldsymbol{0} \\ \boldsymbol{0} & \boldsymbol{0} & \boldsymbol{H}_{\mathfrak{f}}^e \end{bmatrix}}_{=:\mathfrak{H}^{*e}} \underbrace{\begin{bmatrix} \bar{\boldsymbol{d}}^e \\ \check{\boldsymbol{d}}^e \\ \mathfrak{f}^e \end{bmatrix}}_{=:\mathfrak{d}^{*e}} = \mathfrak{H}^*(\boldsymbol{\xi})\mathfrak{d}^*\,,$$

and accordingly $\delta\mathfrak{u}_h^* = \mathfrak{H}^*(\boldsymbol{\xi})\delta\mathfrak{d}^*$. The approximation of the global constitutive state array $\mathfrak{c}^*$ is conceptually written in the same way:

$$\mathfrak{c}_h^* = \mathfrak{B}^*(\boldsymbol{\xi})\mathfrak{d}^*\,,$$

where $\mathfrak{B}^*(\boldsymbol{\xi}) := \mathfrak{D}^*\mathfrak{H}^*(\boldsymbol{\xi})$ with $\mathfrak{D}^*$ being a generalized differential operator matrix. Of course $\delta_{\mathfrak{u}_h^*}\mathfrak{c}_h^* = \mathfrak{B}^*(\boldsymbol{\xi})\delta\mathfrak{d}^*$.
Let the Lagrange-element-family interpolation space be denoted by $\mathcal{S}_h(\mathscr{B}_h) \subset \mathcal{H}^1(\mathscr{B}_h)$ and let

$$\begin{aligned} \mathcal{V}_{\bar{\boldsymbol{u}}h} &:= \mathcal{V}_{\bar{\boldsymbol{u}}}(\mathscr{B}_h) \cap [\mathcal{S}_h(\mathscr{B}_h)]^3\,, \\ \mathcal{V}_{\check{\boldsymbol{u}}h} &:= \mathcal{V}_{\check{\boldsymbol{u}}}(\mathscr{B}_h) \cap [\mathcal{S}_h(\mathscr{B}_h)]^m\,, \\ \mathcal{V}^0_{\bar{\boldsymbol{u}}h} &:= \mathcal{V}^0_{\bar{\boldsymbol{u}}}(\mathscr{B}_h) \cap [\mathcal{S}_h(\mathscr{B}_h)]^3\,, \\ \mathcal{V}^0_{\check{\boldsymbol{u}}h} &:= \mathcal{V}^0_{\check{\boldsymbol{u}}}(\mathscr{B}_h) \cap [\mathcal{S}_h(\mathscr{B}_h)]^m \end{aligned}$$

be the conform ansatz spaces. Then the discrete variational principle reads

$$\{\bar{\boldsymbol{u}}_h, \check{\boldsymbol{u}}_h, \boldsymbol{\mathcal{I}}, \mathfrak{f}_h, \boldsymbol{\mathcal{F}}\} = \arg\{\min_{\bar{\boldsymbol{u}}_h \in \mathcal{V}_{\bar{\boldsymbol{u}}h}} \min_{\check{\boldsymbol{u}}_h \in \mathcal{V}_{\check{\boldsymbol{u}}h}} \min_{\boldsymbol{\mathcal{I}}} \max_{\mathfrak{f}_h \in \mathcal{S}_h} \max_{\boldsymbol{\mathcal{F}}} [\Pi^{*\tau}_{\eta h}]\}$$

with $\Pi^{*\tau}_{\eta h} := \Pi^{*\tau}_{\eta}(\bar{\boldsymbol{u}}_h, \check{\boldsymbol{u}}_h, \boldsymbol{\mathcal{I}}, \mathfrak{f}_h, \boldsymbol{\mathcal{F}})$, where the local fields $\boldsymbol{\mathcal{I}}$ and $\boldsymbol{\mathcal{F}}$ will be evaluated by a local update algorithm on integration point level, and therefore are not discretized globally. The discrete reduced necessary condition is

$$\delta_{\mathfrak{u}_h^*}\Pi^{*\tau}_{\eta h} = \int_{\mathscr{B}_h} \partial_{\mathfrak{c}_h^*}\pi^{*\tau}_{\eta h} \cdot \delta_{\mathfrak{u}_h^*}\mathfrak{c}_h^* \,\mathrm{d}v - \int_{\mathscr{B}_h} \rho\mathfrak{g} \cdot \delta\mathfrak{u}_h^* \,\mathrm{d}v - \int_{\partial\mathscr{B}_{\mathfrak{t}h}} \mathfrak{t}_N \cdot \delta\mathfrak{u}_h^* \,\mathrm{d}s_{\boldsymbol{x}} = \boldsymbol{0}$$

for all $\delta\bar{\boldsymbol{u}}_h \in \mathcal{V}^0_{\bar{\boldsymbol{u}}h}$, $\delta\check{\boldsymbol{u}}_h \in \mathcal{V}^0_{\check{\boldsymbol{u}}h}$ and $\delta\mathfrak{f}_h \in \mathcal{S}_h$, with $\pi^{*\tau}_{\eta h} := \pi^{*\tau}_{\eta}(\mathfrak{c}_h^*, \mathfrak{c}_{nh}^*, \mathfrak{s}, \mathfrak{s}_n)$. Plugging in all above relations, we obtain a system of nonlinear equations in $\mathfrak{d}^*$:

$$\boldsymbol{F}(\mathfrak{d}^*) := \int_{\mathscr{B}_h} \mathfrak{B}^{*T}\boldsymbol{\sigma}^* \,\mathrm{d}v - \int_{\mathscr{B}_h} \mathfrak{H}^{*T}\rho\mathfrak{g} \,\mathrm{d}v - \int_{\partial\mathscr{B}_{\mathfrak{t}h}} \mathfrak{H}^{*T}\mathfrak{t}_N \,\mathrm{d}s_{\boldsymbol{x}} = \boldsymbol{0}\,, \tag{2.20}$$

where

$$\boldsymbol{\sigma}^* := [\partial_{\mathfrak{c}_h^*}\pi^{*\tau}_{\eta h}(\mathfrak{c}_h^*(\mathfrak{d}^*), \mathfrak{c}_{nh}^*(\mathfrak{d}_n^*), \mathfrak{s}, \mathfrak{s}_n)] \tag{2.21}$$

is a row matrix containing generalized stresses. Because of its nonlinearity, the system (2.20) must be solved iteratively. This will be done by a Newton-Raphson scheme. Let a solution estimate $\mathfrak{d}^{*k}$ at iteration $k+1$, obtained by iteration k, be given, which is not an equilibrium state. A new solution

$$\mathfrak{d}^{*k+1} = \mathfrak{d}^{*k} + \Delta\mathfrak{d}^{*k}$$

in terms of an increment $\Delta\mathfrak{d}^{*k}$ is obtained by a linearisation of (2.20) around $\mathfrak{d}^{*k}$:

$$\begin{aligned}\boldsymbol{F}(\mathfrak{d}^{*k+1}) &\approx \boldsymbol{F}(\mathfrak{d}^{*k}) + \partial_{\mathfrak{d}^*}\boldsymbol{F}(\mathfrak{d}^*)|_{\mathfrak{d}^{*k}}\,\Delta\mathfrak{d}^{*k} \\ &= \boldsymbol{F}(\mathfrak{d}^{*k}) + \int_{\mathscr{B}_h} \mathfrak{B}^{*T}[\partial^2_{\mathfrak{c}^*_h\mathfrak{c}^*_h}\pi^{*\tau}_{\eta h}]|_{\mathfrak{d}^{*k}}\partial_{\mathfrak{d}^*}\mathfrak{c}^*_h\,\mathrm{d}v\,\Delta\mathfrak{d}^{*k} \\ &=: \boldsymbol{F}(\mathfrak{d}^{*k}) + \int_{\mathscr{B}_h} \mathfrak{B}^{*T}\mathbb{C}^{*k}\mathfrak{B}^*\,\mathrm{d}v\,\Delta\mathfrak{d}^{*k} = \mathbf{0}\,,\end{aligned}$$

where we introduced the material tangent moduli $\mathbb{C}^{*k}$.

Remark 5. The use of partial differentials in the above Taylor expansion is mathematically a bit improper, and concerning the material tangent moduli it can be misleading. Suppressing the dependency of the rate potential per unit volume on the global and local state at t_n, a proper definition of $\mathbb{C}^{*k}$ reads

$$\mathbb{C}^{*k} := \left\{\frac{\mathrm{d}}{\mathrm{d}\mathfrak{c}^*_h}\left[\frac{\partial}{\partial\mathfrak{c}^*_h}\pi^{*\tau}_\eta(\mathfrak{c}^*_h,\mathfrak{s})\right]\right\}\Big|_{\mathfrak{d}^{*k}}\,.$$

This means, that for the outer derivation the dependency of the local set $\mathfrak{s}$ on the global field variables, coming from the local update algorithm, must be respected. However, to make writing easier, we will use the notation

$$\mathbb{C}^{*k} = [\partial^2_{\mathfrak{c}^*_h\mathfrak{c}^*_h}\pi^{*\tau}_{\eta h}]|_{\mathfrak{d}^{*k}}\,, \tag{2.22}$$

given in the above Taylor expansion.

With the stiffness matrix

$$\boldsymbol{K}^{*k} := \int_{\mathscr{B}_h} \mathfrak{B}^{*T}\mathbb{C}^{*k}\mathfrak{B}^*\,\mathrm{d}v\,,$$

the vector of internal forces

$$\boldsymbol{f}^{*k}_{int} := \int_{\mathscr{B}_h} \mathfrak{B}^{*T}\boldsymbol{\sigma}^{*k}\,\mathrm{d}v$$

and the vector of external forces

$$\boldsymbol{f}^*_{ext} := \int_{\mathscr{B}_h} \mathfrak{H}^{*T}\rho\mathfrak{g}\,\mathrm{d}v + \int_{\partial\mathscr{B}_{\mathfrak{t}h}} \mathfrak{H}^{*T}\mathfrak{t}_N\,\mathrm{d}s_{\boldsymbol{x}}\,, \tag{2.23}$$

we obtain the linear system of equations

$$\boldsymbol{K}^{*k}\Delta\mathfrak{d}^{*k} = \underbrace{-\boldsymbol{f}^{*k}_{int} + \boldsymbol{f}^*_{ext}}_{=:\boldsymbol{r}^{*k}}$$

from which we can calculate $\Delta\mathfrak{d}^{*k}$ and get the new solution $\mathfrak{d}^{*k+1}$. With this at hand the new stresses $\boldsymbol{\sigma}^{*k+1}$ can be computed via the nonlinear constitutive law, and accordingly the new residuum $\boldsymbol{r}^{*k+1}$ is known. One should also note, that at every iteration a new stiffness matrix must be calculated. However, this disadvantage is compensated by a quadratic order of convergence, in contrast to, e.g., the modified Newton-Raphson scheme, where throughout the iteration the same initial stiffness matrix is used, but only a linear order of convergence is achieved. On the other hand, since we remain in the geometrically linear theory, the $\mathfrak{B}^{*e}$ matrices must only be computed one time for every integration point. For one-dimensional problems the Newton-Raphson scheme is illustrated in Figure 2.3.

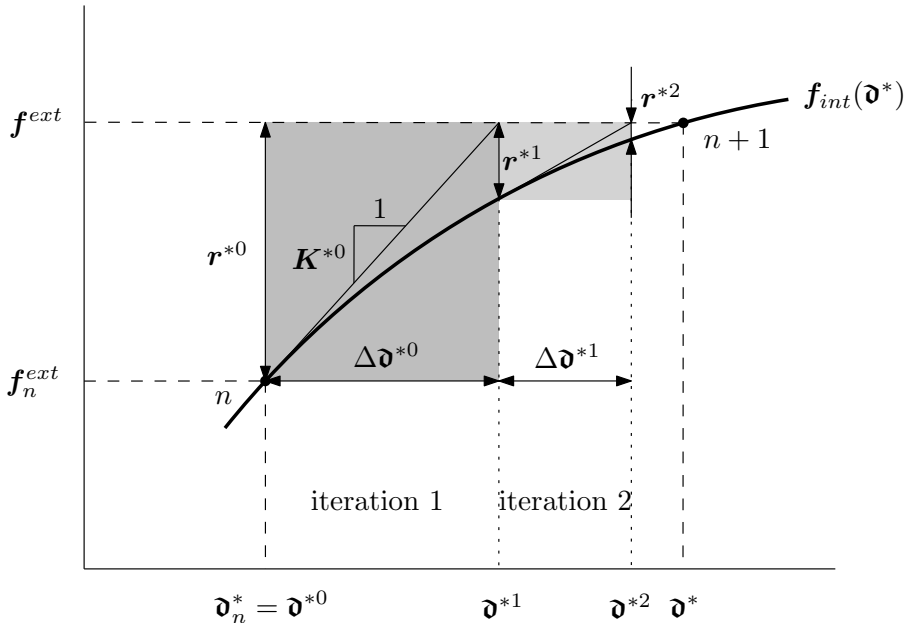

Figure 2.3. The Newton-Raphson scheme. Here $\boldsymbol{f}_{int}(\mathfrak{d}^*)$ denotes a function in terms of the independent variable $\mathfrak{d}^*$, which is not only meant to be evaluated at $n+1$. The grey rectangles display the corresponding unbalanced energies ue^0 and ue^1.

As measure how far we are still away from equilibrium, we introduce the unbalanced energy at iteration $k+1$

$$ue^k := \left\| [\boldsymbol{r}^{*k}]^T \Delta\mathfrak{d}^{*k} \right\| ,$$

and break off the iteration if we fall bellow a given tolerance *tol*:

$$ue^k \leq tol\,.$$

Remark 6. It is important to note, that the Newton-Raphson scheme is locally convergent and may fail if the solution estimate $\mathfrak{d}^{*0}$ is too far away from the exact solution.

Remark 7. Since the incremental Dirichlet boundary conditions are exactly fulfilled after the first Newton-Raphson iteration step, they have to be set zero for all remaining steps within an increment.

2.5. Enhanced-strain method

In order to prevent locking, several mixed methods are used today, e.g. methods based on the Hu-Washizu principle. Beside the displacements, it also treats the stresses and strains as independent variables. This of course comes along with an increase of degrees of freedom. The enhanced strain method [25] bases on the idea to treat the additional degrees of freedom only on element level, which allows them to be eliminated by a static condensation. Hence, the advantage of such an adaption lies in the circumstance, that the number of degrees of freedom is the same as in a pure displacement formulation. To realize this idea, we enhance the macroscopic strain field $\bar{\boldsymbol{\varepsilon}}$ by some additional strains ${}^e\bar{\boldsymbol{\varepsilon}}$, i.e.

$$\bar{\boldsymbol{\varepsilon}}(\bar{\boldsymbol{u}}, {}^e\bar{\boldsymbol{\varepsilon}}) = \frac{1}{2}\left[\nabla\bar{\boldsymbol{u}} + (\nabla\bar{\boldsymbol{u}})^T\right] + {}^e\bar{\boldsymbol{\varepsilon}} \tag{2.24}$$

and use ${}^e\bar{\boldsymbol{\varepsilon}}$ instead of $\bar{\boldsymbol{\varepsilon}}$ as independent variable in the Hu-Washizu potential formulation. Writing (2.24) as ${}^e\bar{\boldsymbol{\varepsilon}} = \bar{\boldsymbol{\varepsilon}} - \frac{1}{2}\left[\nabla\bar{\boldsymbol{u}} + (\nabla\bar{\boldsymbol{u}})^T\right]$ we see, that the introduction of enhanced

strains ${}^e\bar{\boldsymbol{\varepsilon}}$ is nothing else than a substitution, and we can interpret ${}^e\bar{\boldsymbol{\varepsilon}}$ as a residuum. Accordingly the constitutive state (2.1) reads

$$\mathfrak{c}(\mathfrak{u}, {}^e\bar{\boldsymbol{\varepsilon}}) := \{\bar{\boldsymbol{\varepsilon}}(\bar{\boldsymbol{u}}, {}^e\bar{\boldsymbol{\varepsilon}}), \check{\boldsymbol{u}}, \nabla\check{\boldsymbol{u}}\} \quad \text{with} \quad \mathfrak{u} = \{\bar{\boldsymbol{u}}, \check{\boldsymbol{u}}\} \,, \tag{2.25}$$

and the extended constitutive state (2.13)

$$\mathfrak{c}^*(\mathfrak{u}^*, {}^e\bar{\boldsymbol{\varepsilon}}) := \{\bar{\boldsymbol{\varepsilon}}(\bar{\boldsymbol{u}}, {}^e\bar{\boldsymbol{\varepsilon}}), \check{\boldsymbol{u}}, \nabla\check{\boldsymbol{u}}, \mathfrak{f}\} \quad \text{with} \quad \mathfrak{u}^* = \{\bar{\boldsymbol{u}}, \check{\boldsymbol{u}}, \mathfrak{f}\} \,.$$

2.5.1. Hu-Washizu principle

Starting point is the potential (2.9) in its viscous-regularized form:

$$\Pi^*_\eta(\dot{\bar{\boldsymbol{u}}}, \dot{\check{\boldsymbol{u}}}, \dot{\boldsymbol{\mathcal{I}}}, \mathfrak{f}, \boldsymbol{\mathcal{F}}) = \int_{\mathscr{B}} \pi^*_\eta(\mathfrak{c}, \boldsymbol{\mathcal{I}}, \dot{\mathfrak{c}}, \dot{\boldsymbol{\mathcal{I}}}, \mathfrak{f}, \boldsymbol{\mathcal{F}}) \,\mathrm{d}v - P_{ext}(\dot{\mathfrak{u}}, t)$$

with π^*_η given in (2.11). The kinematic constraint ${}^e\dot{\bar{\boldsymbol{\varepsilon}}} = \boldsymbol{0}$ is considered in the potential by a Lagrange multiplier $\boldsymbol{\lambda}$, i.e.

$$\tilde{\Pi}^*_\eta(\dot{\bar{\boldsymbol{u}}}, \dot{\check{\boldsymbol{u}}}, \dot{\boldsymbol{\mathcal{I}}}, \mathfrak{f}, \boldsymbol{\mathcal{F}}, \boldsymbol{\lambda}, {}^e\dot{\bar{\boldsymbol{\varepsilon}}}) := \int_{\mathscr{B}} (\pi^*_\eta - \boldsymbol{\lambda} : {}^e\dot{\bar{\boldsymbol{\varepsilon}}}) \,\mathrm{d}v - P_{ext}(\dot{\mathfrak{u}}, t) \,.$$

To make this potential stationary the necessary condition reads

$$\delta\tilde{\Pi}^*_\eta = \delta_{\dot{\bar{\boldsymbol{u}}}}\tilde{\Pi}^*_\eta + \delta_{\dot{\check{\boldsymbol{u}}}}\tilde{\Pi}^*_\eta + \delta_{\dot{\boldsymbol{\mathcal{I}}}}\tilde{\Pi}^*_\eta + \delta_{\mathfrak{f}}\tilde{\Pi}^*_\eta + \delta_{\boldsymbol{\mathcal{F}}}\tilde{\Pi}^*_\eta + \delta_{\boldsymbol{\lambda}}\tilde{\Pi}^*_\eta + \delta_{{}^e\dot{\bar{\boldsymbol{\varepsilon}}}}\tilde{\Pi}^*_\eta = 0$$

for all $\delta\dot{\bar{\boldsymbol{u}}} \in \mathcal{V}^0_{\bar{\boldsymbol{u}}}$, $\delta\dot{\check{\boldsymbol{u}}} \in \mathcal{V}^0_{\check{\boldsymbol{u}}}$, $\delta\dot{\boldsymbol{\mathcal{I}}} \in \mathcal{L}_2$, $\delta\mathfrak{f} \in \mathcal{L}_2$, $\delta\boldsymbol{\mathcal{F}} \in \mathcal{L}_2$, $\delta\boldsymbol{\lambda} \in \mathcal{L}_2$ and $\delta{}^e\dot{\bar{\boldsymbol{\varepsilon}}} \in \mathcal{L}_2$, where

$$\begin{aligned}
\delta_{\boldsymbol{\lambda}}\tilde{\Pi}^*_\eta &= \int_{\mathscr{B}} {}^e\dot{\bar{\boldsymbol{\varepsilon}}} : \delta\boldsymbol{\lambda} \,\mathrm{d}v \,, \\
\delta_{{}^e\dot{\bar{\boldsymbol{\varepsilon}}}}\tilde{\Pi}^*_\eta &= \int_{\mathscr{B}} (\partial_{{}^e\dot{\bar{\boldsymbol{\varepsilon}}}}\dot{\psi} + \bar{\boldsymbol{\mathcal{F}}} - \boldsymbol{\lambda}) : \delta\,{}^e\dot{\bar{\boldsymbol{\varepsilon}}} \,\mathrm{d}v \,.
\end{aligned}$$

Note that according to (2.4) $\partial_{{}^e\dot{\bar{\boldsymbol{\varepsilon}}}}\dot{\psi} = \partial_{\bar{\boldsymbol{\varepsilon}}}\psi$, and a localization argument gives

$$\boldsymbol{\lambda} = \partial_{\bar{\boldsymbol{\varepsilon}}}\psi + \bar{\boldsymbol{\mathcal{F}}} \quad \text{and} \quad {}^e\dot{\bar{\boldsymbol{\varepsilon}}} = \boldsymbol{0} \,.$$

From this we see, that the Lagrange multiplier $\boldsymbol{\lambda}$ equals the total stress tensor[2] $\bar{\boldsymbol{\sigma}}$ in the weak sense. Hence, we define a rate potential per unit volume of Hu-Washizu type as

$$\tilde{\pi}^*_\eta(\mathfrak{c}, \boldsymbol{\mathcal{I}}, \dot{\mathfrak{c}}, \dot{\boldsymbol{\mathcal{I}}}, \mathfrak{f}, \boldsymbol{\mathcal{F}}, \bar{\boldsymbol{\sigma}}) := \frac{\mathrm{d}}{\mathrm{d}t}\psi(\mathfrak{c}, \boldsymbol{\mathcal{I}}) - \bar{\boldsymbol{\sigma}} : {}^e\dot{\bar{\boldsymbol{\varepsilon}}} + \mathfrak{f} \cdot \dot{\mathfrak{c}} + \boldsymbol{\mathcal{F}} \cdot \dot{\boldsymbol{\mathcal{I}}} - \frac{1}{2\eta}\langle\varphi(\mathfrak{f}, \boldsymbol{\mathcal{F}}, \mathfrak{c}, \boldsymbol{\mathcal{I}})\rangle^2 \,.$$

A consistent time incrementation reads

$$\begin{aligned}
\tilde{\pi}^{*\tau}_\eta(\mathfrak{c}^*, \mathfrak{c}^*_n, \mathfrak{s}, \mathfrak{s}_n, \bar{\boldsymbol{\sigma}}, \bar{\boldsymbol{\sigma}}_n) = \psi(\mathfrak{c}, \boldsymbol{\mathcal{I}}) - \psi(\mathfrak{c}_n, \boldsymbol{\mathcal{I}}_n) - \bar{\boldsymbol{\sigma}} : {}^e\bar{\boldsymbol{\varepsilon}} + \bar{\boldsymbol{\sigma}}_n : {}^e\bar{\boldsymbol{\varepsilon}}_n \\
+ \mathfrak{f} \cdot (\mathfrak{c} - \mathfrak{c}_n) + \boldsymbol{\mathcal{F}} \cdot (\boldsymbol{\mathcal{I}} - \boldsymbol{\mathcal{I}}_n) \\
- \frac{\tau}{2\eta}\langle\varphi(\mathfrak{f}, \boldsymbol{\mathcal{F}}, \mathfrak{c}_n, \boldsymbol{\mathcal{I}}_n)\rangle^2 \,,
\end{aligned}$$

where again quantities without sub index are meant to be evaluated at time t_{n+1}. Accordingly

$$\tilde{\Pi}^{*\tau}_\eta(\mathfrak{u}^*, \mathfrak{s}, {}^e\bar{\boldsymbol{\varepsilon}}, \bar{\boldsymbol{\sigma}}) = \int_{\mathscr{B}} \tilde{\pi}^{*\tau}_\eta(\mathfrak{c}^*, \mathfrak{c}^*_n, \mathfrak{s}, \mathfrak{s}_n, \bar{\boldsymbol{\sigma}}, \bar{\boldsymbol{\sigma}}_n) \,\mathrm{d}v - P^\tau_{ext}(\mathfrak{u}, \mathfrak{u}_n)$$

[2] The total stress tensor also contains the dissipative stresses $\bar{\boldsymbol{\mathcal{F}}}$.

and the variational principle reads

$$\{\bar{\boldsymbol{u}}, \check{\boldsymbol{u}}, \boldsymbol{\mathcal{I}}, \mathfrak{f}, \boldsymbol{\mathcal{F}}, {}^e\bar{\boldsymbol{\varepsilon}}, \bar{\boldsymbol{\sigma}}\} = \arg\{\min_{\bar{\boldsymbol{u}}\in\mathcal{V}_{\bar{\boldsymbol{u}}}} \min_{\check{\boldsymbol{u}}\in\mathcal{V}_{\check{\boldsymbol{u}}}} \min_{\boldsymbol{\mathcal{I}}\in\mathcal{L}_2} \max_{\mathfrak{f}\in\mathcal{L}_2} \max_{\boldsymbol{\mathcal{F}}\in\mathcal{L}_2} \min_{{}^e\bar{\boldsymbol{\varepsilon}}\in\mathcal{L}_2} \max_{\bar{\boldsymbol{\sigma}}\in\mathcal{L}_2} [\tilde{\Pi}_\eta^{*\tau}(\bar{\boldsymbol{u}}, \check{\boldsymbol{u}}, \boldsymbol{\mathcal{I}}, \mathfrak{f}, \boldsymbol{\mathcal{F}}, {}^e\bar{\boldsymbol{\varepsilon}}, \bar{\boldsymbol{\sigma}})]\}\,.$$

As discussed in the end of Section 2.3, the necessary condition for this problem can be reduced to

$$\delta\tilde{\Pi}_\eta^{*\tau} = \delta_{\mathfrak{u}^*}\tilde{\Pi}_\eta^{*\tau} + \delta_{e\bar{\boldsymbol{\varepsilon}}}\tilde{\Pi}_\eta^{*\tau} + \delta_{\bar{\boldsymbol{\sigma}}}\tilde{\Pi}_\eta^{*\tau} = 0$$

for all $\delta\bar{\boldsymbol{u}} \in \mathcal{V}_{\bar{\boldsymbol{u}}}^0$, $\delta\check{\boldsymbol{u}} \in \mathcal{V}_{\check{\boldsymbol{u}}}^0$, $\delta\mathfrak{f} \in \mathcal{L}_2$, $\delta^e\bar{\boldsymbol{\varepsilon}} \in \mathcal{L}_2$ and $\delta\bar{\boldsymbol{\sigma}} \in \mathcal{L}_2$, with

$$\begin{aligned}
\delta_{\mathfrak{u}^*}\tilde{\Pi}_\eta^{*\tau} &= \int_{\mathscr{B}} \partial_{\mathfrak{c}^*}\tilde{\pi}_\eta^{*\tau} \cdot \delta_{\mathfrak{u}^*}\mathfrak{c}^* \,\mathrm{d}v - \int_{\mathscr{B}} \rho\mathfrak{g} \cdot \delta\mathfrak{u}^* \,\mathrm{d}v - \int_{\partial\mathscr{B}_\mathfrak{t}} \mathfrak{t}_N \cdot \delta\mathfrak{u}^* \,\mathrm{d}s_{\boldsymbol{x}}\,,\\
\delta_{e\bar{\boldsymbol{\varepsilon}}}\tilde{\Pi}_\eta^{*\tau} &= \int_{\mathscr{B}} \partial_{e\bar{\boldsymbol{\varepsilon}}}\tilde{\pi}_\eta^{*\tau} : \delta^e\bar{\boldsymbol{\varepsilon}} \,\mathrm{d}v = \int_{\mathscr{B}} (\partial_{\bar{\boldsymbol{\varepsilon}}}\tilde{\pi}_\eta^{*\tau} - \bar{\boldsymbol{\sigma}}) : \delta^e\bar{\boldsymbol{\varepsilon}} \,\mathrm{d}v\,,\\
\delta_{\bar{\boldsymbol{\sigma}}}\tilde{\Pi}_\eta^{*\tau} &= \int_{\mathscr{B}} \partial_{\bar{\boldsymbol{\sigma}}}\tilde{\pi}_\eta^{*\tau} : \delta\bar{\boldsymbol{\sigma}} \,\mathrm{d}v\,,
\end{aligned}$$

where $\partial_{\bar{\boldsymbol{\varepsilon}}}\tilde{\pi}_\eta^{*\tau} = \partial_{\bar{\boldsymbol{\varepsilon}}}\psi + \bar{\boldsymbol{\mathcal{F}}}$ and $\partial_{\bar{\boldsymbol{\sigma}}}\tilde{\pi}_\eta^{*\tau} = -{}^e\bar{\boldsymbol{\varepsilon}}$, from which we follow, that $\tilde{\pi}_\eta^{*\tau}$ indeed comes from a consistent integration algorithm. However, note that in the finite element approximation ${}^e\bar{\boldsymbol{\varepsilon}}_h \neq \mathbf{0}$ in $\mathscr{B}_h$.

2.5.2. Finite element discretization

Again, the discretized global fields are denoted by the sub index h. The discrete variational principle reads

$$\{\bar{\boldsymbol{u}}_h, \check{\boldsymbol{u}}_h, \boldsymbol{\mathcal{I}}, \mathfrak{f}_h, \boldsymbol{\mathcal{F}}, {}^e\bar{\boldsymbol{\varepsilon}}_h, \bar{\boldsymbol{\sigma}}_h\} = \arg\{\min_{\bar{\boldsymbol{u}}_h\in\mathcal{V}_{\bar{\boldsymbol{u}}h}} \min_{\check{\boldsymbol{u}}_h\in\mathcal{V}_{\check{\boldsymbol{u}}h}} \min_{\boldsymbol{\mathcal{I}}} \max_{\mathfrak{f}_h\in\mathcal{S}_h} \max_{\boldsymbol{\mathcal{F}}} \min_{{}^e\bar{\boldsymbol{\varepsilon}}_h} \max_{\bar{\boldsymbol{\sigma}}_h} [\tilde{\Pi}_{\eta h}^{*\tau}]\}\,,$$

with $\tilde{\Pi}_{\eta h}^{*\tau} := \tilde{\Pi}_\eta^{*\tau}(\mathfrak{u}_h^*, \mathfrak{s}, {}^e\bar{\boldsymbol{\varepsilon}}_h, \bar{\boldsymbol{\sigma}}_h)$, where, as already mentioned before, the local solution pair $\mathfrak{s} = \{\boldsymbol{\mathcal{I}}, \boldsymbol{\mathcal{F}}\}$ is computed by a local update algorithm on integration point level. The ansatz spaces for the discrete stresses $\bar{\boldsymbol{\sigma}}_h$ and for the discrete enhanced strains ${}^e\bar{\boldsymbol{\varepsilon}}_h$ remain unspecified yet. The reduced necessary condition is

$$\delta_{\mathfrak{u}_h^*}\tilde{\Pi}_{\eta h}^{*\tau} + \delta_{e\bar{\boldsymbol{\varepsilon}}_h}\tilde{\Pi}_{\eta h}^{*\tau} + \delta_{\bar{\boldsymbol{\sigma}}_h}\tilde{\Pi}_{\eta h}^{*\tau} = 0$$

for all $\delta\bar{\boldsymbol{u}}_h \in \mathcal{V}_{\bar{\boldsymbol{u}}h}^0$, $\delta\check{\boldsymbol{u}}_h \in \mathcal{V}_{\check{\boldsymbol{u}}h}^0$, $\delta\mathfrak{f}_h \in \mathcal{S}_h$, $\delta^e\bar{\boldsymbol{\varepsilon}}_h$ and $\delta\bar{\boldsymbol{\sigma}}_h$. To lower the computational costs we want to eliminate $\bar{\boldsymbol{\sigma}}_h$. For this purpose we assume the discrete stresses and enhanced strains to fulfil the orthogonality relation

$$\int_{\mathscr{B}_h} \bar{\boldsymbol{\sigma}}_h : {}^e\bar{\boldsymbol{\varepsilon}}_h \,\mathrm{d}v = 0\,. \tag{2.26}$$

This condition is a first specification of the ansatz spaces for discrete stresses and discrete enhanced strains, which are now not independent any more. With (2.26) at hand we can say

$$\int_{\mathscr{B}_h} \bar{\boldsymbol{\sigma}}_h : \delta^e\bar{\boldsymbol{\varepsilon}}_h \,\mathrm{d}v = 0 \quad \text{and} \quad \int_{\mathscr{B}_h} {}^e\bar{\boldsymbol{\varepsilon}}_h : \delta\bar{\boldsymbol{\sigma}}_h \,\mathrm{d}v = 0\,,$$

and get the simplified system of equations

$$\mathbf{0} = \begin{bmatrix} \delta_{\mathfrak{u}_h^*}\tilde{\Pi}_{\eta h}^{*\tau} \\ \delta_{e\bar{\boldsymbol{\varepsilon}}_h}\tilde{\Pi}_{\eta h}^{*\tau} \end{bmatrix}$$

with

$$\delta_{\mathbf{u}_h^*}\tilde{\Pi}_{\eta h}^{*\tau} = \int_{\mathscr{B}_h} \partial_{\mathfrak{c}_h^*}\tilde{\pi}_{\eta h}^{*\tau}\cdot\delta_{\mathbf{u}_h^*}\mathfrak{c}_h^*\,\mathrm{d}v - \int_{\mathscr{B}_h}\rho\mathfrak{g}\cdot\delta\mathbf{u}_h^*\,\mathrm{d}v\,,$$
$$\delta_{^e\bar{\boldsymbol{\varepsilon}}_h}\tilde{\Pi}_{\eta h}^{*\tau} = \int_{\mathscr{B}_h} \partial_{\bar{\boldsymbol{\varepsilon}}_h}\tilde{\pi}_{\eta h}^{*\tau} : \delta^e\bar{\boldsymbol{\varepsilon}}_h\,\mathrm{d}v\,,$$

where $\tilde{\pi}_{\eta h}^{*\tau} := \tilde{\pi}_{\eta}^{*\tau}(\mathfrak{c}_h^*, \mathfrak{c}_{nh}^*, \mathfrak{s}, \mathfrak{s}_n, \bar{\boldsymbol{\sigma}}_h, \bar{\boldsymbol{\sigma}}_{nh})$. According to Section 2.4, we have $\delta\mathbf{u}_h^* = \mathfrak{H}^*(\boldsymbol{\xi})\delta\mathfrak{d}^*$ and $\delta_{\mathbf{u}_h^*}\mathfrak{c}_h^* = \mathfrak{B}^*(\boldsymbol{\xi})\delta\mathfrak{d}^*$. The enhanced strains $^e\bar{\boldsymbol{\varepsilon}}_h$ and its variation $\delta^e\bar{\boldsymbol{\varepsilon}}_h$ are approximated in Voigt's notation on element level by

$$^e\bar{\boldsymbol{\varepsilon}}_h =: \mathop{\mathsf{A}}_{e=1}^{n} \boldsymbol{A}^e(\boldsymbol{\xi})\bar{\boldsymbol{a}}^e =: \boldsymbol{A}(\boldsymbol{\xi})\bar{\boldsymbol{a}} \quad\text{and}\quad \delta^e\bar{\boldsymbol{\varepsilon}}_h = \boldsymbol{A}(\boldsymbol{\xi})\delta\bar{\boldsymbol{a}}\,, \tag{2.27}$$

where $\boldsymbol{A}^e(\boldsymbol{\xi})$ is the element interpolation matrix, and $\bar{\boldsymbol{a}}^e$ a row matrix containing the element degrees of freedom of the enhanced strain $^e\bar{\boldsymbol{\varepsilon}}_h$. It should be mentioned, that $\bar{\boldsymbol{a}}^e$ does not contain any nodal values; its entries are constant over the element e. The structure of the matrix $\boldsymbol{A}^e(\boldsymbol{\xi})$ will be derived at the end of the next chapter. Note that due to the geometrical linearity, the $\boldsymbol{A}^e$ matrices, like the $\mathfrak{B}^{*e}$ matrices, do not change in the integration points during the whole incrementation and iteration process.
With all these approximations at hand, the system of nonlinear equations in $\mathfrak{d}^*$ and $\bar{\boldsymbol{a}}$ reads

$$\boldsymbol{F}(\mathfrak{d}^*, \bar{\boldsymbol{a}}) = \begin{bmatrix} \int_{\mathscr{B}_h}\mathfrak{B}^{*T}\boldsymbol{\sigma}^*\,\mathrm{d}v - \int_{\mathscr{B}_h}\mathfrak{H}^{*T}\rho\mathfrak{g}\,\mathrm{d}v - \int_{\partial\mathscr{B}_{\mathfrak{t}h}}\mathfrak{H}^{*T}\mathbf{t}_N\,\mathrm{d}s_{\boldsymbol{x}} \\ \int_{\mathscr{B}_h}\boldsymbol{A}^T[\partial_{\bar{\boldsymbol{\varepsilon}}_h}\pi_{\eta h}^{*\tau}]\,\mathrm{d}v \end{bmatrix} = \mathbf{0}\,, \tag{2.28}$$

where we have considered that $\partial_{\mathfrak{c}_h^*}\pi_{\eta h}^{*\tau} = \partial_{\mathfrak{c}_h^*}\tilde{\pi}_{\eta h}^{*\tau}$, and used the definition of the generalized stresses (2.21)

$$\boldsymbol{\sigma}^* = [\partial_{\mathfrak{c}_h^*}\pi_{\eta h}^{*\tau}(\mathfrak{c}_h^*(\mathfrak{d}^*, \bar{\boldsymbol{a}}), \mathfrak{c}_{nh}^*(\mathfrak{d}_n^*, \bar{\boldsymbol{a}}_n), \mathfrak{s}, \mathfrak{s}_n)]\,.$$

To solve the nonlinear system (2.28) we again make use of the Newton-Raphson procedure. For this, we do a linearisation of $\boldsymbol{F}(\mathfrak{d}^*, \bar{\boldsymbol{a}})$ around $(\mathfrak{d}^{*k}, \bar{\boldsymbol{a}}^k)$:

$$\boldsymbol{F}(\mathfrak{d}^{*k+1}, \bar{\boldsymbol{a}}^{k+1}) \approx \boldsymbol{F}(\mathfrak{d}^{*k}, \bar{\boldsymbol{a}}^k) + \begin{bmatrix} \boldsymbol{K}_{\mathfrak{d}^*\mathfrak{d}^*}^{*k} & \boldsymbol{K}_{\mathfrak{d}^*\bar{\boldsymbol{a}}}^{*k} \\ \boldsymbol{K}_{\bar{\boldsymbol{a}}\mathfrak{d}^*}^{*k} & \boldsymbol{K}_{\bar{\boldsymbol{a}}\bar{\boldsymbol{a}}}^{*k} \end{bmatrix} \begin{bmatrix} \Delta\mathfrak{d}^{*k} \\ \Delta\bar{\boldsymbol{a}}^k \end{bmatrix}$$

with the single sub stiffness matrices

$$\begin{aligned}
\boldsymbol{K}_{\mathfrak{d}^*\mathfrak{d}^*}^{*k} &= \int_{\mathscr{B}_h}\mathfrak{B}^{*T}[\partial^2_{\bar{\boldsymbol{\varepsilon}}_h\bar{\boldsymbol{\varepsilon}}_h}\pi_{\eta h}^{*\tau}]|_{(\mathfrak{d}^{*k},\bar{\boldsymbol{a}}^k)}\mathfrak{B}^*\,\mathrm{d}v\,,\\
\boldsymbol{K}_{\mathfrak{d}^*\bar{\boldsymbol{a}}}^{*k} &= \int_{\mathscr{B}_h}\mathfrak{B}^{*T}[\partial^2_{\mathfrak{c}_h^*\bar{\boldsymbol{\varepsilon}}_h}\pi_{\eta h}^{*\tau}]|_{(\mathfrak{d}^{*k},\bar{\boldsymbol{a}}^k)}\boldsymbol{A}\,\mathrm{d}v\\
\boldsymbol{K}_{\bar{\boldsymbol{a}}\mathfrak{d}^*}^{*k} &= \int_{\mathscr{B}_h}\boldsymbol{A}^T[\partial^2_{\bar{\boldsymbol{\varepsilon}}_h\mathfrak{c}_h^*}\pi_{\eta h}^{*\tau}]|_{(\mathfrak{d}^{*k},\bar{\boldsymbol{a}}^k)}\mathfrak{B}^*\,\mathrm{d}v = [\boldsymbol{K}_{\mathfrak{d}^*\bar{\boldsymbol{a}}}^{*k}]^T\\
\boldsymbol{K}_{\bar{\boldsymbol{a}}\bar{\boldsymbol{a}}}^{*k} &= \int_{\mathscr{B}_h}\boldsymbol{A}^T[\partial^2_{\bar{\boldsymbol{\varepsilon}}_h\bar{\boldsymbol{\varepsilon}}_h}\pi_{\eta h}^{*\tau}]|_{(\mathfrak{d}^{*k},\bar{\boldsymbol{a}}^k)}\boldsymbol{A}\,\mathrm{d}v\,.
\end{aligned} \tag{2.29}$$

Then, together with the vector of internal forces at iteration k

$$\begin{bmatrix} \boldsymbol{f}_{int\,\mathfrak{d}^*}^{*k} \\ \boldsymbol{f}_{int\,\bar{\boldsymbol{a}}}^{*k} \end{bmatrix} := \begin{bmatrix} \int_{\mathscr{B}_h}\mathfrak{B}^{*T}\boldsymbol{\sigma}^{*k}\,\mathrm{d}v \\ \int_{\mathscr{B}_h}\boldsymbol{A}^T[\partial_{\bar{\boldsymbol{\varepsilon}}_h}\pi_{\eta}^{*\tau}]|_{(\mathfrak{d}^{*k},\bar{\boldsymbol{a}}^k)}\,\mathrm{d}v \end{bmatrix},$$

and the vector of external forces (2.23), we obtain the block system

$$\begin{bmatrix} \boldsymbol{K}_{\mathfrak{d}^*\mathfrak{d}^*}^{*k} & \boldsymbol{K}_{\mathfrak{d}^*\bar{\boldsymbol{a}}}^{*k} \\ \boldsymbol{K}_{\bar{\boldsymbol{a}}\mathfrak{d}^*}^{*k} & \boldsymbol{K}_{\bar{\boldsymbol{a}}\bar{\boldsymbol{a}}}^{*k} \end{bmatrix} \begin{bmatrix} \Delta\mathfrak{d}^{*k} \\ \Delta\bar{\boldsymbol{a}}^k \end{bmatrix} = \begin{bmatrix} -\boldsymbol{f}_{int\,\mathfrak{d}^*}^{*k} + \boldsymbol{f}_{ext}^* \\ -\boldsymbol{f}_{int\,\bar{\boldsymbol{a}}}^{*k} \end{bmatrix} =: \begin{bmatrix} \boldsymbol{r}_{\mathfrak{d}^*}^{*k} \\ \boldsymbol{r}_{\bar{\boldsymbol{a}}}^{*k} \end{bmatrix}, \tag{2.30}$$

from which $\Delta\mathfrak{d}^{*k}$ and $\Delta\bar{\boldsymbol{a}}^k$ could be calculated. However, since the additional degrees of freedom $\bar{\boldsymbol{a}}$, stemming from the enhanced strains, are defined on element level, we can do a static condensation. The block system (2.30) reads for an arbitrary element e

$$[\boldsymbol{K}^{*e}_{\mathfrak{d}^*\mathfrak{d}^*}]^k[\Delta\mathfrak{d}^{*e}]^k + [\boldsymbol{K}^{*e}_{\mathfrak{d}^*\bar{\boldsymbol{a}}}]^k[\Delta\bar{\boldsymbol{a}}^e]^k = [\boldsymbol{r}^{*e}_{\mathfrak{d}^*}]^k\,, \tag{2.31}$$

$$[\boldsymbol{K}^{*e}_{\bar{\boldsymbol{a}}\mathfrak{d}^*}]^k[\Delta\mathfrak{d}^{*e}]^k + [\boldsymbol{K}^{*e}_{\bar{\boldsymbol{a}}\bar{\boldsymbol{a}}}]^k[\Delta\bar{\boldsymbol{a}}^e]^k = [\boldsymbol{r}^{*e}_{\bar{\boldsymbol{a}}}]^k\,. \tag{2.32}$$

Expressing $[\Delta\bar{\boldsymbol{a}}^e]^k$ from (2.32)

$$[\Delta\bar{\boldsymbol{a}}^e]^k = -\{[\boldsymbol{K}^{*e}_{\bar{\boldsymbol{a}}\bar{\boldsymbol{a}}}]^k\}^{-1}[\boldsymbol{K}^{*e}_{\bar{\boldsymbol{a}}\mathfrak{d}^*}]^k[\Delta\mathfrak{d}^{*e}]^k + \{[\boldsymbol{K}^{*e}_{\bar{\boldsymbol{a}}\bar{\boldsymbol{a}}}]^k\}^{-1}[\boldsymbol{r}^{*e}_{\bar{\boldsymbol{a}}}]^k\,, \tag{2.33}$$

and inserting this into (2.31), yields

$$\underbrace{\left([\boldsymbol{K}^{*e}_{\mathfrak{d}^*\mathfrak{d}^*}]^k - [\boldsymbol{K}^{*e}_{\mathfrak{d}^*\bar{\boldsymbol{a}}}]^k\{[\boldsymbol{K}^{*e}_{\bar{\boldsymbol{a}}\bar{\boldsymbol{a}}}]^k\}^{-1}[\boldsymbol{K}^{*e}_{\bar{\boldsymbol{a}}\mathfrak{d}^*}]^k\right)}_{=:[\mathsf{S}^{*e}]^k}[\Delta\mathfrak{d}^{*e}]^k = \underbrace{[\boldsymbol{r}^{*e}_{\mathfrak{d}^*}]^k - [\boldsymbol{K}^{*e}_{\mathfrak{d}^*\bar{\boldsymbol{a}}}]^k\{[\boldsymbol{K}^{*e}_{\bar{\boldsymbol{a}}\bar{\boldsymbol{a}}}]^k\}^{-1}[\boldsymbol{r}^{*e}_{\bar{\boldsymbol{a}}}]^k}_{=:[\mathsf{f}^{*e}]^k}\,.$$

Then, the global vector $\Delta\mathfrak{d}^{*k}$ can be obtained from the reduced linear system of equations

$$\mathsf{S}^{*k}\Delta\mathfrak{d}^{*k} = \mathsf{f}^{*e} \tag{2.34}$$

with

$$\mathsf{S}^{*k} = \mathop{\mathsf{A}}_{e=1}^{N}[\mathsf{S}^{*e}]^k \quad \text{and} \quad \mathsf{f}^{*e} = \mathop{\mathsf{A}}_{e=1}^{N}[\mathsf{f}^{*e}]^k\,.$$

With known $\Delta\mathfrak{d}^{*k}$ the incremental element enhanced strains $[\Delta\bar{\boldsymbol{a}}^e]^k$ are calculated via (2.33), what makes it necessary to store the corresponding element sub stiffness matrices. Finally, the degrees of freedom have to be updated:

$$\mathfrak{d}^{*k+1} = \mathfrak{d}^{*k} + \Delta\mathfrak{d}^{*k} \quad \text{and} \quad [\bar{\boldsymbol{a}}^e]^{k+1} = [\bar{\boldsymbol{a}}^e]^k + [\Delta\bar{\boldsymbol{a}}^e]^k \quad \text{for } e = 1,\dots,N\,.$$

The new strains can be computed on element level at any point $\boldsymbol{\xi}$ by the discrete version of (2.24), i.e. by an interpolation via the element matrices $\mathfrak{B}^{*e}$ and $\boldsymbol{A}^e$. For the later discussed local update algorithm, the strains must be known at the integration points after every Newton-Raphson iteration step.

3. Application to plasticity with gradient-type softening

Following [28] we will apply the developed model of gradient-type rate-dependent plasticity to von-Mises plasticity with gradient-type softening and hardening, respectively. However, before doing this we look at some general considerations on plasticity on a phenomenological level. Most of the information collected in Section 3.1 and Section 3.3 is taken from [6], [10], [13] and [15]. To explain the effect of localization we will look at an one-dimensional example and discuss some arising problems concerning the physics and the numerics. Finally we will specify the emerging finite element matrices when using the enhanced-strain method.

3.1. Basics on phenomenological plasticity and material stability

We take a cylindric specimen of initial length L made out of some metal and do a tension test. From this we get a stress-strain curve, which gives a relationship between the nominal stress

$$\sigma := \frac{F}{A}\,,$$

where F denotes the applied force and A the original cross-sectional area of the specimen, and the engineering strain

$$\varepsilon := \frac{\Delta L}{L}$$

with Δ being the incremental operator. Typical results are given in Figure 3.1 for annealed mild steel and aluminium alloy. The elastic behaviour of many metals can be sufficiently described by Hooke's law. If the yield stress y_0, which in most cases cannot be determined exactly from the experiment, is exceeded, we observe plastic deformations. In big contrast to elastic deformations, plastic ones are irreversible and depend on the load history.
In general the velocity with which the specimen is loaded has an influence on the magnitude of the stress (rate-dependency). Further, two typical time effects are relaxation and creep. Former names the observation, that at constant prescribed deformation the stress declines in time. On the other hand, if we keep the stress constant, the deformation of the specimen will increase continuously in time - this effect is called creep.
To do a mathematical modelling of plasticity, several simplifications are commonly made. First of all, we assume that the unloading curve is linear with slope equal to that of Hooke's line. In reality the unloading-loading process undergoes a small hysteresis. If we completely neglect rate-dependency and the effect of hardening and softening, respectively, we end up with the model of classical plasticity, see Figure 3.2(a). For stress-driven processes the strain can reach arbitrary values in the plastic range, whereas for strain-driven processes the stress is uniquely determined. If we take a hardening law into account, we have a unique assignment between stress and strain and observe, that strain can only be increased by increasing the stress, see Figure 3.2(b). This means the work of the additional stress $\Delta\sigma$ on the additional strain $\Delta\varepsilon$ is positive. Therefore, according to Drucker, we call a material stable if

$$\Delta\sigma\Delta\varepsilon > 0\,,$$

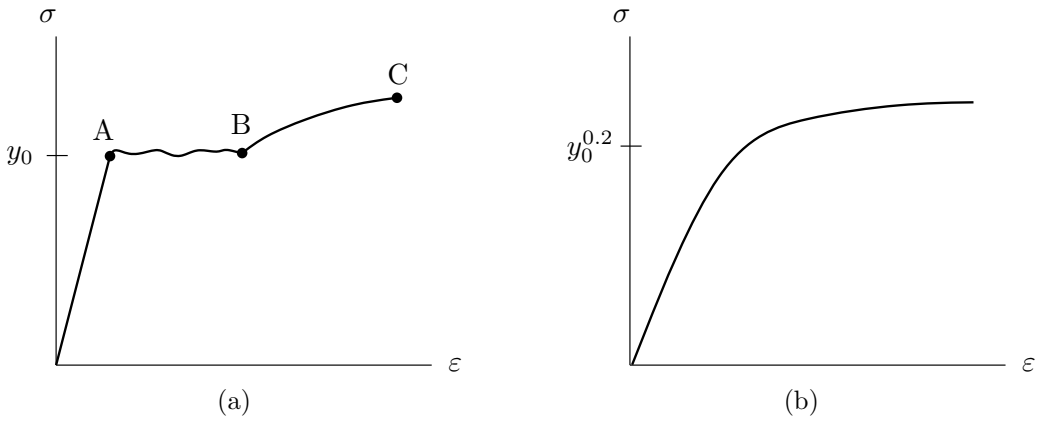

Figure 3.1. Typical stress-strain curves obtained by a tension test: (a) annealed mild steel with typical yield plateau AB at yield stress y_0 and hardening region BC and (b) aluminium alloy, where $y_0^{0.2}$ denotes the stress, at which a strain of 0.2% remains after unloading.

or in the multi-axial case, if $\dot{\boldsymbol{\sigma}} : \dot{\boldsymbol{\varepsilon}} > 0$. Following this definition, the model of ideal plasticity is not stable, but neutral stable, since $\Delta\sigma\Delta\varepsilon = 0$. When considering softening, see Figure 3.2(c), we see that $\Delta\sigma\Delta\varepsilon < 0$. Hence, the behaviour of a softening material is unstable. However, it is important to note explicitly, that we do not look at the work of the total stresses σ on $\Delta\varepsilon$, which is of course always positive for $\sigma > 0$ and $\Delta\varepsilon > 0$.

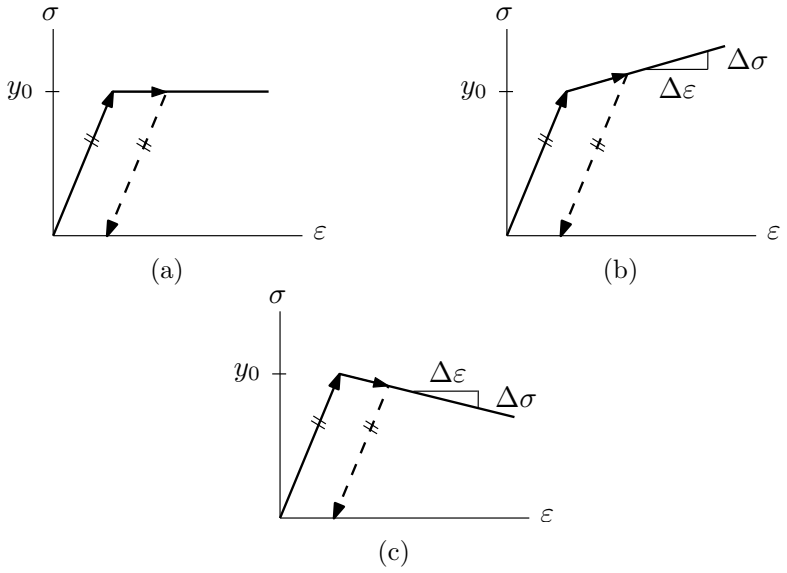

Figure 3.2. Stress-strain curves for (a) perfect plasticity, (b) plasticity with linear hardening and (c) plasticity with linear softening.

To disable the supposition, that softening materials violate the second law of thermodynamics, we look at the reduced dissipation inequality (1.13). The plastic strain $\boldsymbol{\varepsilon}^p$ serves as an internal variable, and the question arises, if we can give the conjugate force $-\partial_{\boldsymbol{\varepsilon}^p}\psi$ a physical meaning. For this we claim the free energy ψ to be a sum of two parts, namely the elastic free energy ψ^e, which only depends on the elastic strain $\boldsymbol{\varepsilon}^e$, and the part ψ^h, which only depends on internal variables $\boldsymbol{\mathcal{I}}^h$ describing the softening of the material. Doing an

additive decomposition of the total strain

$$\boldsymbol{\varepsilon} = \boldsymbol{\varepsilon}^e + \boldsymbol{\varepsilon}^p \,,$$

we can say

$$-\partial_{\boldsymbol{\varepsilon}^p}\psi(\boldsymbol{\varepsilon}, \boldsymbol{\mathcal{I}}^h) = -\partial_{\boldsymbol{\varepsilon}^p}\psi^e(\boldsymbol{\varepsilon} - \boldsymbol{\varepsilon}^p) = \partial_{\boldsymbol{\varepsilon}^e}\psi^e(\boldsymbol{\varepsilon}^e) = \partial_{\boldsymbol{\varepsilon}}\psi(\boldsymbol{\varepsilon}, \boldsymbol{\mathcal{I}}^h) = \boldsymbol{\sigma} \,,$$

where the last equality sign only holds if we exclude dissipative stresses. Hence, we conclude the dissipation inequality as

$$\boldsymbol{\sigma} : \dot{\boldsymbol{\varepsilon}}^p \geq 0 \,. \tag{3.1}$$

Looking at the one-dimensional counterpart $\sigma\dot{\varepsilon}^p \geq 0$, it is easily seen from Figure 3.2(c), that softening materials are in agreement with the second law of thermodynamics, although they are not stable in Drucker's sense.
Let us now look at a cyclic process of loading and unloading, see Figure 3.3(a).

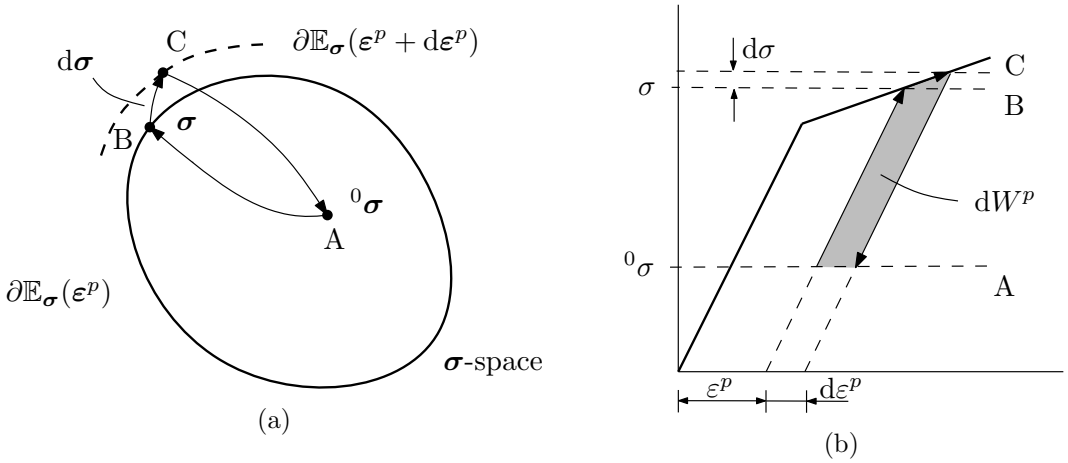

Figure 3.3. Complete load cycle for (a) the multi-axial case and (b) the one-dimensional case. The line AB characterises elastic loading, the line BC infinitesimally small plastic loading and the line CA elastic unloading. For the one-dimensional case the infinitesimal irreversible plastic work is, by neglecting higher order terms, $\mathrm{d}W^p := (\sigma - {}^0\sigma)\,\mathrm{d}\varepsilon^p$.

Let $\partial\mathbb{E}_{\boldsymbol{\sigma}}(\boldsymbol{\varepsilon}^p)$ be the yield surface in stress space at plastic strain $\boldsymbol{\varepsilon}^p$. The initial stress ${}^0\boldsymbol{\sigma}$ (point A) lies either inside the yield surface, which corresponds to an elastic state, or on the yield surface, which corresponds to a plastic state. When we do a further loading, this point moves closer and closer to $\partial\mathbb{E}_{\boldsymbol{\sigma}}(\boldsymbol{\varepsilon}^p)$ until the plastic state with stress $\boldsymbol{\sigma}$ (point B) is reached, which means that the point lies on the yield surface. An infinitesimal growth of stress $\mathrm{d}\boldsymbol{\sigma}$ (point C) of course causes an additional elastic strain $\mathrm{d}\boldsymbol{\varepsilon}^e$ and an additional plastic strain $\mathrm{d}\boldsymbol{\varepsilon}^p$. Now, by elastic unloading, we return to the initial state (point A). Motivated by the one-dimensional case, see Figure 3.3(b), the irreversible plastic work is postulated to be non-negative for all admissible ${}^0\boldsymbol{\sigma}$:

$$\mathrm{d}W_p := (\boldsymbol{\sigma} - {}^0\boldsymbol{\sigma}) : \mathrm{d}\boldsymbol{\varepsilon}^p \geq 0 \,,$$

and correspondingly

$$(\boldsymbol{\sigma} - {}^0\boldsymbol{\sigma}) : \dot{\boldsymbol{\varepsilon}}^p \geq 0 \,, \tag{3.2}$$

where the equality sign holds for ideal plastic materials. This inequality also goes back to Drucker and is identical to (3.1) for ${}^0\boldsymbol{\sigma} = \mathbf{0}$. Writing (3.2) as $\boldsymbol{\sigma} : \dot{\boldsymbol{\varepsilon}}^p \geq {}^0\boldsymbol{\sigma} : \dot{\boldsymbol{\varepsilon}}^p$, we can see, that the stress $\boldsymbol{\sigma}$ corresponding to $\dot{\boldsymbol{\varepsilon}}^p$ maximizes the plastic dissipation $d^p := {}^0\boldsymbol{\sigma} : \dot{\boldsymbol{\varepsilon}}^p$ under all admissible stresses ${}^0\boldsymbol{\sigma}$. This is nothing else than the principle of maximum plastic dissipation, which has been discussed in Section 1.4. Applying Voigt's notation in terms of the principal normal stresses on inequality (3.2), we can conclude, that (3.2) is fulfilled if, and only if

- the yield surface is convex and
- the vector $\dot{\boldsymbol{\varepsilon}}^p$ is directed along the outward normal of the yield surface, see (1.19).

Finally, it should also be noted, that (3.2) is not a sufficient condition for a material to be stable, since it also allows softening, which can be easily seen if we once again look at the one-dimensional case in Figure 3.2(c).
So far, we looked at rate-independent plasticity. If we apply a big enough strain, which does not violate the assumption of geometrical linearity, rather quickly on a viscoplastic specimen, the stress exceeds the yield limit y_0 by following the linear elastic law, see Figure 3.4. After the total strain has been applied and is hold constant, the overstress decreases and plastic deformation occurs. The state, which would be reached by a specimen with zero viscosity under the same applied total strain (point P, when ignoring the effect of hardening and softening), is reached asymptotically. Of course the unloading is elastic again.

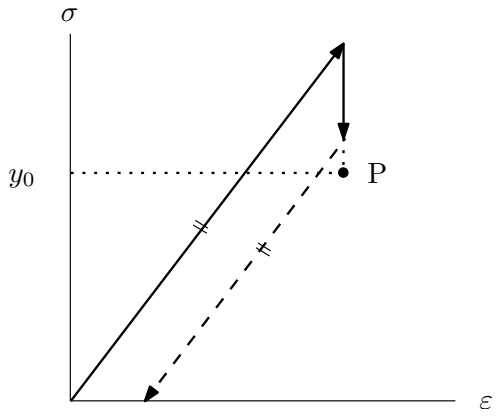

Figure 3.4. Stress-strain curve of a viscoplastic specimen. The point P belongs to a state which would be reached by ideal plasticity. If we take hardening or softening into account the point P would lie above or below the line $\sigma = y_0$.

3.2. Localization phenomena and mesh sensitivity

Softening is an effect which is strongly related to damage. The sliding of the stress in the plastic state can be microscopically explained by merging of defects and by arising of microcracks, what reduces the effective area of the specimen. In experiments one can observe the phenomena of localization. In localized zones high plastic deformations occur and may cause failure. A famous example of such a localization phenomena are shear bands, which are observed in many ductile materials.
It will be seen by the following one-dimensional, rate-independent example, that we will run into some trouble concerning the physics and numerics, when we try to describe

softening by a local continuum theory. A resort is provided by a nonlocal continuum theory. The information of the two following subsections is taken from [23] and [22].

3.2.1. Softening bar: local theory

We look at a bar with length L and unit cross sectional area loaded by an uni-axial stress σ. The body is decomposed into two (finite) elements denoted by A and B with length a and b such that $L = a+b$, see Figure 3.5(a). Both elements are assumed to follow the same constitutive relation and time dependencies are excluded. The elastic region is described by Hooke's law with Young's modulus E, and the softening region by a linear relationship with proportionality factor hE and the hardening parameter h being negative, see Figure 3.5(b).

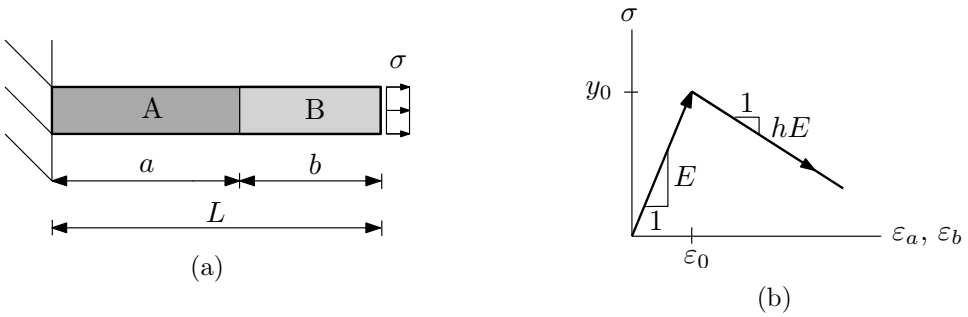

Figure 3.5. (a) One-dimensional model problem with weakened element B, and (b) constitutive behaviour of element A and element B.

To simulate localization, we assume the yield stress y_0 in element B to be a little bit smaller than in element A. We are interested now in the constitutive response of the composite and do a strain-driven tension test. From zero upward to the strain which belongs to the yield stress of element B, the constitutive relation of the composite equals the constitutive relation for either elements. This does not hold for the softening region. For this, we look at an actual total engineering strain ε of the composite, which is given by

$$\varepsilon = \frac{a}{L}\varepsilon_a + \frac{b}{L}\varepsilon_b \,, \tag{3.3}$$

where ε_a and ε_b are the actual engineering strains of element A and element B. Now we impose an increment $\Delta\varepsilon_b$ on element B and assume that the new strain causes a plastification of element B. The incremental constitutive relation of element B reads

$$\Delta\sigma = hE\Delta\varepsilon_b < 0 \,.$$

Because of equilibrium $\frac{\mathrm{d}}{\mathrm{d}x}\sigma(x) = 0$, the stress σ must be constant over the whole composite. As a result the applied increment $\Delta\varepsilon_b$ causes an elastic unloading of element A, and consequently the change of the engineering strain in element A reads

$$\Delta\varepsilon_a = \frac{\Delta\sigma}{E} = h\Delta\varepsilon_b < 0 \,.$$

Inserting this into the incremental form of (3.3) yields

$$\Delta\varepsilon = \frac{ha+b}{L}\Delta\varepsilon_b \,.$$

Then the incremental constitutive relation of the composite reads by using $a = L - b$

$$\Delta\sigma = -E\chi\Delta\varepsilon \quad \text{with} \quad \chi := \frac{-hL}{b(1-h)+hL}\,.$$

Here it is important to note, that the incremental stress depends on the length b of the softening element B. Physically spoken this element forms a damaged zone. In contrast, the element A remains in the elastic region since its yield stress is not exceeded. The crucial point here is, that the length b of the damaged zone is not known. So far we have an infinite number of solutions, see Figure 3.6.

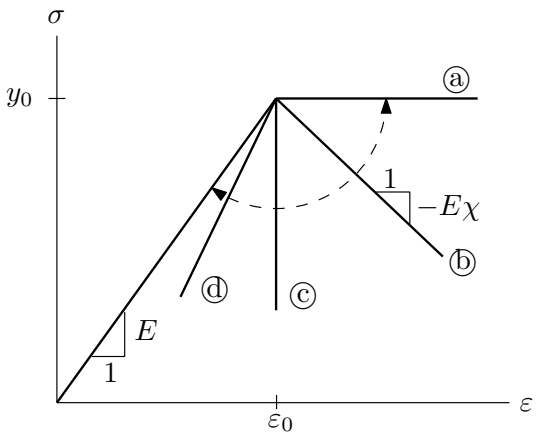

Figure 3.6. Constitutive behaviour of the composite. Since b remains undetermined, we obtain an infinite number of solutions for the softening regime: ⓐ $\chi = 0$, ⓑ $\chi > 0$, ⓒ $\chi \to \pm\infty$ and ⓓ $-1 > \chi > -\infty$.

The first problem is in the offing. If we do a simulation by the finite element method, the plastic zone cannot spread over the weakened element, the size of which in fact corresponds to the length b. Accordingly, the stress response of the composite is mesh-dependent and the line representing the softening range of the stress-strain diagram will rotate clockwise about the point (ε_0, y_0) by using finer and finer meshes. The mathematical reason for this lies in the loss of ellipticity of the governing differential equations, see [28] and the references therein.
But not only a numerical problem occurs. Of course every material has defects and some regions tolerate more strain than others before plastification takes place. Because in our example the local strains are uniformly distributed up to the yield stress, the weakest region of our composite (element B) is the first one which reaches the softening range. Corresponding to the above discussion it is also the only one, since all other "stronger" regions (element A) undergo an elastic unloading. Of course the weakest region can be arbitrarily small ($b \to 0$), which means, that the corresponding softening branch can be arbitrarily close to the elastic line in the stress-strain diagram ($\chi \to -1$), see again Figure 3.6. Not only that softening zones of negligible thickness are not observed in experiments, such arbitrarily small zones do not effect energy dissipation. In order to describe softening zones of finite thickness a nonlocal continuum theory is used, which is presented in the next subsection.

3.2.2. Softening bar: nonlocal theory

We again look at the same bar with length L, but with the difference that we do not decompose it into two elements with slightly different yield stresses. Instead we identify

the point P_1 to be weakest location of the material, see Figure 3.7(a). Again we assume the constitutive behaviour of the bar to be linear in the elastic range and to be also linear in the softening regime, see Figure 3.7(b). Because of the uniformity of the local elastic strain, the point P_1 will plastify at first.

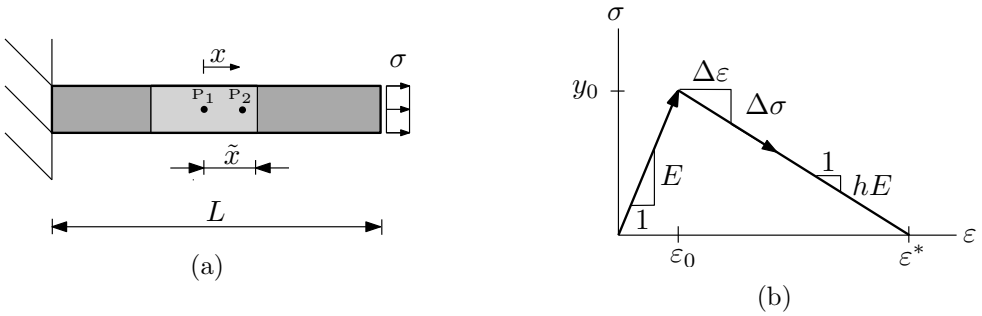

Figure 3.7. (a) One-dimensional model problem with spreading out softening zone of length $2\tilde{x}$, and (b) constitutive behaviour of the bar.

Doing a strain driven tension test, we can write for the stress after exceeding the yield limit

$$\sigma = y_0 + \Delta\sigma \quad \text{with} \quad \Delta\sigma < 0\,. \tag{3.4}$$

As it will be seen later, it is convenient to express this relation in terms of the global plastic strain ε^p. For this we additively decompose the total engineering strain $\varepsilon = \varepsilon^p + \varepsilon^e$, where ε^e denotes the global elastic strain, which equals the local one in every point of the specimen. Together with the incremental relations $\Delta\sigma = E\Delta\varepsilon^e$ and $\Delta\sigma = hE\Delta\varepsilon$ we obtain

$$\Delta\varepsilon^e = h\Delta\varepsilon \quad \text{and} \quad \Delta\varepsilon^p = (1-h)\Delta\varepsilon\,,$$

and consequently we can write the incremental stress in terms of the incremental plastic strain as

$$\Delta\sigma = \frac{hE}{1-h}\Delta\varepsilon^p\,. \tag{3.5}$$

Since in (3.4) the strain increment is counted from ε_0, see again Figure 3.7(b), we can say $\Delta\varepsilon^p = \varepsilon^p$, and inserting (3.5) into (3.4) yields

$$\sigma = y_0 + \frac{hE}{1-h}\varepsilon^p\,,$$

or in terms of $\varepsilon^* := -\frac{1-h}{hE}y_0$

$$\sigma = y_0\left(1 - \frac{\varepsilon^p}{\varepsilon^*}\right)\,. \tag{3.6}$$

Note that this statement is a global one. However since the tensile stress σ is constant over the whole specimen, (3.6) also holds locally for the softening region. So far there is no difference to the local theory treated in the last subsection. To enforce the softening region to spread over, and in fact not to remain in the weakened finite element, we do a gradient-type expansion of the plastic strain, i.e.

$$\varepsilon^p_\nabla(x) := \varepsilon^p(x) + l^2\left[\frac{\mathrm{d}}{\mathrm{d}x}\varepsilon^p(x)\right]^2\,,$$

where the micro-scale parameter $l \in \mathbb{R}^+$ has the dimension of a length. Replacing the plastic strain in the local version of (3.6) by the nonlocal representation ε^p_∇, gives a

nonlinear and inhomogeneous ordinary differential equation in ε^p:

$$l^2 \left[\frac{\mathrm{d}}{\mathrm{d}x}\varepsilon^p(x)\right]^2 + \varepsilon^p(x) = \left(1 - \frac{\sigma}{y_0}\right)\varepsilon^* .$$

For $l = 0$ we simply get the solution

$$\varepsilon^p(x) = \left(1 - \frac{\sigma}{y_0}\right)\varepsilon^* ,$$

which provides the local plastic strain to be constant over the whole softening region. For $l > 0$ the solution reads

$$\varepsilon^p(x) = \left(1 - \frac{\sigma}{y_0}\right)\varepsilon^* - \frac{1}{4}\frac{x^2}{l^2} , \tag{3.7}$$

and we see that the plastic strain field is not uniform in this case. At the beginning of the softening ($\sigma = y_0$), the plastic strain ε^p is just zero at the softening's origin P_1 to which the coordinate $x = 0$ belongs. We are interested in the size of the softening zone subject to a given load σ. Since ε^p must be positive, the nonlocal solution (3.7) is valid for $-\tilde{x} \leq x \leq +\tilde{x}$, where $\tilde{x}$ is obtained from the condition $\varepsilon^p(\tilde{x}) = 0$. This gives

$$\tilde{x} = 2l\sqrt{\left(1 - \frac{\sigma}{y_0}\right)\varepsilon^*} .$$

We see that for $l = 0$ the softening zone remains at $x = 0$ for all values of σ and does not spread out. The plastic strain over the whole specimen for $l = 0$ can then be written by a Dirac-distribution as

$$\varepsilon^p(x) = \left(1 - \frac{\sigma}{y_0}\right)\varepsilon^*\delta(x) .$$

On the other hand for $l > 0$ the softening zone becomes broader and broader with increasing strain increment, and $\tilde{x}$ reaches a maximal value at $\varepsilon = \varepsilon^*$, where $\sigma = 0$, of

$$\tilde{x}_{max} = 2l\sqrt{\varepsilon^*} .$$

To understand the mechanism behind the spreading of the softening zone in case of the nonlocal theory, we look at the point P_1 and at another point P_2, see again Figure 3.7(a). Initially the point P_2 unloads elastically until the gradient-type plastic strain, which, due to the gradient, can be relatively high, causes a sufficient reduction of the term $y_0\left(1 - \varepsilon^p_\nabla/\varepsilon^*\right)$, see (3.6), such that the yield function

$$\varphi(\sigma, \varepsilon^p_\nabla) := \sigma - y_0\left(1 - \frac{\varepsilon^p_\nabla}{\varepsilon^*}\right)$$

becomes zero at a stress smaller than y_0. Consequently the softening branch of point P_2 is shifted downward in parallel to the softening branch of point P_1 in the local stress strain diagram, see Figure 3.8.

3.3. Yield Criterion

To decide when a plastic state is reached we need a yield criterion. Such a yield criterion is conceptionally derived from physical assumptions, which are, depending on the material under focus, more or less confirmed by experiments. Hence, there does not exist a master criterion which provides good results for every type of material. Our focus lies on metals for which the von-Mises yield criterion is commonly used. A great advantage of this criterion lies undoubtfully in its simple structure.

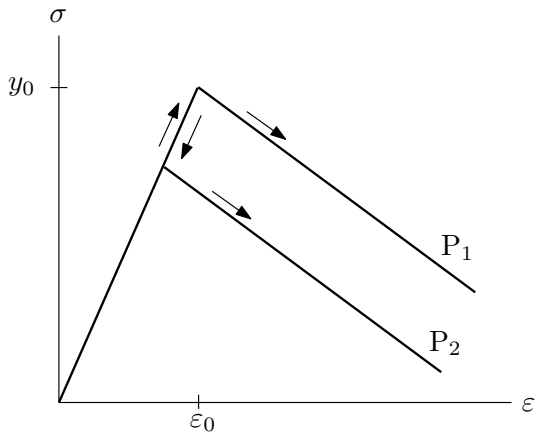

Figure 3.8. Local constitutive behaviour of points P_1 and P_2, where P_1 is the activator of the softening zone.

3.3.1. General remarks

We assume the material under focus to be isotropic and ignore for the present hardening and softening, respectively. Because of isotropy any yield function φ can only depend on the invariants of the stress tensor $\boldsymbol{\sigma}$ given by

$$J_{\boldsymbol{\sigma}}^{(1)} = \mathrm{tr}[\boldsymbol{\sigma}]\,, \quad J_{\boldsymbol{\sigma}}^{(2)} = \frac{1}{2}\left[(\mathrm{tr}[\boldsymbol{\sigma}])^2 - \mathrm{tr}[\boldsymbol{\sigma}^2]\right]\,, \quad J_{\boldsymbol{\sigma}}^{(3)} = \det[\boldsymbol{\sigma}]\,,$$

see e.g. [12]. In terms of the principal normal stresses σ_{11}, σ_{22} and σ_{33}, they simply read

$$J_{\boldsymbol{\sigma}}^{(1)} = \sigma_{11} + \sigma_{22} + \sigma_{33}\,, \quad J_{\boldsymbol{\sigma}}^{(2)} = \sigma_{11}\sigma_{22} + \sigma_{22}\sigma_{33} + \sigma_{33}\sigma_{11}\,, \quad J_{\boldsymbol{\sigma}}^{(3)} = \sigma_{11}\sigma_{22}\sigma_{33}\,.$$

One should notice the symmetry of the three invariants in the three principal normal stresses, which means that they are not changed by a permutation of σ_{11}, σ_{22} and σ_{33}.
It is useful to decompose the stress tensor into its hydrostatic part $\boldsymbol{\sigma}^{hyd}$ and into its deviatoric part $\boldsymbol{s}$:

$$\boldsymbol{\sigma} = \boldsymbol{\sigma}^{hyd} + \boldsymbol{s}\,.$$

A hydrostatic stress state is characterized by vanishing shear stresses and is given by

$$\boldsymbol{\sigma}^{hyd} = p\boldsymbol{I} \quad \text{with} \quad p := \frac{1}{3}(\sigma_{11} + \sigma_{22} + \sigma_{33}) = \frac{1}{3}\,\mathrm{tr}[\boldsymbol{\sigma}]$$

being the mean or hydrostatic pressure and with $\boldsymbol{I}$ denoting the second order unity tensor. Consequently the remaining deviatoric stress tensor, which contains the shear stresses, can be written as

$$\boldsymbol{s} = \boldsymbol{\sigma} - \frac{1}{3}\,\mathrm{tr}[\boldsymbol{\sigma}]\boldsymbol{I}\,.$$

This motivates the general definition of a deviator of a second order tensor:

$$\mathrm{dev}[\cdot] := [\cdot] - \frac{1}{3}\,\mathrm{tr}[\cdot]\boldsymbol{I}\,.$$

For metals, which are our considered materials here, it is known from experiments, that the influence of a hydrostatic stress state on plastic deformation is negligible. Therefore, in the yield function the invariants of the stress tensor can be replaced by the invariants of the deviatoric stress tensor

$$J_{\boldsymbol{s}}^{(1)} = s_{11} + s_{22} + s_{33}\,, \quad J_{\boldsymbol{s}}^{(2)} = s_{11}s_{22} + s_{22}s_{33} + s_{33}s_{11}\,, \quad J_{\boldsymbol{s}}^{(3)} = s_{11}s_{22}s_{33}\,.$$

Since $J_{\boldsymbol{s}}^{(1)} = 0$, we conclude

$$\varphi = \varphi(J_{\boldsymbol{s}}^{(2)}, J_{\boldsymbol{s}}^{(3)})\,.$$

The yield surface itself is given by $\varphi(J_{\boldsymbol{s}}^{(2)}, J_{\boldsymbol{s}}^{(3)}) = 0$. A further consequence of the independence of plastic states on $\boldsymbol{\sigma}^{hyd}$ concerns the plastic strains itself. Since dilatation is due to a hydrostatic stress state, we conclude it to be an elastic deformation and hence, plastic deformation does not come along with volumetric changes, i.e.

$$\mathrm{tr}[\boldsymbol{\varepsilon}^p] = 0\,, \tag{3.8}$$

because we are assuming small strains here.
Considering the yield surface to lie in the space of principal normal stresses, we can observe some geometrical properties, see Figure 3.9(a). Let a stress state $\mathbf{S} = (\sigma_{11}, \sigma_{22}, \sigma_{33})$ be given, which lies on the yield surface. The vector **OS**, pointing from the origin **O** to point **S**, can additively be decomposed into $\mathbf{OS} = \mathbf{OD} + \mathbf{DS}$, where $\mathbf{D} = (s_{11}, s_{22}, s_{33})$ contains the principle deviatoric normal stresses and where **DS** represents the hydrostatic stress state $(p, p, p)^T$. Because of $J_{\boldsymbol{s}}^{(1)} = 0$ the vector **OD** must always lie in the plane $\mathscr{E}$: $\sigma_{11} + \sigma_{22} + \sigma_{33} = 0$ (called deviator plane) with normal vector $\boldsymbol{n} = (1/\sqrt{3}, 1/\sqrt{3}, 1/\sqrt{3})^T$. The vector **DS** is parallel to the line $\sigma_{11} = \sigma_{22} = \sigma_{33}$ and is therefore perpendicular to $\mathscr{E}$. Since plasticity is unaffected by hydrostatic stress states, we can conclude that the yield surface is a cylindrical surface with a template lying in $\mathscr{E}$ and a generatrix being normal to $\mathscr{E}$. Consequently it is sufficient for further considerations to look at the template itself.

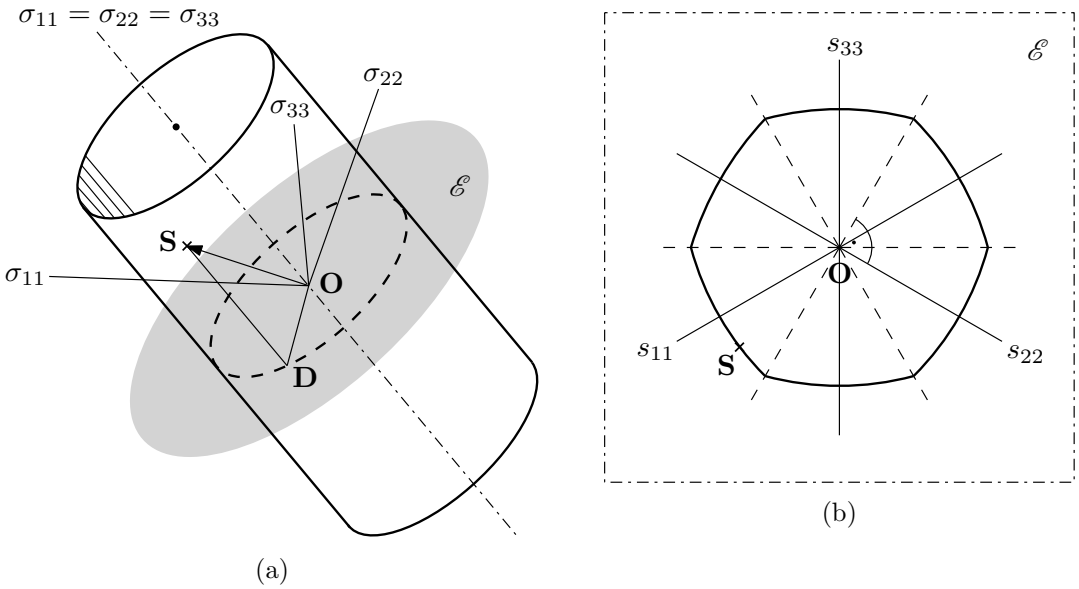

Figure 3.9. (a) Yield surface in space of principal normal stresses [10] and (b) allowed template of the yield surface [10].

Some characteristics of the template can be derived from physical properties of the material, see Figure 3.9(b). First of all the assumed isotropy results in a symmetry of the template about the s_{11}-, s_{22}- and s_{33}-axis. Secondly the template does not go through the origin **O** since a purely hydrostatic stress state causes no plastic deformations. And thirdly, by assuming that the material's behaviour is the same under tension and compression, i.e. we do not take Bauschinger's effect into account, we can follow, that, starting from a

plastic state on the template, unloading and reloading into the opposite direction along a straight line going through the origin **O**, leads to a state on the template which has the same distance from the origin as the original plastic state. Therefore, the template is also symmetrical about straight lines perpendicular to the s_{11}-, s_{22}- and s_{33}-axis. Finally it should be mentioned again, that the template must be convex in order to fulfil inequality (3.2).

3.3.2. Von-Mises yield criterion

The von-Mises yield criterion bases on the assumption, that the comparison stress σ_V can be obtained by the postulation, that the octahedral shear stress of the complex loaded body equals the octahedral shear stress of the tensile loaded specimen used in tension tests. The octahedral shear stress is

$$\tau_{oct} := \frac{1}{3}\sqrt{2[J_{\boldsymbol{\sigma}}^{(1)}]^2 - 6J_{\boldsymbol{\sigma}}^{(2)}}\,,$$

see [5], and is an invariant quantity. It reads in terms of the principal normal stresses

$$\tau_{oct} = \frac{1}{3}\sqrt{(\sigma_{11}-\sigma_{22})^2 + (\sigma_{22}-\sigma_{33})^2 + (\sigma_{33}-\sigma_{11})^2}\,.$$

The reduction to the one-dimensional case $\sigma_1 = \sigma_V$ and $\sigma_2 = \sigma_3 = 0$ gives

$$[\tau_{oct}]_{1d} = \frac{\sqrt{2}}{3}\sigma_V\,,$$

and the above mentioned postulate $\tau_{oct} = [\tau_{oct}]_{1d}$ yields the comparison stress

$$\sigma_V = \sqrt{\frac{1}{2}\left[(\sigma_{11}-\sigma_{22})^2 + (\sigma_{22}-\sigma_{33})^2 + (\sigma_{33}-\sigma_{11})^2\right]}\,.$$

With this at hand, we define the yield function as $\varphi(\boldsymbol{\sigma}) := \sigma_V - y_0$. For non-viscous materials a plastic state is reached if, and only if, $\varphi = 0$, whereas for viscous materials plastic states are characterized by φ being greater than zero and being equal zero in the asymptotic limit. Using the invariants of the stress tensor $\boldsymbol{\sigma}$, the yield function can be expressed as

$$\varphi(J_{\boldsymbol{\sigma}}^{(1)}, J_{\boldsymbol{\sigma}}^{(2)}) = \sqrt{[J_{\boldsymbol{\sigma}}^{(1)}]^2 - 3J_{\boldsymbol{\sigma}}^{(2)}} - y_0\,.$$

Since yielding is assumed not to be affected by hydrostatic stress states, it is convenient to express the yield function in terms of the invariants of the deviatoric stress tensor $\boldsymbol{s}$. Again we make use of $J_{\boldsymbol{s}}^{(1)} = 0$ and obtain the relation $J_{\boldsymbol{\sigma}}^{(2)} = J_{\boldsymbol{s}}^{(2)} + \frac{1}{3}[J_{\boldsymbol{\sigma}}^{(1)}]^2$. This gives

$$\varphi(J_{\boldsymbol{s}}^{(2)}) = \sqrt{-3J_{\boldsymbol{s}}^{(2)}} - y_0\,,$$

and we see, that the yield function only depends on the second invariant of $\boldsymbol{s}$. Finally, we will derive a form of the yield function which will be used later on. From $[J_{\boldsymbol{s}}^{(1)}]^2 = (s_{11}+s_{22}+s_{33})^2 = 0$ we get

$$s_{11}^2 + s_{22}^2 + s_{33}^2 = -2(s_{11}s_{22} + s_{22}s_{33} + s_{33}s_{11})$$

and hence $J_{\boldsymbol{s}}^{(2)} = -\frac{1}{2}\|\boldsymbol{s}\|_2^2$, where $\|\cdot\|_2$ denotes the Euclidean matrix norm. Hence, we obtain for the yield function after a redefinition by the factor $\sqrt{2/3}$

$$\varphi(\boldsymbol{s}) = \|\boldsymbol{s}\|_2 - \sqrt{\frac{2}{3}}y_0\,, \quad \text{or} \quad \varphi(\boldsymbol{\sigma}) = \|\mathrm{dev}[\boldsymbol{\sigma}]\|_2 - \sqrt{\frac{2}{3}}y_0\,.$$

With this form at hand we can identify the template of the yield surface in the deviator plane $\mathscr{E}$ as a circle with radius $\sqrt{2/3}y_0$ and with midpoint lying in $\mathbf{O}$. The requested symmetry properties and the convexity are obviously fulfilled, see Example 2 in Appendix A. Finally, we verify the von-Mises yield function by checking the condition of plastic incompressibility (3.8) in its infinitesimal form. Looking at $(1.19)_2$ and (1.24), respectively, we have

$$\mathrm{tr}[\mathrm{d}\boldsymbol{\varepsilon}^p] \propto \mathrm{tr}[\partial_{\boldsymbol{\sigma}}\varphi(\boldsymbol{\sigma})]\,.$$

According to (3.12) we get $\mathrm{tr}\left[\partial_{\boldsymbol{\sigma}}\|\mathrm{dev}[\boldsymbol{\sigma}]\|_2\right] = 0$, and together with its symmetry properties and convexity, we identify the von-Mises yield criterion to be physically reasonable.

Remark 8. We obtain the same yield surface if we postulate, that the comparison stress can be derived by setting the strain energy of distortion of the complex loaded body equal to the strain energy of distortion of the tensile loaded specimen. This is known as hypothesis of Huber-Hencky, see [6].

3.3.3. Incorporation of hardening and softening

So far we ignored the effect of hardening and softening, respectively. For simplicity we will only look at isotropic hardening/softening[1], which means that the template of the yield surface is blown up (hardening) or shrunken (softening) by keeping its shape, i.e. its convexity and symmetries, and its origin. In case of the von-Mises criterion this means, that the radius of the circle lying in $\mathscr{E}$ becomes larger (hardening) or lower (softening). Mathematically speaking we extend the dependency of the yield function by internal variables describing the hardening/softening of the material. Since only the yield stress y_0 is affected by the internal variables, we can take into account hardening and softening by a single scalar quantity α, and we can split the yield function in the following way:

$$\varphi(\boldsymbol{\sigma}, \alpha) = F(\boldsymbol{\sigma}) - f(\alpha)\,.$$

To clear the physical meaning of α, let us first look at the one dimensional case with a tensile loaded specimen made out of a metal following a linear hardening law, see Figure 3.2(b) and Figure 3.2(c). Defining the material parameter $H := hE$, we write

$$F(\sigma) = |\sigma| \quad \text{and} \quad f(\alpha) = y_0 + H\alpha\,,$$

with $H > 0$ for hardening and $H < 0$ for softening. Clearly, for the one-dimensional case, the internal variable α equals the plastic strain ε^p. The situation is a bit more complicated for the multi-axial case. We need a scalar quantity, which, depending on the plastic strain tensor $\boldsymbol{\varepsilon}^p$, changes the yield stress y_0. We define, see [15],

$$\alpha := \int_0^t \sqrt{\frac{2}{3}\dot{\boldsymbol{\varepsilon}}^p : \dot{\boldsymbol{\varepsilon}}^p}\,\mathrm{d}\bar{t}\,, \tag{3.9}$$

and call this quantity equivalent plastic strain. From this definition we see, that $\dot{\alpha} = 0$ whenever $\dot{\boldsymbol{\varepsilon}}^p = \mathbf{0}$, and $\dot{\alpha} > 0$ whenever $\dot{\boldsymbol{\varepsilon}}^p \neq \mathbf{0}$. The factor $2/3$ comes from the above observation, that in the one-dimensional case $\dot{\alpha} = |\dot{\varepsilon}^p|$. This should be checked here: for a specimen of which the material is isotropic and plastically incompressible, the plastic strain rate tensor reads

$$\dot{\boldsymbol{\varepsilon}}^p = \begin{bmatrix} \dot{\varepsilon}^p & 0 & 0 \\ 0 & -\frac{1}{2}\dot{\varepsilon}^p & 0 \\ 0 & 0 & -\frac{1}{2}\dot{\varepsilon}^p \end{bmatrix},$$

[1] Kinematic hardening is related to Bauschinger's effect, which was not taken into account when discussing the geometrical properties of the yield surface's template.

and we obtain $\sqrt{\frac{2}{3}\dot{\boldsymbol{\varepsilon}}^p : \dot{\boldsymbol{\varepsilon}}^p} = |\dot{\varepsilon}^p|$ by direct calculation.
As an example we finally look at von-Mises plasticity. Incorporation of a linear hardening law gives

$$\varphi(\boldsymbol{\sigma}, \alpha) = \|\mathrm{dev}[\boldsymbol{\sigma}]\|_2 - \sqrt{\frac{2}{3}}(y_0 + H\alpha)\,, \tag{3.10}$$

with α being defined in (3.9).

3.4. Von-Mises plasticity with gradient-type softening

In this section the gradient-extended theory presented in Chapter 2 will be applied to von-Mises plasticity at small strains for the rate-dependent case. We will set up the governing strong form of the problem and specify the extended internal rate potential per unit volume $\pi_\eta^{*\tau}$. Finally we will derive an update algorithm for the local plastic strains.

3.4.1. Governing equations

In a first step we have to specify the constitutive state, i.e. the generalized internal variables $\check{\boldsymbol{u}}$, and the local internal variables $\boldsymbol{\mathcal{I}}$. Beside the macroscopic displacement field $\boldsymbol{u}$ we introduce a scalar hardening field α serving as a generalized internal variable, which has, at the moment, nothing to do with the equivalent plastic strain. Furthermore the macroscopic plastic strain $\boldsymbol{\varepsilon}^p$ serves as a local internal variable. Together we have

$$\bar{\boldsymbol{u}} = \{\boldsymbol{u}\}\,, \quad \check{\boldsymbol{u}} = \{\alpha\} \quad \text{and} \quad \boldsymbol{\mathcal{I}} = \{\boldsymbol{\varepsilon}^p\}\,,$$

and the constitutive state reads

$$\mathfrak{c} = \{\boldsymbol{u}, \alpha, \nabla\alpha\}\,.$$

We ignore dissipative macroscopic stresses represented by $\bar{\boldsymbol{\mathcal{F}}}$ and take only thermodynamic driving forces conjugate to α and $\boldsymbol{\varepsilon}^p$ into account, i.e.

$$\check{\boldsymbol{f}} =: \{\beta\} \quad \text{and} \quad \boldsymbol{\mathcal{F}} =: \{\boldsymbol{B}\}\,.$$

Looking at Table 2.1, we need to specify the free energy ψ. We decompose it additively as

$$\psi(\mathfrak{c}, \boldsymbol{\varepsilon}^p) = \bar{\psi}_{loc}(\boldsymbol{\varepsilon}^e(\boldsymbol{\varepsilon}, \boldsymbol{\varepsilon}^p)) + \check{\psi}_{loc}(\alpha) + \check{\psi}_{non}(\nabla\alpha)\,,$$

where $\bar{\psi}_{loc}$ describes the elastic macroscopic distortion with $\boldsymbol{\varepsilon}^e = \boldsymbol{\varepsilon} - \boldsymbol{\varepsilon}^p$, $\check{\psi}_{loc}$ the local microscopic hardening/softening process, and $\check{\psi}_{non}$ the nonlocal microscopic hardening/softening process. The single terms take the specific form

$$\begin{aligned}
\bar{\psi}_{loc}(\boldsymbol{\varepsilon}^e(\boldsymbol{\varepsilon}, \boldsymbol{\varepsilon}^p)) &= \frac{1}{2}\kappa(\mathrm{tr}[\boldsymbol{\varepsilon}^e(\boldsymbol{\varepsilon}, \boldsymbol{\varepsilon}^p)])^2 + \mu\|\mathrm{dev}[\boldsymbol{\varepsilon}^e(\boldsymbol{\varepsilon}, \boldsymbol{\varepsilon}^p)]\|_2^2\,,\\
\check{\psi}_{loc}(\alpha) &= \frac{1}{2}H\alpha^2\,,\\
\check{\psi}_{non}(\nabla\alpha) &= \frac{1}{2}\mu l^2\|\nabla\alpha\|_2^2\,,
\end{aligned}$$

where κ denotes the bulk modulus, μ the shear modulus, H the isotropic hardening modulus, and l a length scale parameter, see Figure 2.1. To evaluate the macroscopic equilibrium, the microscopic balance equation and the conjugate problem for the local

internal variable $\boldsymbol{\varepsilon}^p$, we need the derivatives $\partial_{\boldsymbol{\varepsilon}}\psi$, $\partial_{\boldsymbol{\varepsilon}^p}\psi$, $\partial_\alpha\psi$ and $\partial_{\nabla\alpha}\psi$, see Table 2.1. Using the condition of plastic incompressibility $\operatorname{tr}[\boldsymbol{\varepsilon}^p]=0$, we can write

$$\|\operatorname{dev}[\boldsymbol{\varepsilon}^e]\|_2^2 = \sum_{i=1}^{3}\left(\varepsilon_{ii}-\varepsilon_{ii}^p-\frac{1}{3}\operatorname{tr}[\boldsymbol{\varepsilon}]\right)^2 + \sum_{\substack{i,j=1\\ i\neq j}}^{3}(\varepsilon_{ij}-\varepsilon_{ij}^p)^2$$

and calculate

$$\begin{aligned}\frac{\partial}{\partial\varepsilon_{ii}}\|\operatorname{dev}[\boldsymbol{\varepsilon}^e]\|_2^2 &= \frac{4}{3}\left(\varepsilon_{ii}-\varepsilon_{ii}^p-\frac{1}{3}\operatorname{tr}[\boldsymbol{\varepsilon}]\right)-\frac{2}{3}\sum_{j=1,j\neq i}^{3}\left(\varepsilon_{jj}-\varepsilon_{jj}^p-\frac{1}{3}\operatorname{tr}[\boldsymbol{\varepsilon}]\right)\\ &= 2\left(\varepsilon_{ii}-\varepsilon_{ii}^p-\frac{1}{3}\operatorname{tr}[\boldsymbol{\varepsilon}-\boldsymbol{\varepsilon}^p]\right) = -\frac{\partial}{\partial\varepsilon_{ii}^p}\|\operatorname{dev}[\boldsymbol{\varepsilon}^e]\|_2^2\,,\\ \frac{\partial}{\partial\varepsilon_{ij}}\|\operatorname{dev}[\boldsymbol{\varepsilon}^e]\|_2^2 &= 2(\varepsilon_{ij}-\varepsilon_{ij}^p) = -\frac{\partial}{\partial\varepsilon_{ij}^p}\|\operatorname{dev}[\boldsymbol{\varepsilon}^e]\|_2^2 \quad \text{for } i\neq j\,.\end{aligned}$$

Furthermore $\partial_{\boldsymbol{\varepsilon}}\operatorname{tr}[\boldsymbol{\varepsilon}]=\boldsymbol{I}$ and hence we get

$$\begin{aligned}\partial_{\boldsymbol{\varepsilon}}\psi &= \kappa\operatorname{tr}[\boldsymbol{\varepsilon}]\boldsymbol{I}+2\mu\operatorname{dev}[\boldsymbol{\varepsilon}-\boldsymbol{\varepsilon}^p]\,,\\ \partial_{\boldsymbol{\varepsilon}^p}\psi &= -2\mu\operatorname{dev}[\boldsymbol{\varepsilon}-\boldsymbol{\varepsilon}^p]\,.\end{aligned}$$

The remaining derivatives read

$$\partial_\alpha\psi = H\alpha \quad\text{and}\quad \partial_{\nabla\alpha}\psi = \mu l^2\nabla\alpha\,.$$

For the evolution laws the yield function φ must be specified. An adapted version of the von-Mises yield function (3.10) reads in space of thermodynamic driving forces $\boldsymbol{B}$ as

$$\varphi(\boldsymbol{B},\beta) = \|\operatorname{dev}[\boldsymbol{B}]\|_2 - \sqrt{\frac{2}{3}}(y_0-\beta)\,, \tag{3.11}$$

where isotropic hardening is modelled by the scalar force $-\beta$. It will be seen later in this section, that the minus sign before β is in agreement with the plus sign before the term $H\alpha$ in (3.10). Now we need to calculate the derivatives $\partial_\beta\varphi$ and $\partial_{\boldsymbol{B}}\varphi$, see again Table 2.1. They read

$$\partial_\beta\varphi = \sqrt{\frac{2}{3}} \quad\text{and}\quad \partial_{\boldsymbol{B}}\varphi = \frac{\operatorname{dev}[\boldsymbol{B}]}{\|\operatorname{dev}[\boldsymbol{B}]\|_2}\,.$$

To follow the result of the derivative of φ witch respect to $\boldsymbol{B}$, we have by the chain rule

$$\begin{aligned}\frac{\partial}{\partial B_{ii}}\|\operatorname{dev}[\boldsymbol{B}]\|_2 &= \frac{1}{\|\operatorname{dev}[\boldsymbol{B}]\|_2}\left(B_{ii}-\frac{1}{3}\operatorname{tr}[\boldsymbol{B}]\right)\,,\\ \frac{\partial}{\partial B_{ij}}\|\operatorname{dev}[\boldsymbol{B}]\|_2 &= \frac{1}{\|\operatorname{dev}[\boldsymbol{B}]\|_2}B_{ij} \quad \text{for } i\neq j\,.\end{aligned} \tag{3.12}$$

Remark 9. The expression

$$\boldsymbol{N} := \partial_{\boldsymbol{B}}\varphi(\boldsymbol{B},\beta) = \frac{\operatorname{dev}[\boldsymbol{B}]}{\|\operatorname{dev}[\boldsymbol{B}]\|_2} \tag{3.13}$$

can be seen as the direction of the evolution of the plastic strain and lies "normal" to the yield surface.

Macroscopic equilibrium:

$$\begin{aligned} -\mathrm{div}[\kappa\,\mathrm{tr}[\boldsymbol{\varepsilon}]\boldsymbol{I} + 2\mu\,\mathrm{dev}[\boldsymbol{\varepsilon} - \boldsymbol{\varepsilon}^p]] - \rho\bar{\boldsymbol{f}}^B &= \boldsymbol{0} && \text{in } \mathscr{B} \\ \boldsymbol{u} &= \bar{\boldsymbol{u}}_D && \text{on } \partial\mathscr{B}_{\bar{\boldsymbol{u}}} \\ \boldsymbol{t} &= \bar{\boldsymbol{t}}_N && \text{on } \partial\mathscr{B}_{\bar{\boldsymbol{t}}} \end{aligned}$$

Microscopic balance equation:

$$\begin{aligned} -\mu l^2\nabla^2\alpha + H\alpha + \beta &= 0 && \text{in } \mathscr{B} \\ \nabla\alpha\cdot\boldsymbol{n} &= 0 && \text{on } \partial\mathscr{B} \end{aligned}$$

Conjugate problem for local plastic strains:

$$-2\mu\,\mathrm{dev}[\boldsymbol{\varepsilon} - \boldsymbol{\varepsilon}^p] + \boldsymbol{B} = \boldsymbol{0} \quad \text{in } \mathscr{B}$$

Evolution equations for hardening field and local plastic strains:

$$\begin{aligned} \dot{\alpha} &= \tfrac{1}{\eta}\langle \|\mathrm{dev}[\boldsymbol{B}]\|_2 - \sqrt{\tfrac{2}{3}}(y_0 - \beta)\rangle\sqrt{\tfrac{2}{3}} && \text{in } \mathscr{B} \\ \alpha(t=0) &= 0 && \text{in } \mathscr{B} \\ \dot{\boldsymbol{\varepsilon}}^p &= \tfrac{1}{\eta}\langle \|\mathrm{dev}[\boldsymbol{B}]\|_2 - \sqrt{\tfrac{2}{3}}(y_0 - \beta)\rangle\boldsymbol{N} && \text{in } \mathscr{B} \\ \boldsymbol{\varepsilon}^p(t=0) &= \boldsymbol{0} && \text{in } \mathscr{B} \end{aligned}$$

Table 3.1. Strong form of rate-dependent coupled system of equations for von-Mises plasticity with gradient-type hardening/softening.

The fully coupled system of equations is summarized in Table 3.1, where we set $\check{\boldsymbol{f}}^B = \boldsymbol{0}$ and choose $\nabla\alpha\cdot\boldsymbol{n} = 0$ on the whole boundary $\partial\mathscr{B}$.
Taking the Euclidean matrix norm of the evolution equation for local plastic strains gives with $\|\boldsymbol{N}\|_2 = 1$

$$\|\dot{\boldsymbol{\varepsilon}}^p\|_2 = \sqrt{\dot{\boldsymbol{\varepsilon}}^p : \dot{\boldsymbol{\varepsilon}}^p} = \frac{1}{\eta}\langle \|\mathrm{dev}[\boldsymbol{B}]\|_2 - \sqrt{\frac{2}{3}}(y_0 - \beta)\rangle\,,$$

and we see from the evolution law for the hardening variable that

$$\dot{\alpha} = \sqrt{\frac{2}{3}\dot{\boldsymbol{\varepsilon}}^p : \dot{\boldsymbol{\varepsilon}}^p}\,.$$

A comparison with the definition (3.9) yields, that the hardening variable α indeed corresponds to the equivalent plastic strain.
Furthermore, it is worth looking at the microscopic balance equation. For $l = 0$ the Laplacian vanishes and we get $H\alpha = -\beta$. Inserting this into the yield function (3.11) and comparing with (3.10), explains the subtraction of β from y_0 in the bracket of (3.11).

Next we do a time discretization of the equations summarized in Table 3.1. Applying the result given in Table 2.2, we obtain the time discrete form of the coupled strong formulation, see Table 3.2, where again the subindex $n+1$, standing for the evaluation at time t_{n+1}, is omitted and $\tau = t_{n+1} - t_n$.
We see, that the consistent integration algorithm results in an implicit Euler scheme for the evolution equations of gradient-type von-Mises plasticity. The reason for this lies in the fact, that the von-Mises yield function (3.11) does not depend on the plastic strains $\boldsymbol{\varepsilon}^p$ and on the constitutive state $\mathfrak{c}$ explicitly. One should remember, that the consistent integration algorithm comes from the time incrementation of the internal rate potential per unit volume. Identifying the extended constitutive state (2.13) as

$$\mathfrak{c}^*(\mathfrak{u}^*) = \{\boldsymbol{\varepsilon}, \alpha, \nabla\alpha, \beta\} \quad \text{with} \quad \mathfrak{u}^* = \{\boldsymbol{u}, \alpha, \beta\}\,,$$

Macroscopic equilibrium:

$$\begin{aligned} -\mathrm{div}[\kappa\,\mathrm{tr}[\boldsymbol{\varepsilon}]\boldsymbol{I} + 2\mu\,\mathrm{dev}[\boldsymbol{\varepsilon} - \boldsymbol{\varepsilon}^p]] - \rho\bar{\boldsymbol{f}}^B &= \boldsymbol{0} && \text{in } \mathscr{B} \\ \boldsymbol{u} &= \bar{\boldsymbol{u}}_D && \text{on } \partial\mathscr{B}_{\bar{\boldsymbol{u}}} \\ \boldsymbol{t} &= \bar{\boldsymbol{t}}_N && \text{on } \partial\mathscr{B}_{\bar{\boldsymbol{t}}} \end{aligned}$$

Microscopic balance equation:

$$\begin{aligned} -\mu l^2\nabla^2\alpha + H\alpha + \beta &= 0 && \text{in } \mathscr{B} \\ \nabla\alpha\cdot\boldsymbol{n} &= 0 && \text{on } \partial\mathscr{B} \end{aligned}$$

Conjugate problem for local plastic strains:

$$-2\mu\,\mathrm{dev}[\boldsymbol{\varepsilon} - \boldsymbol{\varepsilon}^p] + \boldsymbol{B} = \boldsymbol{0} \quad \text{in } \mathscr{B}$$

Evolution equations for hardening field and local plastic strains:

$$\begin{aligned} \alpha &= \alpha_n + \tfrac{\tau}{\eta}\langle \|\mathrm{dev}[\boldsymbol{B}]\|_2 - \sqrt{\tfrac{2}{3}}(y_0 - \beta)\rangle\sqrt{\tfrac{2}{3}} && \text{in } \mathscr{B} \\ \alpha_0 &= 0 && \text{in } \mathscr{B} \\ \boldsymbol{\varepsilon}^p &= \boldsymbol{\varepsilon}^p_n + \tfrac{\tau}{\eta}\langle \|\mathrm{dev}[\boldsymbol{B}]\|_2 - \sqrt{\tfrac{2}{3}}(y_0 - \beta)\rangle\boldsymbol{N} && \text{in } \mathscr{B} \\ \boldsymbol{\varepsilon}^p_0 &= \boldsymbol{0} && \text{in } \mathscr{B} \end{aligned}$$

Table 3.2. Time discrete strong form of rate-dependent coupled system of equations for von-Mises plasticity with gradient-type hardening/softening.

and the set (2.14) of local internal variables together with its dual forces as

$$\mathfrak{s} = \{\boldsymbol{\varepsilon}^p, \boldsymbol{B}\}\ ,$$

we can, according to (2.15), write the time incremental extended internal rate potential per unit volume as

$$\begin{aligned} \pi^{*\tau}_\eta(\mathfrak{c}^*, \mathfrak{c}^*_n, \mathfrak{s}, \mathfrak{s}_n) = {} & \frac{1}{2}\kappa(\mathrm{tr}[\boldsymbol{\varepsilon}])^2 + \mu\|\mathrm{dev}[\boldsymbol{\varepsilon} - \boldsymbol{\varepsilon}^p]\|_2^2 + \frac{1}{2}H\alpha^2 + \frac{1}{2}\mu l^2\|\nabla\alpha\|_2^2 \\ & - \frac{1}{2}\kappa(\mathrm{tr}[\boldsymbol{\varepsilon}_n])^2 - \mu\|\mathrm{dev}[\boldsymbol{\varepsilon}_n - \boldsymbol{\varepsilon}^p_n]\|_2^2 - \frac{1}{2}H\alpha_n^2 - \frac{1}{2}\mu l^2\|\nabla\alpha_n\|_2^2 \\ & + \beta(\alpha - \alpha_n) + \boldsymbol{B} : (\boldsymbol{\varepsilon}^p - \boldsymbol{\varepsilon}^p_n) - \frac{\tau}{2\eta}\langle\varphi(\boldsymbol{B}, \beta)\rangle^2\,. \end{aligned}$$

Taking a closer look at the equations summarized in Table 3.2, we see, that for a given total strain $\boldsymbol{\varepsilon}$, we can solve the local pair $\mathfrak{s}$ by a decoupled subproblem formed by the conjugate problem for local plastic strains and the time discrete evolution problem for local plastic strains. A solution algorithm is derived in the next subsection.

3.4.2. Update algorithm for local plastic strains

We look at the following decoupled subproblem to find $\boldsymbol{\varepsilon}^p$ and $\boldsymbol{B}$ for $\boldsymbol{\varepsilon}$ being given:

$$-2\mu\,\mathrm{dev}[\boldsymbol{\varepsilon} - \boldsymbol{\varepsilon}^p] + \boldsymbol{B} = \boldsymbol{0}\,, \tag{3.14}$$

$$\boldsymbol{\varepsilon}^p = \boldsymbol{\varepsilon}^p_n + \frac{\tau}{\eta}\langle\|\mathrm{dev}[\boldsymbol{B}]\|_2 - \sqrt{\frac{2}{3}}(y_0 - \beta)\rangle\boldsymbol{N}\,, \tag{3.15}$$

where also the actual plastic flow direction $\boldsymbol{N}$ is an unknown quantity. By considering plastic incompressibility, we first of all observe

$$\mathrm{tr}[\boldsymbol{B}] = 2\mu\,(\varepsilon_{11} + \varepsilon_{22} + \varepsilon_{33} - \mathrm{tr}[\boldsymbol{\varepsilon}] - \varepsilon^p_{11} - \varepsilon^p_{22} - \varepsilon^p_{33}) = 0\,,$$

which allows (3.14) to be written as

$$\operatorname{dev}[\boldsymbol{B}] = 2\mu \operatorname{dev}[\boldsymbol{\varepsilon} - \boldsymbol{\varepsilon}^p] \,. \tag{3.16}$$

From (3.15) we get

$$\operatorname{dev}[\boldsymbol{\varepsilon}^p] = \operatorname{dev}[\boldsymbol{\varepsilon}_n^p] + \Delta\gamma \boldsymbol{N} \quad \text{with} \quad \Delta\gamma := \frac{\tau}{\eta}\langle \|\operatorname{dev}[\boldsymbol{B}]\|_2 - \sqrt{\frac{2}{3}}(y_0 - \beta)\rangle \tag{3.17}$$

being the plastic consistency parameter. Inserting this into (3.16) gives

$$\operatorname{dev}[\boldsymbol{B}] = \underbrace{2\mu \operatorname{dev}\left[\boldsymbol{\varepsilon} - \boldsymbol{\varepsilon}_n^p\right]}_{=:\operatorname{dev}[\boldsymbol{B}^{tr}]} - 2\mu\Delta\gamma \boldsymbol{N} \,, \tag{3.18}$$

with $\operatorname{dev}[\boldsymbol{B}^{tr}]$ being the deviatoric trial thermodynamic driving force, which only consists of known values. Introducing the trial direction of plastic flow

$$\boldsymbol{N}^{tr} := \frac{\operatorname{dev}[\boldsymbol{B}^{tr}]}{\|\operatorname{dev}[\boldsymbol{B}^{tr}]\|_2} \,,$$

we can write (3.18) as

$$\|\operatorname{dev}[\boldsymbol{B}]\|_2 \boldsymbol{N} = \left\|\operatorname{dev}[\boldsymbol{B}^{tr}]\right\|_2 \boldsymbol{N}^{tr} - 2\mu\Delta\gamma \boldsymbol{N} \,, \tag{3.19}$$

where for the term on the left hand side we made use of (3.13). Taking the Euclidean matrix norm of (3.18) yields with $\|\boldsymbol{N}\|_2 = 1$

$$\|\operatorname{dev}[\boldsymbol{B}]\|_2 = \left\|\operatorname{dev}[\boldsymbol{B}^{tr}]\right\|_2 - 2\mu\Delta\gamma \,, \tag{3.20}$$

and by a comparison with (3.19) the yet unknown direction of plastic flow $\boldsymbol{N}$ can be identified as

$$\boldsymbol{N} = \boldsymbol{N}^{tr} \,. \tag{3.21}$$

Hence, only the plastic consistency parameter remains unknown. By inserting (3.20) into the definition of $\Delta\gamma$ given in (3.17), we get a linear equation in $\Delta\gamma$:

$$\Delta\gamma = \frac{\tau}{\eta}\langle \underbrace{\left\|\operatorname{dev}[\boldsymbol{B}^{tr}]\right\|_2 - 2\mu\Delta\gamma - \sqrt{\frac{2}{3}}(y_0 - \beta)}_{=\varphi(\boldsymbol{B},\beta)} \rangle \,. \tag{3.22}$$

Assuming $\varphi > 0$, the trial solution $\widetilde{\Delta\gamma}$ of (3.22) reads

$$\widetilde{\Delta\gamma} = \frac{\tau}{2\mu\tau + \eta}\left[\left\|\operatorname{dev}[\boldsymbol{B}^{tr}]\right\|_2 - \sqrt{\frac{2}{3}}(y_0 - \beta)\right]$$

with which we can calculate via (3.18)

$$\operatorname{dev}[\widetilde{\boldsymbol{B}}] = \operatorname{dev}[\boldsymbol{B}^{tr}] - 2\mu\widetilde{\Delta\gamma}\boldsymbol{N} \,.$$

To confirm or confute the trial plastic consistency parameter $\widetilde{\Delta\gamma}$, we have to check backwards and obtain the plastic consistency parameter as

$$\Delta\gamma = \begin{cases} \widetilde{\Delta\gamma} & \text{if } \varphi(\widetilde{\boldsymbol{B}}, \beta) > 0 \,, \\ 0 & \text{if } \varphi(\widetilde{\boldsymbol{B}}, \beta) < 0 \end{cases}$$

with which the actual plastic strain $\boldsymbol{\varepsilon}^p$ can be computed via (3.17).

Remark 10. Looking at (3.18) we see, that the trial state is corrected by a term with "direction" $\boldsymbol{N}$. Because of (3.21), the direction of plastic flow $\boldsymbol{N}$, embedded in the space of principal deviatoric thermodynamic driving forces, is radial to the template of the von-Mises yield surface, see Figure 3.10. Therefore the presented update algorithm can be seen as a radial-return algorithm.

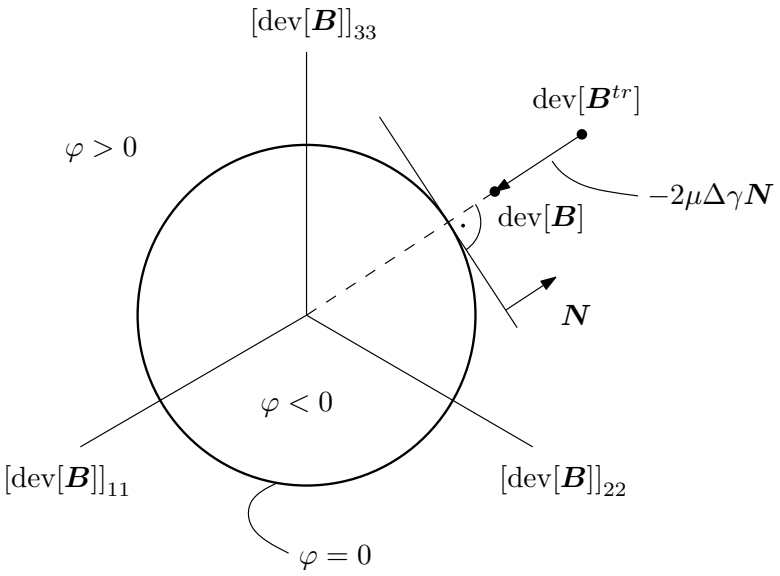

Figure 3.10. Radial-return algorithm.

3.4.3. Generalized stresses and material tangent moduli

In order to evaluate the stiffness matrix and the vector of internal forces, we have to compute the material tangent moduli and the vector of generalized stresses at every integration point. For this we switch to Voigt's notation. Since we are only considering plane strain problems in our numerical examples, we write

$$\mathfrak{e}_h^* = \{\varepsilon_{11h}, \varepsilon_{22h}, \varepsilon_{12h}, \varepsilon_{21h}, \alpha_h, \nabla\alpha_h, \beta_h\} \quad \text{and} \quad \mathfrak{u}_h^* = \{u_{1h}, u_{2h}, \alpha_h, \beta_h\}\,, \tag{3.23}$$

where we do not consider the symmetry of the strain tensor. Following the notation used in Section 2.4, the nodal values of the node with global number j are

$$\mathfrak{d}_j^* = \left\{\bar{\boldsymbol{u}}_j, \check{\boldsymbol{u}}_j, \mathfrak{f}_j\right\}$$

with $\bar{\boldsymbol{u}}_j = [d_j^1,\, d_j^1]^T$ being the nodal macroscopic displacements, $\check{\boldsymbol{u}}_j = \alpha_j$ being the nodal hardening variable and $\mathfrak{f}_j = \beta_j$ being the nodal conjugate force.
As defined in (2.21) and already given in (2.17), the vector of generalized stresses $\boldsymbol{\sigma}^{*k}$ is

$$\boldsymbol{\sigma}^{*k} = \begin{bmatrix} [\partial_{\boldsymbol{\varepsilon}_h}\pi^{*\tau}_{\eta h}]_{4\times1} \\ \partial_{\alpha_h}\pi^{*\tau}_{\eta h} \\ \partial_{\nabla\alpha_h}\pi^{*\tau}_{\eta h} \\ \partial_{\beta_h}\pi^{*\tau}_{\eta h} \end{bmatrix}^k = \begin{bmatrix} [\partial_{\boldsymbol{\varepsilon}_h}\psi]_{4\times1} \\ \partial_{\alpha_h}\psi + \beta_h \\ \partial_{\nabla\alpha_h}\psi \\ \alpha_h - \alpha_{nh} - m\left[\frac{\tau}{\eta}\varphi(\boldsymbol{B},\beta_h)\partial_{\beta_h}\varphi(\boldsymbol{B},\beta_h)\right] \end{bmatrix}^k,$$

with

$$m := \begin{cases} 1 & \text{if } \varphi(\boldsymbol{B},\beta_h) > 0\,, \\ 0 & \text{if } \varphi(\boldsymbol{B},\beta_h) < 0\,. \end{cases} \tag{3.24}$$

The emerging derivatives, which have already been calculated, are

$$\begin{aligned} \partial_{\boldsymbol{\varepsilon}_h}\psi &= \kappa\,\mathrm{tr}[\boldsymbol{\varepsilon}_h]\boldsymbol{I} + 2\mu\,\mathrm{dev}[\boldsymbol{\varepsilon}_h - \boldsymbol{\varepsilon}^p]\,, \\ \partial_{\alpha_h}\psi &= H\alpha_h + \beta_h\,, \\ \partial_{\nabla\alpha_h}\psi &= \mu l^2\nabla\alpha_h\,, \\ \partial_{\beta_h}\varphi &= \sqrt{\frac{2}{3}}\,. \end{aligned}$$

The needed values α_h and β_h in the integration points are calculated via an element-wise interpolation of the nodal values α_j and β_j, which are actually known from $\mathfrak{d}^{*k} = \mathfrak{d}^{*k-1} + \Delta\mathfrak{d}^{*k-1}$. Similarly we get $\boldsymbol{\varepsilon}_h$ and $\nabla\alpha_h$ by just considering the appropriate derivatives, which are concluded in the $\mathfrak{B}^*$ matrix[2]. The local variables $\boldsymbol{\varepsilon}^p$ and $\boldsymbol{B}$ are obtained by the update algorithm derived in the last subsection. Here one has to be very careful in the calculation of $\left\|\mathrm{dev}[\boldsymbol{B}^{tr}]\right\|_2$ since the defined deviatoric operator just makes sense for a 3×3 array. Therefore we have to expand the 2×2 arrays $\boldsymbol{\varepsilon}_h$ and $\boldsymbol{\varepsilon}^p$ by one row and one column containing zeros. We obtain $[\mathrm{dev}[\boldsymbol{B}]]_{33} \neq 0$, which means, that, although we are doing a two-dimensional calculation here, the thermodynamic driving forces $\boldsymbol{B}^{tr}$ and $\boldsymbol{B}$, respectively, must be treated as 3×3 arrays.
Voigt's notation transforms every quantity, which can be represented by a two-dimensional array, in a one-dimensional array:

$$\begin{bmatrix} [\cdot]_{11} & [\cdot]_{12} & [\cdot]_{13} \\ [\cdot]_{21} & [\cdot]_{22} & [\cdot]_{23} \\ [\cdot]_{31} & [\cdot]_{32} & [\cdot]_{33} \end{bmatrix} \rightsquigarrow [[\cdot]_{11}, [\cdot]_{22}, [\cdot]_{33}, [\cdot]_{12}, [\cdot]_{23}, [\cdot]_{31}, [\cdot]_{21}, [\cdot]_{32}, [\cdot]_{13}]^T ,$$

e.g.

$$\begin{bmatrix} 1 & 0 \\ 0 & 1 \end{bmatrix} \rightsquigarrow \mathbf{1} := \begin{bmatrix} 1 \\ 1 \\ 0 \\ 0 \end{bmatrix}$$

Then we can conclude

$$[\partial_{\boldsymbol{\varepsilon}_h}\psi]_{4\times1} = \kappa\,\mathrm{tr}[\boldsymbol{\varepsilon}_h]\mathbf{1} + 2\mu \begin{bmatrix} [\mathrm{dev}[\boldsymbol{\varepsilon}_h - \boldsymbol{\varepsilon}^p]]_{11} \\ [\mathrm{dev}[\boldsymbol{\varepsilon}_h - \boldsymbol{\varepsilon}^p]]_{22} \\ [\mathrm{dev}[\boldsymbol{\varepsilon}_h - \boldsymbol{\varepsilon}^p]]_{12} \\ [\mathrm{dev}[\boldsymbol{\varepsilon}_h - \boldsymbol{\varepsilon}^p]]_{21} \end{bmatrix} ,$$

where again it should be noted, that $[\mathrm{dev}[\boldsymbol{\varepsilon}_h - \boldsymbol{\varepsilon}^p]]_{33} \neq 0$, which identifies the stress σ_{33h} to be nonzero for the plane strain case.

Furthermore, for the realization of the Newton-Raphson scheme, we need to compute the material tangent moduli. They read

$$\mathbb{C}^{*k} = \begin{bmatrix} [\partial^2_{\boldsymbol{\varepsilon}_h\boldsymbol{\varepsilon}_h}\pi^{*\tau}_{\eta h}]_{4\times4} & [\mathbf{0}]_{4\times1} & [\mathbf{0}]_{4\times3} & [\partial^2_{\boldsymbol{\varepsilon}_h\beta_h}\pi^{*\tau}_{\eta h}]_{4\times1} \\ [\mathbf{0}]_{1\times4} & \partial^2_{\alpha_h\alpha_h}\pi^{*\tau}_{\eta h} & [\mathbf{0}]_{1\times3} & 1 \\ [\mathbf{0}]_{2\times4} & [\mathbf{0}]_{2\times1} & \partial^2_{\nabla\alpha_h\nabla\alpha_h}\pi^{*\tau}_{\eta h} & [\mathbf{0}]_{2\times1} \\ [\partial^2_{\beta_h\boldsymbol{\varepsilon}_h}\pi^{*\tau}_{\eta h}]_{1\times4} & 1 & [\mathbf{0}]_{1\times3} & \partial^2_{\beta_h\beta_h}\pi^{*\tau}_{\eta h} \end{bmatrix}^k . \tag{3.25}$$

As mentioned in Remark 5, it is important here to consider the dependencies of the local fields $\boldsymbol{\varepsilon}^p$ and $\boldsymbol{B}$ on the global ones, specialized by the local update algorithm. Let us first look at the elastic case for which $m = 0$ and $\mathrm{dev}[\boldsymbol{\varepsilon}^p] = \mathbf{0}$, and hence no local fields occur. Then, by using

$$\partial_{\boldsymbol{\varepsilon}_h}\,\mathrm{dev}[\boldsymbol{\varepsilon}_h - \boldsymbol{\varepsilon}^p_n] = \mathbb{I} - \frac{1}{3}\boldsymbol{I}\otimes\boldsymbol{I} =: \mathbb{P}$$

[2]For $\boldsymbol{\varepsilon}_h$ also the matrix $\boldsymbol{A}$ is needed, which will be constructed in the next subsection.

with $(\mathbb{I})_{ijkl} := \delta_{ij}\delta_{kl}$ being a fourth order unity tensor, where the symmetry of $\boldsymbol{\varepsilon}$ has not been taken into account, the unknown terms in (3.25) read

$$\begin{aligned}
\partial^2_{\boldsymbol{\varepsilon}_h\boldsymbol{\varepsilon}_h}\pi^{*\tau}_{\eta h} &= \kappa \boldsymbol{I}\otimes\boldsymbol{I} + 2\mu\mathbb{P}\,,\\
\partial^2_{\alpha_h\alpha_h}\pi^{*\tau}_{\eta h} &= H\,,\\
\partial^2_{\nabla\alpha_h\nabla\alpha_h}\pi^{*\tau}_{\eta h} &= \mu l^2 \boldsymbol{I}\,,\\
\partial^2_{\beta_h\beta_h}\pi^{*\tau}_{\eta h} &= 0\,,\\
\partial^2_{\boldsymbol{\varepsilon}_h\beta_h}\pi^{*\tau}_{\eta h} &= \boldsymbol{0}\,.
\end{aligned} \tag{3.26}$$

Remark 11. When explicitly using the symmetry of a symmetric tensor of second order $\boldsymbol{P}$, i.e. $P_{ij} = P_{ji}$, we have $\partial_{\boldsymbol{P}}\boldsymbol{P} = \mathbb{I}^s$ with $(\mathbb{I}^s)_{ijkl} := \frac{1}{2}(\delta_{ik}\delta_{jl} + \delta_{il}\delta_{jk})$ being the symmetric fourth order unity tensor.

If we reach the plastic state ($m = 1$), some components in (3.26) have to be corrected by additional terms, i.e.

$$\begin{aligned}
\partial^2_{\boldsymbol{\varepsilon}_h\boldsymbol{\varepsilon}_h}\pi^{*\tau}_{\eta h} &= \kappa \boldsymbol{I}\otimes\boldsymbol{I} + 2\mu\mathbb{P} - 2\mu\partial_{\boldsymbol{\varepsilon}_h}\operatorname{dev}[\boldsymbol{\varepsilon}^p(\boldsymbol{\varepsilon}_h,\beta_h)]\,,\\
\partial^2_{\beta_h\beta_h}\pi^{*\tau}_{\eta h} &= -\frac{\tau}{\eta}\sqrt{\frac{2}{3}}\partial_{\beta_h}\varphi(\boldsymbol{B}(\boldsymbol{\varepsilon}_h,\beta_h),\beta_h)\,,\\
\partial^2_{\boldsymbol{\varepsilon}_h\beta_h}\pi^{*\tau}_{\eta h} &= -2\mu\partial_{\beta_h}\operatorname{dev}[\boldsymbol{\varepsilon}^p(\boldsymbol{\varepsilon}_h,\beta_h)]\,.
\end{aligned}$$

From the local update algorithm we conclude

$$\operatorname{dev}[\boldsymbol{\varepsilon}^p] = \operatorname{dev}[\boldsymbol{\varepsilon}^p_n] + \frac{\tau}{2\mu\tau+\eta}\left[2\mu\|\operatorname{dev}[\boldsymbol{\varepsilon}_h - \boldsymbol{\varepsilon}^p_n]\|_2 - \sqrt{\frac{2}{3}}(y_0 - \beta_h)\right]\frac{\operatorname{dev}[\boldsymbol{\varepsilon}_h - \boldsymbol{\varepsilon}^p_n]}{\|\operatorname{dev}[\boldsymbol{\varepsilon}_h - \boldsymbol{\varepsilon}^p_n]\|_2}\,,$$

$$\varphi = \left\|\operatorname{dev}[\boldsymbol{B}^{tr}]\right\|_2 - \frac{2\mu\tau}{2\mu\tau+\eta}\left[\left\|\operatorname{dev}[\boldsymbol{B}^{tr}]\right\|_2 - \sqrt{\frac{2}{3}}(y_0 - \beta_h)\right] - \sqrt{\frac{2}{3}}(y_0 - \beta_h)\,.$$

With

$$\partial_{\boldsymbol{\varepsilon}_h}\|\operatorname{dev}[\boldsymbol{\varepsilon}_h - \boldsymbol{\varepsilon}^p_n]\|_2 = \frac{\operatorname{dev}[\boldsymbol{\varepsilon}_h - \boldsymbol{\varepsilon}^p_n]}{\|\operatorname{dev}[\boldsymbol{\varepsilon}_h - \boldsymbol{\varepsilon}^p_n]\|_2} = \frac{\operatorname{dev}[\boldsymbol{B}^{tr}]}{\|\operatorname{dev}[\boldsymbol{B}^{tr}]\|_2} = \boldsymbol{N}^{tr}$$

we obtain

$$\begin{aligned}
\partial_{\boldsymbol{\varepsilon}_h}\operatorname{dev}[\boldsymbol{\varepsilon}^p(\boldsymbol{\varepsilon}_h,\beta_h)] &= \frac{2\mu\tau}{2\mu\tau+\eta}\boldsymbol{N}^{tr}\otimes\boldsymbol{N}^{tr} - \Delta\gamma\frac{2\mu\operatorname{dev}[\boldsymbol{B}^{tr}]}{\|\operatorname{dev}[\boldsymbol{B}^{tr}]\|_2^2}\otimes\boldsymbol{N}^{tr} + \frac{\Delta\gamma}{\|\operatorname{dev}[\boldsymbol{\varepsilon}_h - \boldsymbol{\varepsilon}^p_n]\|_2}\mathbb{P}\\
&= \frac{2\mu\tau}{2\mu\tau+\eta}\boldsymbol{N}^{tr}\otimes\boldsymbol{N}^{tr} + \frac{2\mu\Delta\gamma}{\|\operatorname{dev}[\boldsymbol{B}^{tr}]\|_2}(\mathbb{P} - \boldsymbol{N}^{tr}\otimes\boldsymbol{N}^{tr})\,.
\end{aligned}$$

Furthermore

$$\partial_{\beta_h}\varphi(\boldsymbol{B}(\boldsymbol{\varepsilon}_h,\beta_h) = -\frac{2\mu\tau}{2\mu\tau+\eta}\sqrt{\frac{2}{3}} + \sqrt{\frac{2}{3}} = \sqrt{\frac{2}{3}}\frac{\eta}{2\mu\tau+\eta}$$

and

$$\partial_{\beta_h}\operatorname{dev}[\boldsymbol{\varepsilon}^p(\boldsymbol{\varepsilon}_h,\beta_h)] = \sqrt{\frac{2}{3}}\frac{\tau}{2\mu\tau+\eta}\boldsymbol{N}^{tr}\,.$$

Finally the according components of the material tangent moduli (3.25) read in Voigt's

notation

$$
\begin{aligned}
[\partial^2_{\boldsymbol{\varepsilon}_h\boldsymbol{\varepsilon}_h}\pi^{*\tau}_{\eta h}]_{4\times4} &= \kappa\mathbf{1}\mathbf{1}^T + 2\mu[\mathbb{P}]_{4\times4} \\
&\quad - m\left[\frac{4\mu^2\tau}{2\mu\tau+\eta}[\boldsymbol{N}^{tr}]_{4\times1}[\boldsymbol{N}^{tr}]^T_{4\times1} + \frac{4\mu^2\Delta\gamma}{\|\mathrm{dev}[\boldsymbol{B}^{tr}]\|_2}([\mathbb{P}]_{4\times4} - [\boldsymbol{N}^{tr}]_{4\times1}[\boldsymbol{N}^{tr}]^T_{4\times1})\right], \\
\partial^2_{\alpha_h\alpha_h}\pi^{*\tau}_{\eta h} &= H\,, \\
\partial^2_{\nabla\alpha_h\nabla\alpha_h}\pi^{*\tau}_{\eta h} &= \mu l^2\boldsymbol{I}\,, \\
\partial^2_{\beta_h\beta_h}\pi^{*\tau}_{\eta h} &= m\left(-\frac{2}{3}\frac{\tau}{2\mu\tau+\eta}\right), \\
[\partial^2_{\boldsymbol{\varepsilon}_h\beta_h}\pi^{*\tau}_{\eta h}]_{4\times1} &= m\left(-\sqrt{\frac{2}{3}}\frac{2\mu\tau}{2\mu\tau+\eta}[\boldsymbol{N}^{tr}]_{4\times1}\right),
\end{aligned}
$$

where $[\mathbb{P}]_{4\times4} = [\boldsymbol{I}]_{4\times4} - \frac{1}{3}\mathbf{1}\mathbf{1}^T$, and m being defined in (3.24).

3.4.4. Finite element matrices

For our numerical examples, given in the next chapter, we will discretize the two-dimensional domain by quadrilaterals of first order. The shape functions are

$$
\begin{aligned}
h_1(\boldsymbol{\xi}) &= \frac{1}{4}(1+\xi^1)(1+\xi^2)\,, \\
h_2(\boldsymbol{\xi}) &= \frac{1}{4}(1-\xi^1)(1+\xi^2)\,, \\
h_3(\boldsymbol{\xi}) &= \frac{1}{4}(1-\xi^1)(1-\xi^2)\,, \\
h_4(\boldsymbol{\xi}) &= \frac{1}{4}(1+\xi^1)(1-\xi^2)\,.
\end{aligned}
\tag{3.27}
$$

For the row matrix $\mathfrak{d}^{*e}$, which contains the macroscopic nodal displacements, the nodal hardening variable and its nodal conjugate force, we choose the ordering

$$
\mathfrak{d}^{*e} = \left[d^1_1\,,\, d^2_1\,,\, \alpha_1\,,\, \beta_1\,,\, \ldots\,,\, d^1_4\,,\, d^2_4\,,\, \alpha_4\,,\, \beta_4\right]^{eT}.
$$

Then, under consideration of the ordering of $\mathbf{u}^*_h$ given in $(3.23)_2$, the interpolation matrix on element level is

$$
\mathfrak{H}^{*e} = \begin{bmatrix}
h_1 & 0 & 0 & 0 & \ldots & h_4 & 0 & 0 & 0 \\
0 & h_1 & 0 & 0 & \ldots & 0 & h_4 & 0 & 0 \\
0 & 0 & h_1 & 0 & \ldots & 0 & 0 & h_4 & 0 \\
0 & 0 & 0 & h_1 & \ldots & 0 & 0 & 0 & h_4
\end{bmatrix}.
$$

Moreover, by looking at the ordering of $\mathfrak{e}^*_h$ given in $(3.23)_1$, the generalized differential operator matrix reads

$$
\mathfrak{D}^* = \begin{bmatrix}
\frac{\partial}{\partial x^1} & 0 & 0 & 0 \\
0 & \frac{\partial}{\partial x^2} & 0 & 0 \\
\frac{1}{2}\frac{\partial}{\partial x^2} & \frac{1}{2}\frac{\partial}{\partial x^1} & 0 & 0 \\
\frac{1}{2}\frac{\partial}{\partial x^2} & \frac{1}{2}\frac{\partial}{\partial x^1} & 0 & 0 \\
0 & 0 & 1 & 0 \\
0 & 0 & \frac{\partial}{\partial x^1} & 0 \\
0 & 0 & \frac{\partial}{\partial x^2} & 0 \\
0 & 0 & 0 & 1
\end{bmatrix}.
$$

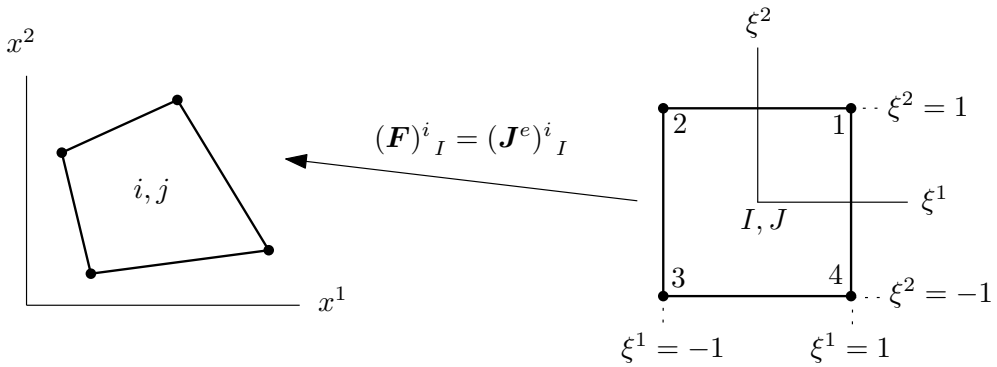

Figure 3.11. Transformation from parameter space to physical space. The local node numbers of the bi-unit square are in agreement with the numbering of the shape functions (3.27).

With this at hand, we can calculate $\mathfrak{B}^{*e} = \mathfrak{D}^* \mathfrak{H}^{*e}$ at every integration point. For the determination of the sub stiffness matrices given in (2.29), we else need the interpolation matrix $\boldsymbol{A}$ for the enhanced strains ${}^e\boldsymbol{\varepsilon}$. Note, that the interpolation of ${}^e\boldsymbol{\varepsilon}$ must be constructed in such a way, that the orthogonality condition (2.26) is fulfilled. For this, as it will be seen soon, it is easier to do a transformation of the element enhanced strains from physical space to parameter space represented by the bi-unit square in the natural coordinate system, i.e.

$$ {}^e\boldsymbol{\varepsilon}^e =: \frac{J^e(\boldsymbol{0})}{J^e(\boldsymbol{\xi})} [\boldsymbol{J}^e(\boldsymbol{0})]^{-T} \boldsymbol{E}^e(\boldsymbol{\xi}) [\boldsymbol{J}^e(\boldsymbol{0})]^{-1} , \tag{3.28} $$

where $\boldsymbol{E}^e(\boldsymbol{\xi})$ denotes the element enhanced strains on the bi-unit square, $\boldsymbol{J}^e(\boldsymbol{\xi})$ the Jacobi matrix

$$ \boldsymbol{J}^e(\boldsymbol{\xi}) := \frac{\partial}{\partial \boldsymbol{\xi}} \boldsymbol{x}_h^e(\boldsymbol{\xi}) = \begin{bmatrix} \frac{\partial x_h^{1e}}{\partial \xi^1} & \frac{\partial x_h^{1e}}{\partial \xi^2} \\ \frac{\partial x_h^{2e}}{\partial \xi^1} & \frac{\partial x_h^{2e}}{\partial \xi^2} \end{bmatrix} $$

and $J^e(\boldsymbol{\xi})$ the Jacobian $J^e(\boldsymbol{\xi}) := \det[\boldsymbol{J}^e(\boldsymbol{\xi})]$.

Remark 12. The transformation (3.28) is motivated by the transformation law of covariant second order tensors, see [12] or [26]:

$$ ({}^e\boldsymbol{\varepsilon})_{ij} = (\boldsymbol{F}^{-T})_i{}^I (\boldsymbol{E})_{IJ} (\boldsymbol{F}^{-1})^J{}_j $$

with the "deformation gradient"

$$ (\boldsymbol{F})^i{}_I := \frac{\partial x^i}{\partial \xi^I} , \tag{3.29} $$

see Figure 3.11.

Remark 13. As mentioned in [30], the evaluation of the Jacobi matrices in (3.28) at the center of the bi-unit square comes from the requirement of the transformation to be invariant. The arising Jacobians are just weighting factors.

Moreover, we do a similar transformation of the element stresses $\boldsymbol{\sigma}^e$ from the physical space to the parameter space, i.e.

$$ \boldsymbol{\sigma}^e =: \boldsymbol{J}^e(\boldsymbol{0}) \boldsymbol{\Sigma}^e(\boldsymbol{\xi}) [\boldsymbol{J}^e(\boldsymbol{0})]^T , \tag{3.30} $$

with $\boldsymbol{\Sigma}^e(\boldsymbol{\xi})$ being the element stress tensor defined on the bi-unit square.

Remark 14. The transformation (3.30) comes from the transformation law of contravariant second order tensors, see again [12] or [26]:

$$(\boldsymbol{\sigma})^{ij} = (\boldsymbol{F})^{i}{}_{I}(\boldsymbol{\Sigma})^{IJ}(\boldsymbol{F}^{T})^{J}{}_{j}\,,$$

where $\boldsymbol{F}$ again denotes the deformation gradient (3.29).

By taking the inner product of the discrete stress tensor and the discrete enhanced strain tensor,

$$\begin{aligned}
\boldsymbol{\sigma}_h^e : {}^e\boldsymbol{\varepsilon}_h^e &= \frac{J^e(\mathbf{0})}{J^e(\boldsymbol{\xi})}\boldsymbol{J}^e(\mathbf{0})\boldsymbol{\Sigma}_h^e(\boldsymbol{\xi})[\boldsymbol{J}^e(\mathbf{0})]^T : [\boldsymbol{J}^e(\mathbf{0})]^{-T}\boldsymbol{E}_h^e(\boldsymbol{\xi})[\boldsymbol{J}^e(\mathbf{0})]^{-1} \\
&= \frac{J^e(\mathbf{0})}{J^e(\boldsymbol{\xi})}[\boldsymbol{J}^e(\mathbf{0})]^{-1}\boldsymbol{J}^e(\mathbf{0})\boldsymbol{\Sigma}_h^e(\boldsymbol{\xi})[\boldsymbol{J}^e(\mathbf{0})]^T : \boldsymbol{E}_h^e(\boldsymbol{\xi})[\boldsymbol{J}^e(\mathbf{0})]^{-1} \\
&= \frac{J^e(\mathbf{0})}{J^e(\boldsymbol{\xi})}\boldsymbol{\Sigma}_h^e(\boldsymbol{\xi})[\boldsymbol{J}^e(\mathbf{0})]^T[\boldsymbol{J}^e(\mathbf{0})]^{-T} : \boldsymbol{E}_h^e(\boldsymbol{\xi}) \\
&= \frac{J^e(\mathbf{0})}{J^e(\boldsymbol{\xi})}\boldsymbol{\Sigma}_h^e(\boldsymbol{\xi}) : \boldsymbol{E}_h^e(\boldsymbol{\xi})\,,
\end{aligned}$$

the orthogonality condition (2.26) can be written on element level as

$$\int_{\mathscr{B}_h^e} \boldsymbol{\sigma}_h^e : {}^e\boldsymbol{\varepsilon}_h^e \,\mathrm{d}v = J^e(\mathbf{0}) \int_{-1}^{1}\int_{-1}^{1} \boldsymbol{\Sigma}_h^e : \boldsymbol{E}_h^e \,\mathrm{d}\xi_1\,\mathrm{d}\xi_2 = 0\,, \tag{3.31}$$

where we have made use of $\mathrm{d}v = J^e(\boldsymbol{\xi})\,\mathrm{d}\xi_1\,\mathrm{d}\xi_2$. Therefore the fulfilment of the orthogonality condition can be reached by the construction of interpolations in the parameter space. Again, we will switch to Voigt's notation, and the transformation (3.28) can be written in matrix-vector product form as

$$\begin{bmatrix} {}^e\varepsilon_{11} \\ {}^e\varepsilon_{22} \\ {}^e\varepsilon_{12} \\ {}^e\varepsilon_{21} \end{bmatrix}^e = \frac{J^e(0)}{J^e(\boldsymbol{\xi})} \underbrace{\begin{bmatrix} J^0_{11}J^0_{11} & J^0_{21}J^0_{21} & J^0_{11}J^0_{21} & J^0_{11}J^0_{21} \\ J^0_{12}J^0_{12} & J^0_{22}J^0_{22} & J^0_{12}J^0_{22} & J^0_{12}J^0_{22} \\ J^0_{11}J^0_{12} & J^0_{21}J^0_{22} & \frac{1}{2}(J^0_{11}J^0_{22}+J^0_{12}J^0_{21}) & \frac{1}{2}(J^0_{11}J^0_{22}+J^0_{12}J^0_{21}) \\ J^0_{11}J^0_{12} & J^0_{21}J^0_{22} & \frac{1}{2}(J^0_{11}J^0_{22}+J^0_{12}J^0_{21}) & \frac{1}{2}(J^0_{11}J^0_{22}+J^0_{12}J^0_{21}) \end{bmatrix}^e}_{=:\boldsymbol{M}^e} \begin{bmatrix} E_{11} \\ E_{22} \\ E_{12} \\ E_{21} \end{bmatrix}^e,$$

where the abbreviation $J^0_{iI} := [\boldsymbol{J}(\mathbf{0})]^{i}{}_{I}$ is used. According to [4] we construct the interpolation of $\boldsymbol{E}$ on element e as

$$\boldsymbol{E}_h^e = \frac{1}{2}\left[\boldsymbol{a}_I^e \otimes \boldsymbol{G}^I(\boldsymbol{\xi}) + \boldsymbol{G}^I(\boldsymbol{\xi}) \otimes \boldsymbol{a}_I^e\right] \qquad \text{(summation on } I\text{; } I\text{=1,2)}$$

with

$$\boldsymbol{a}_I^e := \begin{bmatrix} a_I^1 \\ a_I^2 \end{bmatrix}^e \quad \text{and} \quad \boldsymbol{G}^1 := \left[\xi^1\,,\,0\right]\,, \quad \boldsymbol{G}^2 := \left[0\,,\,\xi^2\right]\,.$$

This yields

$$\boldsymbol{E}_h^e = \frac{1}{2}\left\{\begin{bmatrix} \xi^1 a_1^1 & \xi^2 a_2^1 \\ \xi^1 a_1^2 & \xi^2 a_2^2 \end{bmatrix} + \begin{bmatrix} \xi^1 a_1^1 & \xi^1 a_1^2 \\ \xi^2 a_2^1 & \xi^2 a_2^2 \end{bmatrix}\right\}^e = \begin{bmatrix} 2\xi^1 a_1^1 & \xi^2 a_2^1 + \xi^1 a_1^2 \\ \xi^1 a_1^2 + \xi^2 a_2^1 & 2\xi^2 a_2^2 \end{bmatrix}^e,$$

which can be written in matrix-vector product form as

$$\begin{bmatrix} E_{11h} \\ E_{22h} \\ E_{12h} \\ E_{21h} \end{bmatrix}^e = \underbrace{\begin{bmatrix} \xi^1 & 0 & 0 & 0 \\ 0 & \xi^2 & 0 & 0 \\ 0 & 0 & \frac{1}{2}\xi^1 & \frac{1}{2}\xi^2 \\ 0 & 0 & \frac{1}{2}\xi^1 & \frac{1}{2}\xi^2 \end{bmatrix}}_{=:\boldsymbol{T}(\boldsymbol{\xi})} \begin{bmatrix} a_1^1 \\ a_2^2 \\ a_1^2 \\ a_2^1 \end{bmatrix}^e .$$

Finally, we obtain in Voigt's notation

$${}^e\boldsymbol{\varepsilon}_h^e = \frac{J^e(\mathbf{0})}{J^e(\boldsymbol{\xi})} \boldsymbol{M}^e \boldsymbol{T}(\boldsymbol{\xi}) \boldsymbol{a}^e ,$$

and a comparison with $(2.27)_1$ identifies the element matrix $\boldsymbol{A}^e$ as

$$\boldsymbol{A}^e(\boldsymbol{\xi}) = \frac{J^e(0)}{J^e(\boldsymbol{\xi})} \boldsymbol{M}^e \boldsymbol{T}(\boldsymbol{\xi}) .$$

It remains to check the orthogonality condition (3.31). For this we assume for simplicity the element stresses $\boldsymbol{\Sigma}_h^e$ to be element-wise constant:

$$\begin{bmatrix} \Sigma_h^{11} \\ \Sigma_h^{22} \\ \Sigma_h^{12} \\ \Sigma_h^{21} \end{bmatrix}^e = \begin{bmatrix} 1 & 0 & 0 & 0 \\ 0 & 1 & 0 & 0 \\ 0 & 0 & 1 & 0 \\ 0 & 0 & 0 & 1 \end{bmatrix} \begin{bmatrix} b_1 \\ b_2 \\ b_3 \\ b_4 \end{bmatrix}^e .$$

Because of

$$\int_{-1}^{1} \int_{-1}^{1} \xi_1 \, \mathrm{d}\xi_1 \, \mathrm{d}\xi_2 = \int_{-1}^{1} \int_{-1}^{1} \xi_2 \, \mathrm{d}\xi_1 \, \mathrm{d}\xi_2 = 0 ,$$

we indeed get with our chosen interpolations

$$J^e(\mathbf{0}) \int_{-1}^{1} \int_{-1}^{1} \boldsymbol{\Sigma}_h^{eT} \boldsymbol{E}_h^e \, \mathrm{d}\xi_1 \, \mathrm{d}\xi_2 = 0 \quad \text{for } e = 1, \ldots, M_e .$$

Now the sub stiffness matrices (2.29) can be computed by a numerical integration rule.

4. Numerical Examples

To show the regularization provided by the gradient-extended theory, two examples, taken from [28], have been computed by the enhanced-strain method, namely a bar under tensile load, and a perforated plate under tensile load. Both problems are monotonically strain driven. To compare the results obtained from the local and the nonlocal theory, meshes with different sizes are used, i.e. to show mesh dependency in the local case, and mesh independency in the nonlocal case. Due to symmetry only the half and the quarter, respectively, of the domains have been discretized.
Starting point for the implementation was a linear version of the FE-code SOOFEA, written in `Python` and developed by Dr. Michael Hammer, which has been largely reprogrammed in the course Finite Element Method - A Seminar for Problem Solving on the Computer (304.082) [9].

4.1. Bar under axial loading

We look at a bar with quadratic cross sectional area under strain-driven tensile load and plane strain state, see Figure 4.1(a). Because of the symmetry of the geometry and the load, only half of the bar is discretized by finite elements (quadrilaterals of first order), see Figure 4.1(b).

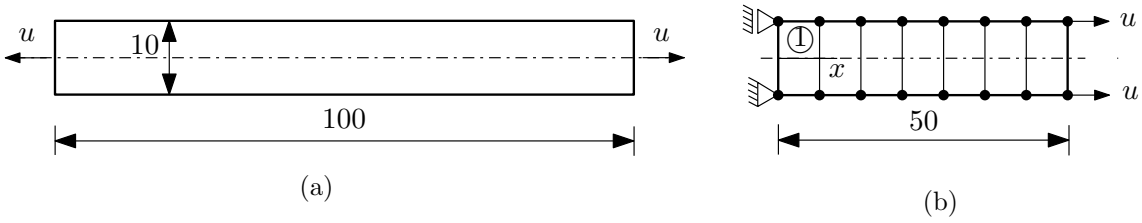

Figure 4.1. (a) Geometry of the bar with quadratic cross sectional area under tensile load and (b) discretization of the halved system by finite elements. In element ① the yield stress y_0 is reduced by 3%.

The material properties are:

κ	164.21	$\mathrm{kN/mm^2}$
μ	80.19	$\mathrm{kN/mm^2}$
y_0	0.45	$\mathrm{kN/mm^2}$
η	10^{-5}	$\mathrm{kNs/mm^2}$
H	-0.129	$\mathrm{kN/mm^2}$

It is maybe of interest to know the corresponding Young's modulus E and Poisson's ratio ν. They are given by the relations

$$E = \frac{9\kappa\mu}{3\kappa+\mu} \quad \text{and} \quad \nu = \frac{3\kappa-2\mu}{2(3\kappa+\mu)},$$

and we get $E \approx 206.892\,215\,879\,\mathrm{kN/mm^2}$ and $\nu \approx 0.290\,012\,569$.
An imperfection is realized by reducing the yield stress y_0 in element ① by 3%, see again

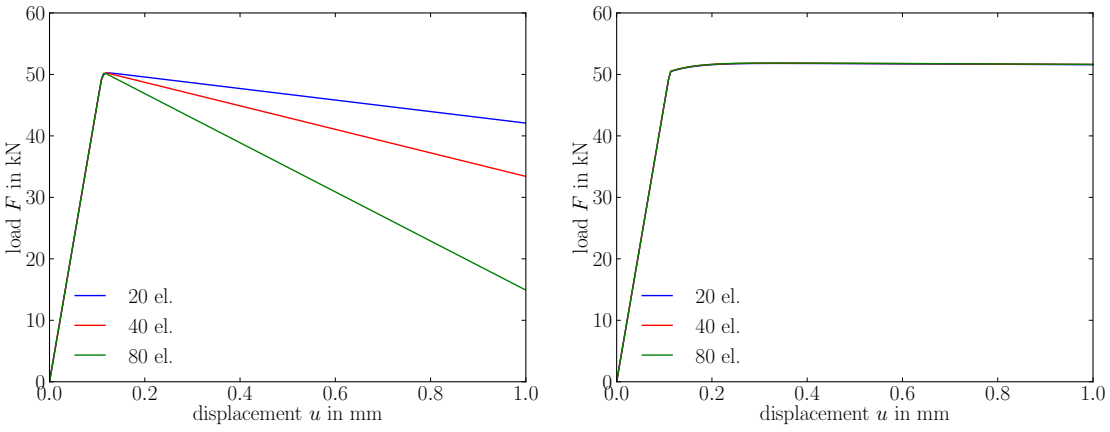

Figure 4.2. Load-displacement curves of the tensile loaded bar for different mesh sizes: (a) $l = 0\,\text{mm}$ and (b) $l = 3\,\text{mm}$.

Figure 4.1(b). To stay in the geometrically linear theory, the total displacement u applied on the halved bar must not be greater than 1 mm. The computation started with a first increment of $\Delta u_1 = 0.1\,\text{mm}$, which does not cause any convergence problems since we are still in the elastic range[1]. If plastic states are reached (in the integration points) a too large displacement increment could cause a failure of the Newton-Raphson procedure because of its local convergence, see Remark 6. Therefore 200 further time steps with $\Delta u_k = 0.0045$ for $k = 2, \ldots, 201$ were done to reach a total displacement of $u = 1\,\text{mm}$. The whole deformation process was chosen to take place within 1 s, accordingly $\tau_k = 0.045\,\text{s}$ for $k = 2, \ldots, 201$. The integration was done by a Gaussian quadrature with 2×2 integration points. The arising linear systems of equations (2.34) are solved by a pre-implemented LU-solver.
The responses of the bar for two different length scales, namely $l = 0\,\text{mm}$, which corresponds to the local theory, and $l = 3\,\text{mm}$, which corresponds to the nonlocal theory, and for three different meshes are shown in Figure 4.2(a) and Figure 4.2(b). As expected from the discussion in Section 3.2, we see a strong mesh dependency of the results for the local case. On the other hand, for $l = 3\,\text{mm}$, we clearly notice the regularization effect of the gradient-extended theory, i.e. the results are mesh independent. Furthermore, by doing a contour plot of the hardening variable α, see Figure 4.3, we indeed observe, that in the local case the softening region remains in the weakened element, whereas in the nonlocal case the softening region spreads out.
Finally it should be noted, that for the force β non-physical oscillations[2] in space occur, which is a classical allusion to stability problems. This issue is intensely discussed in [19]. However, these oscillations can be identified as being of minor influence on the solution.

4.2. Perforated plate under tensile loading

The second numerical example is a monotonically strain driven, tensile loaded quadratic plate under plane strain state with a circular hole in the middle, see Figure 4.4(a). Because

[1] To be precise, the Newton-Raphson procedure reaches the equilibrium state after one iteration.
[2] Note, that from a physical point of view $\beta \geq 0$ for softening plasticity, and $\beta \leq 0$ for hardening plasticity.

Figure 4.3. Contour plots of the hardening variable α over the halved bar under tensile load for $l = 0\,\text{mm}$ (left) and $l = 3\,\text{mm}$ (right) and different mesh sizes: (a)-(b) 20 elements, (c)-(d) 40 elements and (e)-(f) 80 elements. The pictures are taken at $u = 1\,\text{mm}$. Note, that the color-coding is not the same for the left and the right pictures.

of the symmetry, only a quarter of the plate is discretized, see Figure 4.4(b). The material properties are the same as in the first numerical example. The geometrically linear theory is not harmed up to a total displacement of $v = 0.02\,\text{mm}$. As first increment we choose $\Delta v_1 = 0.001\,\text{mm}$, and continue the iteration process with 200 further time steps with $\Delta v_k = 0.95 \cdot 10^{-4}\,\text{mm}$ for $k = 2, \ldots, 201$. Again, the time at which the total displacement is applied is 1 s, and accordingly $\tau_k = 0.00475\,\text{s}$ for $k = 2, \ldots, 201$. As before the integration was done by a 2×2 Gaussian quadrature and the linear system of equations (2.34) is again solved by a pre-implemented LU-solver.
The load-displacements curves for $l = 0\,\text{mm}$ and $l = 0.004\,\text{mm}$ and two different meshes are shown in Figure 4.5(a) and Figure 4.5(b). As expected, we observe a strong mesh dependency of the results obtained from the local theory, whereas this is not the case for the results obtained from the nonlocal theory. The contour plots of the hardening variable α over the whole quarter plate are shown in Figure 4.6. In the case $l = 0\,\text{mm}$ we can clearly identify a shear band, whose width becomes smaller with finer mesh. From Figure 4.7(a) and Figure 4.7(c) it can be seen, that in the local theory the shear band is related to strong deformations. Because of element distortion the solution becomes bad at the corners, which can be seen in Figure 4.6(c). On the other hand, for $l = 0.004\,\text{mm}$ we observe the softening zone to spread over several elements, no matter which mesh size is used. Looking at Figure 4.7(b) and Figure 4.7(d) we see that the nonlocal theory provides a regularization of the shear band.

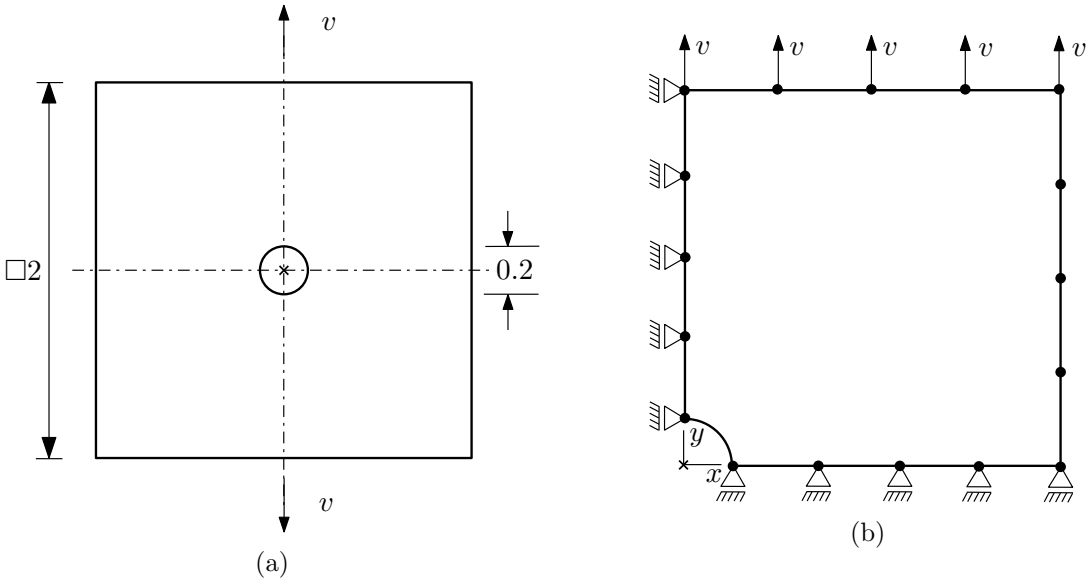

Figure 4.4. (a) Geometry of the perforated quadratic plate (thickness 1 mm) under tensile load and (b) quarter system with boundary conditions

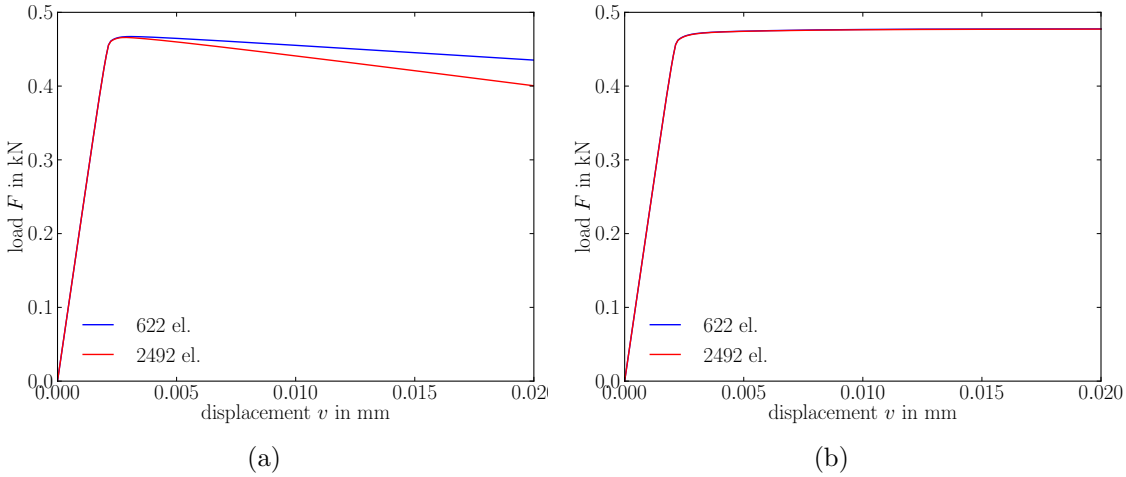

Figure 4.5. Load-displacement curves of the tensile loaded perforated plate for different mesh sizes: (a) $l = 0\,\text{mm}$ and (b) $l = 3\,\text{mm}$.

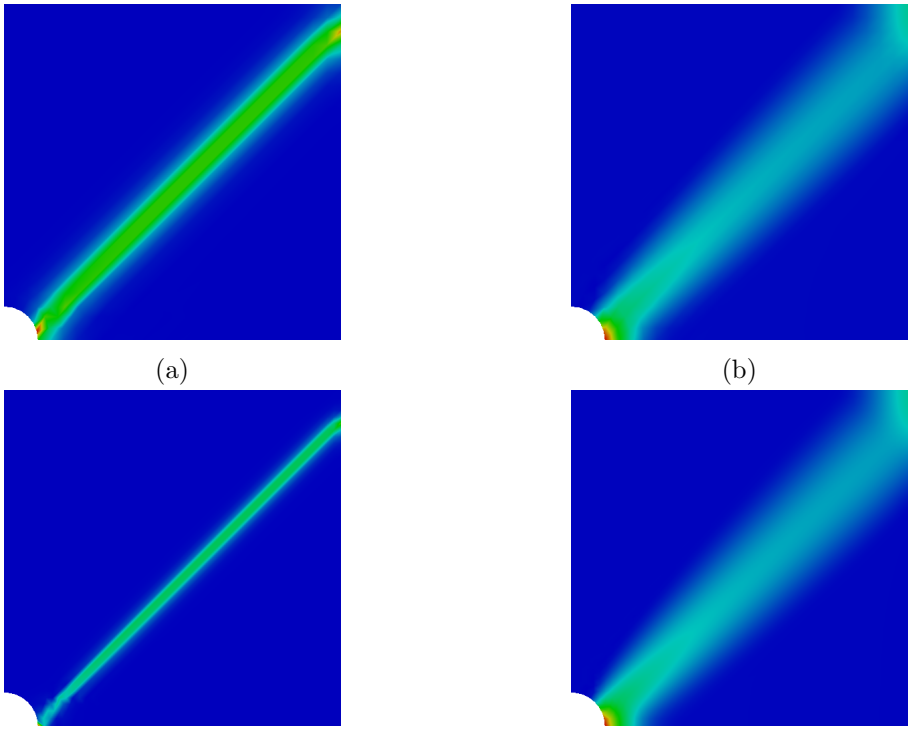

(a) (b)

(c) (d)

Figure 4.6. Contour plots of the hardening variable α over the quarter perforated plate under tensile load for $l = 0\,\text{mm}$ (left) and $l = 0.004\,\text{mm}$ (right) and different mesh sizes: (a)-(b) 622 elements and (c)-(d) 2492 elements. The pictures are taken at $v = 0.02\,\text{mm}$. Note, that the color-coding is not exactly the same for the left and the right pictures.

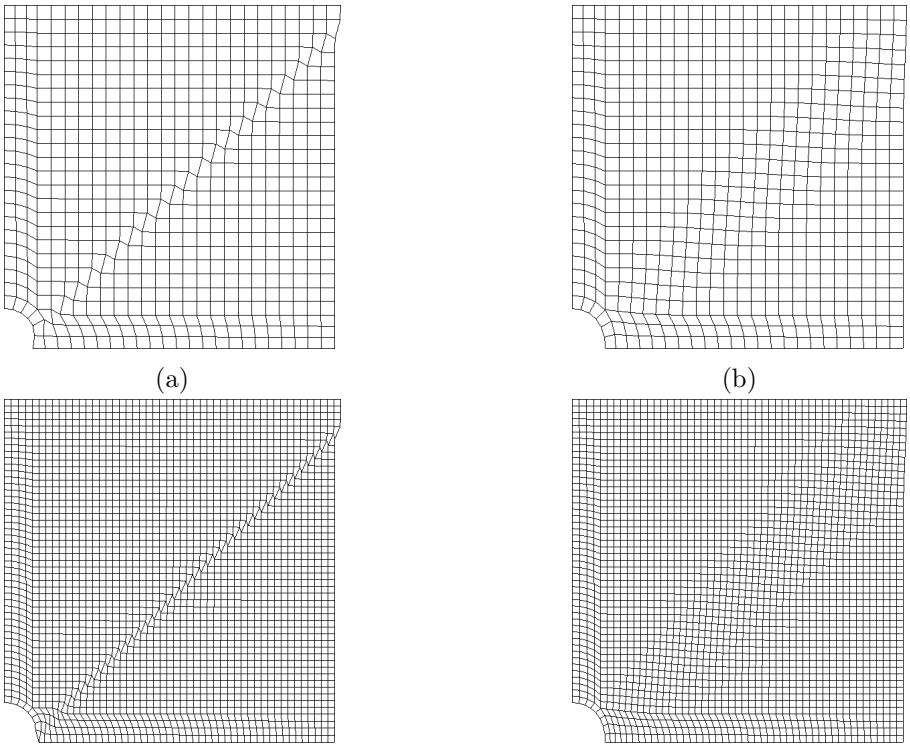

Figure 4.7. Deformed meshes of the perforated plate for $l = 0\,\text{mm}$ (left) and $l = 0.004\,\text{mm}$ (right) and different meshes: (a)-(b) 622 elements and (c)-(d) 2492 elements. The pictures are taken at $v = 0.02\,\text{mm}$.

Appendix A.

Mathematical tools

In this appendix several mathematical definitions and relations are summarized, which are needed in the text. Much of the information collected here is taken from [7].

Convexity

Definition 1. Let $\mathcal{V}$ be a linear vector space. A set $\mathcal{Z} \subset \mathcal{V}$ is called convex, if for all $x, y \in \mathcal{Z}$ and $\lambda \in [0, 1]$

$$\lambda x + (1 - \lambda)y \in \mathcal{Z}\,.$$

Geometrically, this definition can be interpreted in the following way: a set $\mathcal{Z}$ is convex, if every straight line, built by any two points x and y within $\mathcal{Z}$, lies completely in $\mathcal{Z}$, see Figure A.1.

Figure A.1. (a) Convex set and (b) non-convex set in $\mathbb{R}^2$.

Definition 2. Let $\mathcal{Z}$ be a convex set. A functional $F\colon \mathcal{Z} \to \mathbb{R}$ is called convex, if for all $x, y \in \mathcal{Z}$ and $\lambda \in [0, 1]$

$$F(\lambda x + (1 - \lambda)y) \leq \lambda F(x) + (1 - \lambda)F(y)\,. \tag{A.1}$$

If we replace in (A.1) the $\leq$ sign by the $<$ sign, we call F strictly convex.

In the one-dimensional case, convex functionals are identified by lying below its secant, built by $(x, F(x))$ and $(y, F(y))$, for all points in $\mathcal{Z}$, see Figure A.2.

Remark 15. Changing the direction of the inequality-sign in (A.1), we end up with the definition of a concave functional. Clearly, a convex/concave functional can be made concave/convex just by changing its sign.

Example 1. It is immediately seen, that every linear functional is also convex.

Example 2. Let the linear vector space $\mathcal{Z}$ be equipped with a norm $\|\cdot\|\colon \mathcal{Z} \to \mathbb{R}$. Then $\|\cdot\|$ forms a convex functional, as can be quickly proven by using two of the three norm axioms, namely the triangle inequality and the homogeneity property:

$$\|\lambda x + (1 - \lambda)y\| \leq \|\lambda x\| + \|(1 - \lambda)y\| = \lambda\|x\| + (1 - \lambda)\|y\|$$

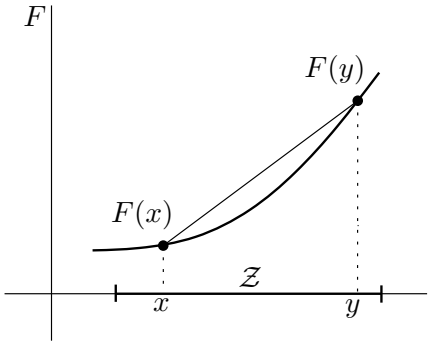

Figure A.2. One-dimensional example of a functional being convex in $\mathcal{Z}$.

for all $x, y \in \mathcal{Z}$ and $\lambda \in [0, 1]$.

Definition 3. The epigraph of a functional $F\colon \mathcal{V} \to \mathbb{R}$ is defined as

$$\operatorname{epi}(F) := \{(x, \alpha) \in \mathcal{V} \times \mathbb{R}\colon \alpha \geq F(x)\} \subset \mathcal{V} \times \mathbb{R}\,.$$

Lemma 1. [21, Theorem 4.6] A functional $F\colon \mathcal{V} \to \mathbb{R}$ is convex if and only if its epigraph $\operatorname{epi}(F)$ is a convex set.

As can be seen from Figure A.3(a), a convex function $F(x)$ can be described by the point wise maximum of all linear functions $t(x)$ satisfying $t(x) \leq F(x)$. In other words, a convex function is given by its tangents $\{t(x)\}$, which are so called supporting hyperplanes. In general a supporting hyperplane of a convex region is the closest possible hyperplane, which does not "cut" the region. At non-smooth points (cones), the supporting hyperplane is not uniquely defined, see Figure A.3(b).

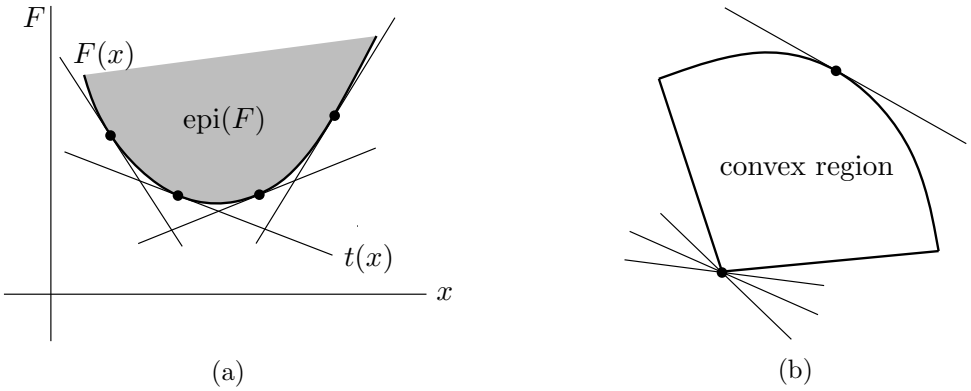

Figure A.3. (a) A convex function (region) described by its supporting hyperplanes and (b) non-uniqueness of supporting hyperplanes at cones.

Definition 4. Let $F\colon \mathcal{V} \to \mathbb{R}$ be a functional. We define the directional derivative at point $x \in \mathcal{V}$ in direction $\chi \in \mathcal{V}$ as

$$\delta F(x; \chi) := \lim_{\varepsilon \to 0} \frac{F(x + \varepsilon\chi) - F(x)}{\varepsilon} = \frac{\mathrm{d}}{\mathrm{d}\varepsilon} F(x + \varepsilon\chi)|_{\varepsilon=0}\,.$$

If δF exists in x in every direction χ, we call F Gateaux-differentiable in x.

Lemma 2. [24, Lemma 2.6.1] Let $\mathcal{V}$ be a convex set. An equivalent condition for a functional $F\colon \mathcal{V} \to \mathbb{R}$ being convex is

$$\partial_y F(y) \cdot (x - y) \leq F(x) - F(y) \tag{A.2}$$

for all $x, y \in \mathcal{V}$.

Proof. For the first equivalence direction we assume F to be convex:

$$F(y + \lambda(x - y)) \leq F(y) + \lambda[F(x) - F(y)]$$

for all $x, y \in \mathcal{V}$ and $\lambda \in [0, 1]$. Division by λ and taking the limit $\lambda \to 0$ yields

$$\begin{aligned} \delta F(y; x - y) &\leq F(x) - F(y) \\ \partial_y F(y) \cdot (x - y) &\leq F(x) - F(y)\,. \end{aligned}$$

For the second equivalence direction, we assume the inequality (A.2) to hold. Further let us define

$$\tilde{y} := \lambda x + (1 - \lambda) y \in \mathcal{V} \quad \text{with } \lambda \in [0, 1]\,.$$

We have

$$\begin{aligned} \partial_{\tilde{y}} F(\tilde{y}) \cdot (x - \tilde{y}) &\leq F(x) - F(\tilde{y}) \\ \partial_{\tilde{y}} F(\tilde{y}) \cdot (x - \lambda x - (1 - \lambda) y) &\leq F(x) - F(\tilde{y}) \\ (1 - \lambda) \partial_{\tilde{y}} F(\tilde{y}) \cdot (x - y) &\leq F(x) - F(\tilde{y})\,, \end{aligned} \tag{A.3}$$

and

$$\begin{aligned} \partial_{\tilde{y}} F(\tilde{y}) \cdot (y - \tilde{y}) &\leq F(y) - F(\tilde{y}) \\ \partial_{\tilde{y}} F(\tilde{y}) \cdot (y - \lambda x - (1 - \lambda) y) &\leq F(y) - F(\tilde{y}) \\ -\lambda \partial_{\tilde{y}} F(\tilde{y}) \cdot (x - y) &\leq F(y) - F(\tilde{y})\,. \end{aligned} \tag{A.4}$$

Multiplying (A.3) by λ and (A.4) by $(1 - \lambda)$ gives after adding these two inequalities

$$0 \leq \lambda F(x) + (1 - \lambda) F(y) - F(\tilde{y})\,,$$

and accordingly $F(\lambda x + (1 - \lambda) y) \leq \lambda F(x) + (1 - \lambda) F(y)$. □

Legendre transformation

First of all we do some general considerations. Let $F\colon \mathbb{R} \to \mathbb{R}$ be a strictly convex and twice continuously differentiable function. Therefore $F''(x) > 0$ and the inverse function of the first derivative $[F'(x)]^{-1} =: g$ exists. Hence, we can say $x = g(k)$ with $k(x) := F'(x)$ being the new variable. The antiderivative of g is given by

$$s(k) := k g(k) - F(g(k)) = \underbrace{F'(x)}_{=k} x - F(x)\,.$$

This can be checked via

$$s'(k) = g(k) + k g'(k) - g'(k) F'(g) = g(k) + k g'(k) - g'(k) k = g(k)\,.$$

For the geometrically motivated introduction of the Legendre transformation, choose an arbitrary $k \in \mathbb{R}$ and build the line $y(x) = kx$. Now check out the point $x(k)$, such that the distance $d(k, x) := kx - F(x)$ becomes a maximum:

$$x(k) = \arg \max_x [d(k, x)]\,.$$

The existence of such a point $x(k)$ is at least guaranteed by the mean value theorem.

Definition 5. The Legendre transformation of a function $F(x)$ is defined as

$$s(k) := \max_x \{d(k,x)\} = kx(k) - F(x(k))\,.$$

Figure A.4 illustrates the Legendre transformation.

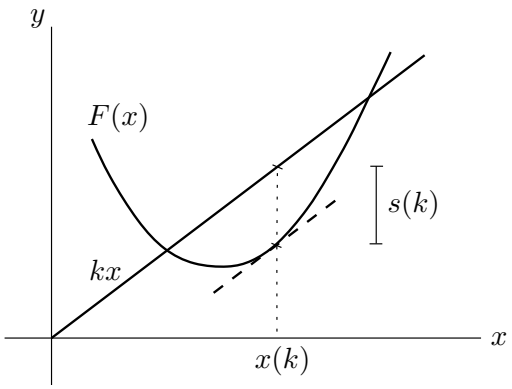

Figure A.4. Geometrical illustration of the Legendre transformation $s(k)$.

Clearly, the Legendre transform $s(k)$ of a function $F(x)$ can be computed via the condition $\frac{\partial}{\partial x} d(k,x) = 0$ in $x = x(k)$.

Example 3. To obtain the Legendre transform $s(k)$ of $F(x) = ax^2$ with $a \in \mathbb{R}$, we get from $\frac{\partial}{\partial x} d(k,x) = 0$ the point at which the maximum arises, namely $x(k) = \frac{k}{2a}$. This gives $s(k) = \frac{k^2}{4a}$.

There is a strong relation between the hyperplanes of a function $F(x)$ and its Legendre transform. As pointed out in the section about convexity, a convex function can be represented by its supporting hyperplanes:

$$F(x) = \max_k \{t(x) = kx - e \quad \text{with } t(x) \leq F(x)\}\,.$$

It can be seen from Figure A.4, that the constraint $t(x) \leq F(x)$ is fulfilled if and only if

$$e \geq s(k) = \max_x \{kx - F(x)\}\,.$$

This yields

$$F(x) = \max_k \{kx - s(k)\}\,,$$

and for convex functions we have shown the following:

Lemma 3. The Legendre transformation is involutoric, this means the Legendre transform of the Legendre transformation of $F(x)$ is again $F(x)$, i.e.

$$s(k) = \max_x \{kx - F(x)\} \quad \text{and} \quad F(x) = \max_k \{xk - s(k)\}\,.$$

The Legendre transformation offers to transform a minimization problem into a saddle-point problem. For this, we exemplarily look at the minimization problem

$$\tilde{x} = \arg\min_x [F(x) + G(x)]\,,$$

with $F(x)$ being convex. Expressing $F(x)$ by its Legendre transform $s(y) = \max_x \{yx - F(x)\}$, we can write

$$\{\tilde{x}, \tilde{y}\} = \arg\{\min_x \max_y [yx - s(y) + G(x)]\}\,.$$

The concept of the Legendre transformation, exemplarily presented for the one-dimensional case, can of course be transferred to the the n-dimensional case with $F\colon \mathbb{R}^n \to \mathbb{R}$. A general and simultaneously abstract treatment of the Legendre transformation is the formulation in Banach spaces.

Definition 6. Let $\mathcal{V}$ be a Banach space and $\mathcal{V}^*$ its dual space with $\langle\cdot,\cdot\rangle_{\mathcal{V}\times\mathcal{V}^*}\colon \mathcal{V}\times\mathcal{V}^* \to \mathbb{R}$ denoting the duality pairing. We look at a convex functional $F\colon \mathcal{Z} \to \mathbb{R}$ over a convex set $\mathcal{Z} \subset \mathcal{V}$. The Legendre transform of F is defined as

$$F^*\colon \mathcal{Z}^* \ni y \mapsto \sup_{x\in\mathcal{Z}}\{\langle y, x\rangle_{\mathcal{V}\times\mathcal{V}^*} - F(x)\} \in \mathbb{R}\,,$$

and is also called dual functional.

Lemma 4. The dual functional $F^*(y)$ is convex.

Proof. We have to show

$$F^*(\lambda y_1 + (1-\lambda)y_2) \le \lambda F^*(y_1) + (1-\lambda)F^*(y_2)$$

for all $y_1, y_2 \in \mathcal{Z}^*$ and $\lambda \in [0,1]$. The single steps are

$$\begin{aligned}
F^*(\lambda y_1 + (1-\lambda)y_2) &= \sup_{x\in\mathcal{Z}}\{\langle \lambda y_1 + (1-\lambda)y_2, x\rangle_{\mathcal{V}\times\mathcal{V}^*} - F(x)\} \\
&= \sup_{x\in\mathcal{Z}}\{\lambda\langle y_1, x\rangle_{\mathcal{V}\times\mathcal{V}^*} + (1-\lambda)\langle y_2, x\rangle_{\mathcal{V}\times\mathcal{V}^*} - F(x) + \lambda F(x) - \lambda F(x)\} \\
&\le \lambda \sup_{x\in\mathcal{Z}}\{\langle y_1, x\rangle_{\mathcal{V}\times\mathcal{V}^*} - F(x)\} + (1-\lambda)\sup_{x\in\mathcal{Z}}\{\langle y_2, x\rangle_{\mathcal{V}\times\mathcal{V}^*} - F(x)\} \\
&= \lambda F^*(y_1) + (1-\lambda)F^*(y_2)\,,
\end{aligned}$$

and we are done. □

For further details we refer to [7] and [21].

Positively homogeneous function

Definition 7. Let $\mathcal{V}$ be a linear vector space. A function $F\colon \mathcal{V} \to \mathbb{R}$ is said to be positively homogeneous of order $0 \neq k \in \mathbb{R}$ if

$$F(\alpha x) = \alpha^k F(x) \quad \text{for all } \alpha > 0\,.$$

Lemma 5. [14, Remark p.46] Let a function $F\colon \mathcal{V} \to \mathbb{R}$ be positively homogeneous of order one ($k = 1$). Then F is convex if and only if

$$F(x+y) \le F(x) + F(y) \quad \text{for all } x, y \in \mathcal{V}\,.$$

Proof. For the first equivalence direction let us assume that

$$F(x+y) \le F(x) + F(y)$$

holds for all $x, y \in \mathcal{V}$. Then we get for $\lambda \in [0,1]$

$$F(\lambda x + (1-\lambda)y) \le F(\lambda x) + F((1-\lambda)y) = \lambda F(x) + (1-\lambda)F(y)\,.$$

For the second equivalence direction we assume F to be convex. For $\lambda = \frac{1}{2}$ we have

$$F(\frac{1}{2}x + \frac{1}{2}y) \le \frac{1}{2}F(x) + \frac{1}{2}F(y)$$

and obtain due to F being positively homogeneous of order one

$$F(x+y) \le F(x) + F(y)\,,$$

which concludes the proof. □

Sobolev spaces of positive integer order

Sobolev spaces are needed for the mathematical treatment of weak formulations of boundary value problems. Let $\mathscr{B} \subset \mathbb{R}^n$ be a bounded and open domain with $n \geq 1$. By $\mathcal{L}_p(\mathscr{B})$ we denote the space of functions $v\colon \mathscr{B} \to \mathbb{R}$, of which the p-th potency is integrable, i.e. the corresponding norm is given by

$$\|v\|_{\mathcal{L}_p(\mathscr{B})} := \left[\int_{\mathscr{B}} |v(x)|^p \,\mathrm{d}x\right]^{1/p} \quad \text{for } 1 \leq p < \infty$$

with $x = (x_1, x_2, \ldots, x_n)$.
For $p = 2$ we get the space of all functions which are square integrable over the domain $\mathscr{B}$. We can define an inner product

$$(u, v)_{\mathcal{L}_2(\mathscr{B})} := \int_{\mathscr{B}} u(x)v(x) \,\mathrm{d}x\,,$$

and it can be shown, that $\mathcal{L}_2(\mathscr{B})$ is by the induced norm $\|v\|_{\mathcal{L}_2(\mathscr{B})} = (v, v)^{1/2}_{\mathcal{L}_2(\mathscr{B})}$ complete and hence a Hilbert space, see e.g. [2].

For integers $k \geq 0$ we define the Sobolev space $\mathcal{H}^k(\mathscr{B})$ as the set of all functions $v \in \mathcal{L}_2(\mathscr{B})$, which possess generalized derivatives through order k. The considered Sobolev spaces are equipped with an inner product

$$(u, v)_{\mathcal{H}^k(\mathscr{B})} := \int_{\mathscr{B}} (uv + u_{,i}v_{,i} + u_{,ij}v_{,ij} + \ldots + u_{,\underbrace{\ldots}_{k \text{ indices}}} v_{,\underbrace{\ldots}_{k \text{ indices}}})\mathrm{d}x\,, \tag{A.5}$$

where $(\cdot)_{,i} := \frac{\partial}{\partial x_i}(\cdot)$ for $i = 1, \ldots, n$ and Einstein's summation convention is used. Again it can be shown, that the induced norm $\|v\|_{\mathcal{H}^k(\mathscr{B})} = (v, v)^{1/2}_{\mathcal{H}^k(\mathscr{B})}$ makes the Sobolev space complete, and therefore $\mathcal{H}^k(\mathscr{B})$ is a Hilbert space for $k \geq 0$.
As an example, we get for $k = 1$ the space of all square integrable functions, of which the first generalized derivative is also square integrable. Its norm reads

$$\|v\|^2_{\mathcal{H}^1(\mathscr{B})} = \|v\|^2_{\mathcal{L}_2(\mathscr{B})} + \|\nabla v\|^2_{\mathcal{L}_2(\mathscr{B})}\,.$$

Clearly from the definition we get

$$\mathcal{L}_2(\mathscr{B}) = \mathcal{H}^0(\mathscr{B}) \supset \mathcal{H}^1(\mathscr{B}) \supset \mathcal{H}^2(\mathscr{B}) \supset \ldots\,.$$

Remark 16. If we are considering m-valued functions $(v_1, v_2, \ldots, v_m)\colon \mathscr{B} \to \mathbb{R}^m$, the inner product (A.5) reads

$$(\boldsymbol{u}, \boldsymbol{v})_{\mathcal{H}^k(\mathscr{B})} := \int_{\mathscr{B}} (u_i v_i + u_{i,j}v_{i,j} + u_{i,jl}v_{i,jl} + \ldots + u_{i,\underbrace{\ldots}_{k \text{ indices}}} v_{i,\underbrace{\ldots}_{k \text{ indices}}})\mathrm{d}x\,.$$

Definition 8. Let $\mathscr{B} \subset \mathbb{R}^n$ be an open set. The space $\mathcal{C}^r(\mathscr{B})$ with $r \in \mathbb{N}_0$ denotes the set of all functions which are bounded on $\mathscr{B}$ and r times continuously differentiable on $\mathscr{B}$.

A very important characterisation of the presented Sobolev spaces is given by Sobolev's embedding theorem:

Theorem 1. [11, p.268] Let $\mathscr{B} \subset \mathbb{R}^n$ be an open set and $\frac{n}{2} + r < k$. Then

$$\mathcal{H}^k(\mathscr{B}) \subset \mathcal{C}^r(\mathscr{B})\,.$$

Example 4. For $n = 2$ and $k = 2$ we get $\mathcal{H}^2(\mathscr{B}) \subset \mathcal{C}^0(\mathscr{B})$. Note, that for $n = 2$ a $\mathcal{H}^1(\mathscr{B})$-function can be discontinuous. However, for $n = 1$ we have $\mathcal{H}^1(\mathscr{B}) \subset \mathcal{C}^0(\mathscr{B})$.

Bibliography

[1] J. Altenbach and H. Altenbach. *Einführung in die Kontinuumsmechanik.* B.G. Teubner-Verlag, Stuttgart, 1994.

[2] K. Burg. *Partielle Differentialgleichungen und funktionalanalytische Grundlagen.* Vieweg+Teubner-Verlag, Wiesbaden, 2010.

[3] R.E. Burkard and U.T. Zimmermann. *Einführung in die Mathematische Optimierung.* Springer-Verlag, Berlin-Heidelberg, 2012.

[4] C.C. Celigoj. *An assumed enhanced displacement gradient ring-element for finite deformation axisymmetric and torsional problems.* International Journal for Numerical Methods in Engineering, 43:1369-1382, 1998.

[5] C.C. Celigoj. *Festigkeitslehre.* Institut für Festigkeitslehre TU Graz, Graz, 2004.

[6] C.C. Celigoj. *Plastizitätstheorie.* Institut für Festigkeitslehre TU Graz, Graz, 2006.

[7] E.W. Gekeler. *Mathematische Methoden zur Mechanik.* Springer-Verlag, Heidelberg u.a., 2010.

[8] M.E. Gurtin, E. Fried, and L. Anand. *The Mechanics and Thermodynamics of Continua.* Cambridge University Press, New York, 2010.

[9] M.E. Hammer. *The Finite Element Method. Linear Structural Analysis. Computer Exercises.* Institut für Festigkeitslehre TU Graz, Graz, 2012.

[10] R. Hill. *The Mathematical Theory of Plasticity.* Oxford University Press, New York, 1950.

[11] T.J.R. Hughes. *The Finite Element Method. Linear Static and Dynamic Finite Element Analysis.* Prentice-Hall, Englewood Cliffs, 1985.

[12] M. Itskov. *Tensor Algebra and Tensor Analysis for Engineers.* Springer-Verlag, Berlin-Heidelberg, 2006.

[13] L.M. Kachanov. *Fundamentals of the Theory of Plasticity.* Dover Publications, New York (Mineola), 2004.

[14] P. Kosmol. *Optimierung und Approximation.* de Gruyter-Verlag, Berlin-New York, 2010.

[15] J. Lubliner. *Plasticity Theory.* Dover Publications, New York (Mineola), 2008.

[16] L.E. Malvern. *Introduction to the mechanics of a continuous medium.* Prentice-Hall, Englewood Cliffs, 1969.

[17] C. Miehe. *Strain-driven homogenization of inelastic microstructures and composites based on an incremental variational formulation.* International Journal for Numerical Methods in Engineering, 55:1285-1322, 2002.

[18] C. Miehe. *A multi-field incremental variational framework for gradient-extended standard dissipative solids.* Journal of the Mechanics and Physics of Solids, 59:898-923, 2011.

[19] C. Miehe, F. Aldakheel, and S. Mauthe. *Mixed variational principles and robust finite element implementations of gradient plasticity at small strains.* International Journal for Numerical Methods in Engineering, 94:1037-1074, 2013.

[20] P. Perzyna. *The constitutive equations for rate sensitive plastic materials.* Quarterly of Applied Mathematics, 20:321-332, 1963.

[21] R.T. Rockafellar. *Convex Analysis.* Princeton University Press, Princeton-New Jersey, 1998.

[22] H.L. Schreyer. *Analytical Solutions for Nonlinear Strain-Gradient Softening and Localization.* Journal of Applied Mechanics, 57:522-528, 1990.

[23] H.L. Schreyer and Z. Chen. *One-dimensional Softening with Localization.* Journal of Applied Mechanics, 53:791-797, 1986.

[24] J.C. Simo and T.J.R. Hughes. *Computational Inelasticity.* Springer-Verlag, New York, 1998.

[25] J.C. Simo and M.S. Rifai. *A class of mixed assumed strain methods and the method of incompatible modes.* International Journal for Numerical Methods in Engineering, 29:1595-1638, 1990.

[26] I. Sokolnikoff. *Tensor Analysis. Theory and Applications to Geometry and Mechanics of Continua.* John Wiley and Sons, New York u.a., 1964.

[27] O. Steinbach. *Mathematische Modellierung 2.* Institut für Numerische Mathematik TU Graz, Graz, 2012.

[28] F.R. Welschinger. *A Variational Framework for Gradient-Extended Dissipative Continua. Application to Damage Mechanics, Fracture and Plasticity.* Bericht Nr.: I-24, Institut für Mechanik (Bauwesen), Lehrstuhl I Universität Stuttgart, Stuttgart, 2011.

[29] O.C. Zienkiewicz, R.L. Taylor, and J.Z. Zhu. *The Finite Element Method for Solid and Structural Mechanics.* Butterworth-Heinemann, Amsterdam u.a., sixth edition, 2005.

[30] O.C. Zienkiewicz, R.L. Taylor, and J.Z. Zhu. *The Finite Element Method. Its Basis and Fundamentals.* Butterworth-Heinemann, Amsterdam u.a., sixth edition, 2005.